New Jersey Institute of Technology
Digital Commons @ NJIT

Dissertations | Electronic Theses and Dissertations

Spring 1985

An analysis of the heating and densification process during rotational molding of a thermoplastic powder in a uniaxially rotating cylindrical cavity

Floyd Steven Ribe
New Jersey Institute of Technology

Follow this and additional works at: https://digitalcommons.njit.edu/dissertations

Part of the Mechanical Engineering Commons

Recommended Citation

Ribe, Floyd Steven, "An analysis of the heating and densification process during rotational molding of a thermoplastic powder in a uniaxially rotating cylindrical cavity" (1985). *Dissertations*. 1203.
https://digitalcommons.njit.edu/dissertations/1203

This Dissertation is brought to you for free and open access by the Electronic Theses and Dissertations at Digital Commons @ NJIT. It has been accepted for inclusion in Dissertations by an authorized administrator of Digital Commons @ NJIT. For more information, please contact digitalcommons@njit.edu.

Copyright Warning & Restrictions

The copyright law of the United States (Title 17, United States Code) governs the making of photocopies or other reproductions of copyrighted material.

Under certain conditions specified in the law, libraries and archives are authorized to furnish a photocopy or other reproduction. One of these specified conditions is that the photocopy or reproduction is not to be "used for any purpose other than private study, scholarship, or research." If a, user makes a request for, or later uses, a photocopy or reproduction for purposes in excess of "fair use" that user may be liable for copyright infringement,

This institution reserves the right to refuse to accept a copying order if, in its judgment, fulfillment of the order would involve violation of copyright law.

Please Note: The author retains the copyright while the New Jersey Institute of Technology reserves the right to distribute this thesis or dissertation

Printing note: If you do not wish to print this page, then select "Pages from: first page # to: last page #" on the print dialog screen

The Van Houten library has removed some of the personal information and all signatures from the approval page and biographical sketches of theses and dissertations in order to protect the identity of NJIT graduates and faculty.

AN ANALYSIS OF THE HEATING AND DENSIFICATION PROCESS DURING ROTATIONAL MOLDING OF A THERMOPLASTIC POWDER IN A UNIAXIALLY ROTATING CYLINDRICAL CAVITY

by
Floyd S. Ribe

Dissertation submitted to the Faculty of the Graduate School of the New Jersey Institute of Technology in partial fulfillment of the requirements for the degree of Doctor of Engineering Science
1985

© 1985

FLOYD S. RIBE

All Rights Reserved

APPROVAL SHEET

Title of Thesis: AN ANALYSIS OF THE HEATING AND DENSIFICATION PROCESS DURING ROTATIONAL MOLDING OF A THERMOPLASTIC POWDER IN A UNIAXIALLY ROTATING CYLINDRICAL CAVITY

Name of Candidate: Floyd S. Ribe
Doctor of Engineering Science, 1985

Thesis and Abstract Approved:

Dr. Richard C. Progelhof Date
Professor of Mechanical Engineering

Dr. John V. Droughton Date

Dr. Benedict C. Sun Date

Dr. Hans E. Pawel Date

Professor Joseph Kopf Date

VITA

Name: Floyd Steven Ribe

Permanent address:

Degree and date to be conferred: D. Eng. Sci., 1985

Date of birth:

Place of birth:

Secondary education: Roxbury High School, 1970.

Collegiate institutions attended	Dates	Degree	Date of Degree
New Jersey Inst. of Tech.	1977-85	D.E.S	1985
New Jersey Inst. of Tech.	1975-76	MSME	1976
Newark College of Eng.	1970-74	BSME	1974

Major: Mechanical Engineering

Publications: 1976 - Master's Thesis: The Heating of Nylon-6 in Matched Die Molds

Positions held: 1976 - 1985 Mechanical Engineer, Picatinny Arsenal Dover, NJ 07801

1975 Consultant, Allied Chemical Corp. Morristown, NJ

ABSTRACT

Title of Thesis: AN ANALYSIS OF THE HEATING AND DENSIFICATION PROCESS DURING ROTATIONAL MOLDING OF A THERMOPLASTIC POWDER IN A UNIAXIALLY ROTATING CYLINDICAL CAVITY

Floyd Steven Ribe, Doctor of Engineering Science, 1985

Thesis directed by: Dr. Richard C. Progelhof
Professor of Mechanical Engineering

This dissertation presents the results of an experimental and theoretical investigation of the heating and densification portion of the rotational molding process in a uniaxial, cylindrical mold.

A thorough literature survey is included which reviewed past analysis of the rotational molding process and other areas that assisted in understanding of the process.

The results presented in this dissertation included an analysis of the densification process by use of Scanning Electronic Microscope (SEM) photography producing intermediate correlations between the physical properties of the densifying material and neck radius of adjacent coalescing spheres. In addition, a hybrid experimental procedure coupled with a small computer simulation was devised to determine the actual initial thermal conductivity and diffusivity of the powdered polymeric material.

Finally, a computer program was written to simulate the heating and densification process during the rotational molding process. Results showed good agreement with actual experimental findings.

ACKNOWLEDGMENTS

The author would like to express appreciation to Dr. R. C. Progelhof for his guidance and assistance throughout the preparation of this dissertation.

Also appreciated for their assistance are my many friends and co-workers at Picatinny Arsenal, Dover, NJ.

TABLE OF CONTENTS

LIST OF TABLES

LIST OF FIGURES

LIST OF FIGURES (CONTINUED)

LIST OF FIGURES (CONTINUED)

I. INTRODUCTION

This dissertation presents the results of an experimental and theoretical investigation of a portion of the rotational molding process of a thermoplastic material in a cylindical mold. In rotational molding or rotomolding of thermoplastic powders, the process consists of the following steps:

1 - Loading the mold with a fixed mass of resin

2 - Simultaineously heating and melting the thermoplastic powder while the mold rotates

3 - Cooling the mold

4 - Unloading the mold

During loading, a premeasured mass of thermoplastic powder is placed in a two or three part split mold of which one section is bolted to a platform. The mold is closed and locked. The mold platform is bolted to an arm which moves the mold from station to station and biaxially rotates the mold at a predetermined rate. Rotational speed and directional speed ratios are adjusted by gearing.

After loading, the arm moves the mold into an oven and the biaxially rotation is started. At this point the powdered material is still cool and due to gravity the powder forms a pool at the bottom of the mold. Figure 1 shows a typical pool flow of a uniaxial clockwise rotating mold and is the type used in this investigation to experimentally verify the theoretical analysis. As the mold rotates, friction causes the material to follow and remains stationary to the motion of the mold surface. When the powder particles reach a point where friction is overcome by gravity, the individual powder granules begin to free fall over the top surface of the following adjacent material of the stationary pool. The stationary and free fall zones are shown in Figure 1. Experiments have shown that the actual motion of the stationary and free falling powder is dependent upon particle geometry, air volume fraction and surface character of the powder.

This rotational process continues until the mold surface reaches a temperature that causes the material to begin to soften and adhere to the mold surface. This temperature is called the "stick temperature". With increasing mold temperature, more material adheres to the mold surface until the mold surface is covered. With a further increase in mold surface temperature, layers of powder will be built on the mold wall causing the pool to deplete. The material adhering to the surface of the mold is a porous powdered layer initially held together by point

Figure 1

TYPICAL POOL FLOW

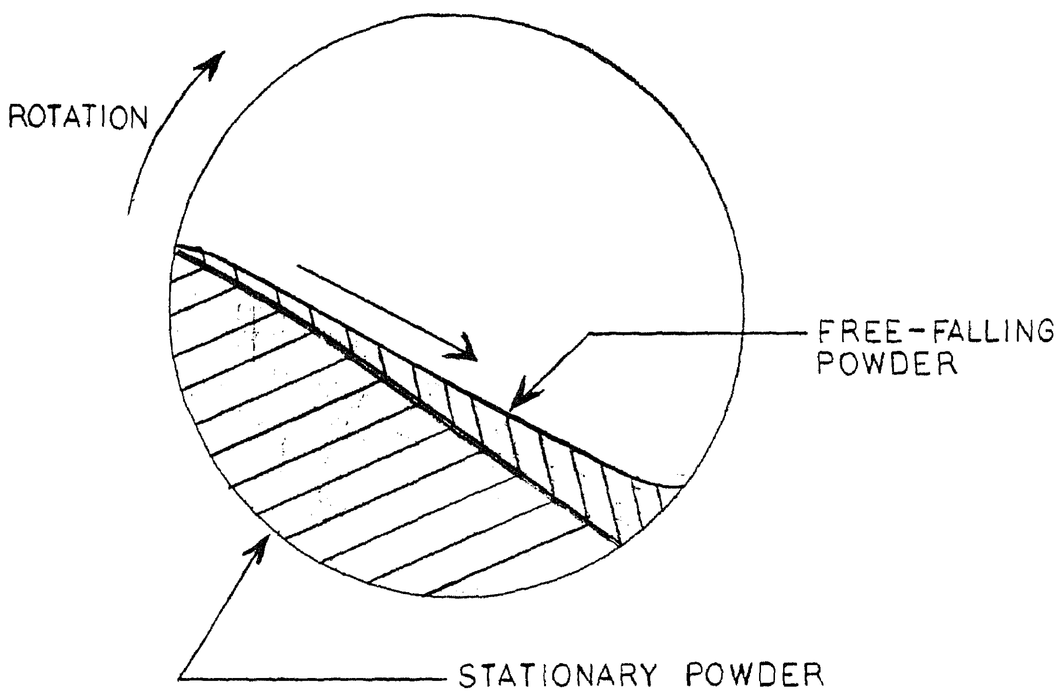

contact of the individual powder particles.

During the period of time for which the particles are adhering to the wall of the mold, the material begins a densification process. During this process the material particles lose their individuality by joining themselves first at the contact points, then "melting" into a solid piece with minute air voids throughout the molten resin. The initial phase of this densification process is similar to the sintering, coalesence and fusion processes in the field of drop coalescense, paint technology, ceramics and glass.

When the heating process is completed, the mold is first air cooled allowing an even temperature distribution within the part and densification of the molded part to complete. Rapid cooing to room temperature is then usually accomplished by water spray on the exterior mold surface.

This investigation will analyze this rotational molding process excluding the cooling portion of the cycle. A literature survey will first be made to review past works. Finally two mathematical models will be developed to predict the material heating process which includes the time for complete densification.

II. LITERATURE SURVEY

The literature available of the rotational molding process and the analysis thereof is very limited. Because of this, the literature survey will first examine the available published works on the subject and then at other related articles that also provide additional insight toward understanding the rotational molding process. These areas include a survey of articles concerning sintering which help describe the densification process in rotational molding, a survey of the thermal conductivity of porous material used to predict the thermal conductivity of powdered material similar to that encountered in the initial phase of the rotational molding system, and a rewiew of previously published works that analyzed the mass flow in a rotating cylinder.

Modeling of the Rotational Molding Process

One of the first to attempts to analytically model the rotational molding process was reported by Rao and Throne (31,32, and 14). They modeled the heat transfer to the mold and powder, the fluid flow of the powder, the sintering-melting and degradation during this process.

In their analysis, the authors' assume that an exponential internal mold surface temperature profile is resultant of a constant ambient oven temperature and convective film coefficient . Assuming a polynomial temperature profile of the penetration thickness of the powdered material adjacent to the mold surface, they computed the amount of material adhering to the mold surface when the mold temperature reaches or exceeds the material stick temperature. By subtracting the predicted amount of powder that adhered to the mold surface, the new volume of the pool was determined. The analysis repeats until all material has left the pool.

Vanderbeck(30) modified Rao and Throne's models by improving some of the basic flow assumptions in the pool. As with Rao and Throne, Vanderbeck also assumes constant physical and thermal properties. Both authors disregard the fact of material that has traveled around the mold and has reentered the powdered pool and thus neglecting the insulating effect of the material adhering to the mold surface.

Throne(33) and Ahdout(34) modeled a rotational system which assumed the powdered material to be evenly distributed around the mold surface, neglecting the actual flow of the powder within the pool region and the mixing zone. Temperature dependent properties were calculated by using a linear interpolation between the known powdered state at the beginning and the final solid state at the end of the process.

The Throne, Rao, Vanderbeck and Adhout models all simulate in a very rough manner, a portion of specific phases of the rotational molding process. However, a complete simulation with temperature dependent properties to predict pool depletion and total densification has yet to be accomplished.

Mass Flow

In the study of mass flow in a rotating cylinder, Lehmverg, Hehl and Schugerl(41) performed experiments using color tracers placed in the pool of powdered material of a rotating drum having transparent ends for visual observations. As the drum rotated, the position of the tracers were recorded. Their results showed an area where most of the material remained stationary relative to the wall during mold rotation and a thin layer of material on top of the stationary pool that mixed as it rolled down the incline of the surface of the material. These results as well as results reported in references 53 and 54, fully concur with the brief description of the typical mass flow in rotational molding made in the introduction.

Sintering

The sintering, coalescence and fusion of particles have been studied in the field of drop coalescence, paint technology, ceramics, glass and polymers. References

1-28,35,51,53,54, and 56 were reviewed with respect to the sintering process of polymers. The following is a brief summary of the major applicable works.

Frenkel(1) analyzed the phenomena of "Cold Welding" of two amorphous spheres. Based on thermodynamic relationships, a relationship to predict the neck radius, x, of two coalesing spheres (Figure 2), is given by:

$$x^2 = 3a\gamma t/2\eta$$

where γ is the surface tension; η , is the Newtonian viscosity; a, is the radius of the sphere; and t is time.

To illustrate the application of Frenkel's equation for isothermal sintering for polyethylene, the properties of which are listed in Table 1, the following sintering equations are generated:

For 105 °C

$$\frac{x^2}{a} = 8.915 \times 10^{-6}\ t$$

where x and a are in cm. and t is seconds

For 150 °C

$$\frac{x^2}{a} = 6.549 \times 10^{-5}\ t$$

For 180 °C

$$\frac{x^2}{a} = 1.959 \times 10^{-4}\ t$$

The predicted results are plotted in Figure 3. Note the linear relationship between $\frac{x^2}{a}$ as a function of time that

Figure 2

SINTERING OF TWO ADJACENT SPHERES

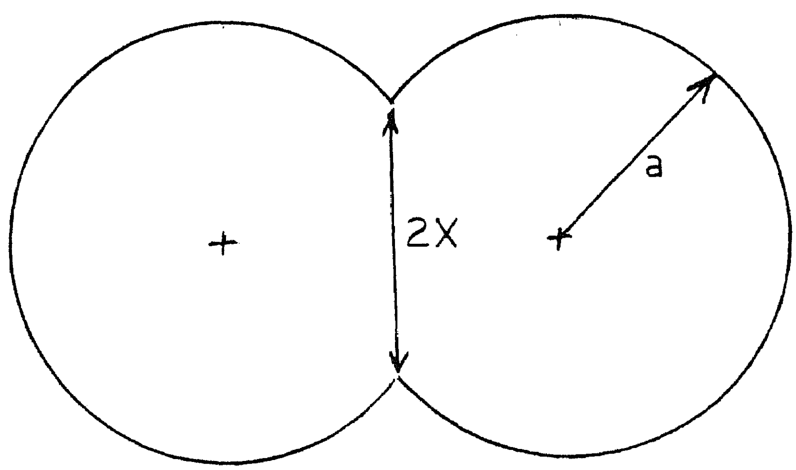

TABLE 1

PROPERTIES OF POLYETHYLENE

Surface Tension(18)

$$\gamma(T) = \gamma_0 - (\partial\gamma/\partial T)(T-T_o)$$

For Polyethylene

$$\gamma(T) = 31 - (0.058)(T-105)$$

Where:
γ is in dynes/cm
T is in degrees C.

Viscosity(6)

$$\eta = \eta_0 \exp\left\{\frac{-E}{R}\,\frac{(T - T_0)}{(T)*(T_0)}\right\}$$

For Polyethylene

$$\eta = 5.22 \times 10^6 \exp\left\{-19.583 + \frac{7402.5}{T}\right\}$$

Where: η is in Poise
T is in degrees K

Figure 3

PLOTS OF FRENKEL'S EQUATIONS FOR POLYETHYLENE

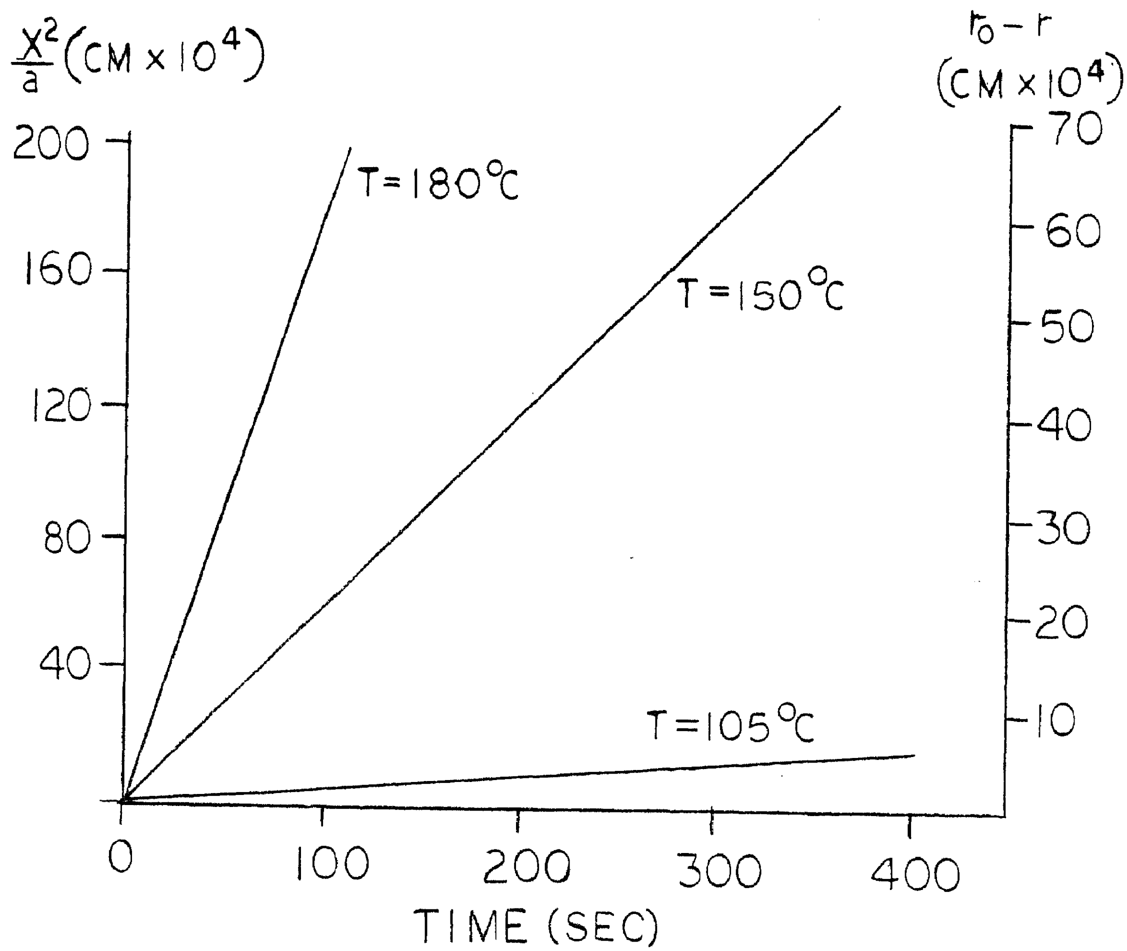

intersects at the origin.

Frenkel also derived the theory of densification of glass for the second stage of sintering where the voids become individual bubbles that slowly reduce in diameter. The equation for the collapse of an individual bubble is given by:

$$r_o - r = \frac{\gamma}{2\eta} t \qquad \text{(eq. 2)}$$

where r_o is the original pore radius at time zero and r is the radius at time t. Using the polyethylene properties in Table 1, the collapse of the voids for the three temperatures used are as follows:

For 105 °C

$$r_o - r = 2.97 \times 10^{-6}\ t$$

For 150 °C

$$r_o - r = 2.18 \times 10^{-5}\ t$$

For 180 °C

$$r_o - r = 6.53 \times 10^{-4}\ t$$

These equations are plotted in Figure 3.

Frenkel's equation(eq 1) was experimentally confirmed by Kuczynski(2) where glass beads were heated on top of a glass plate having the same composition as the beads. After heating, the samples were rapidly cooled and mounted in Bakelite. The dimensions were measured and plotted in

Figure 4

KUCZYNSKI'S RESULTS OF SINTERING GLASS SPHERES

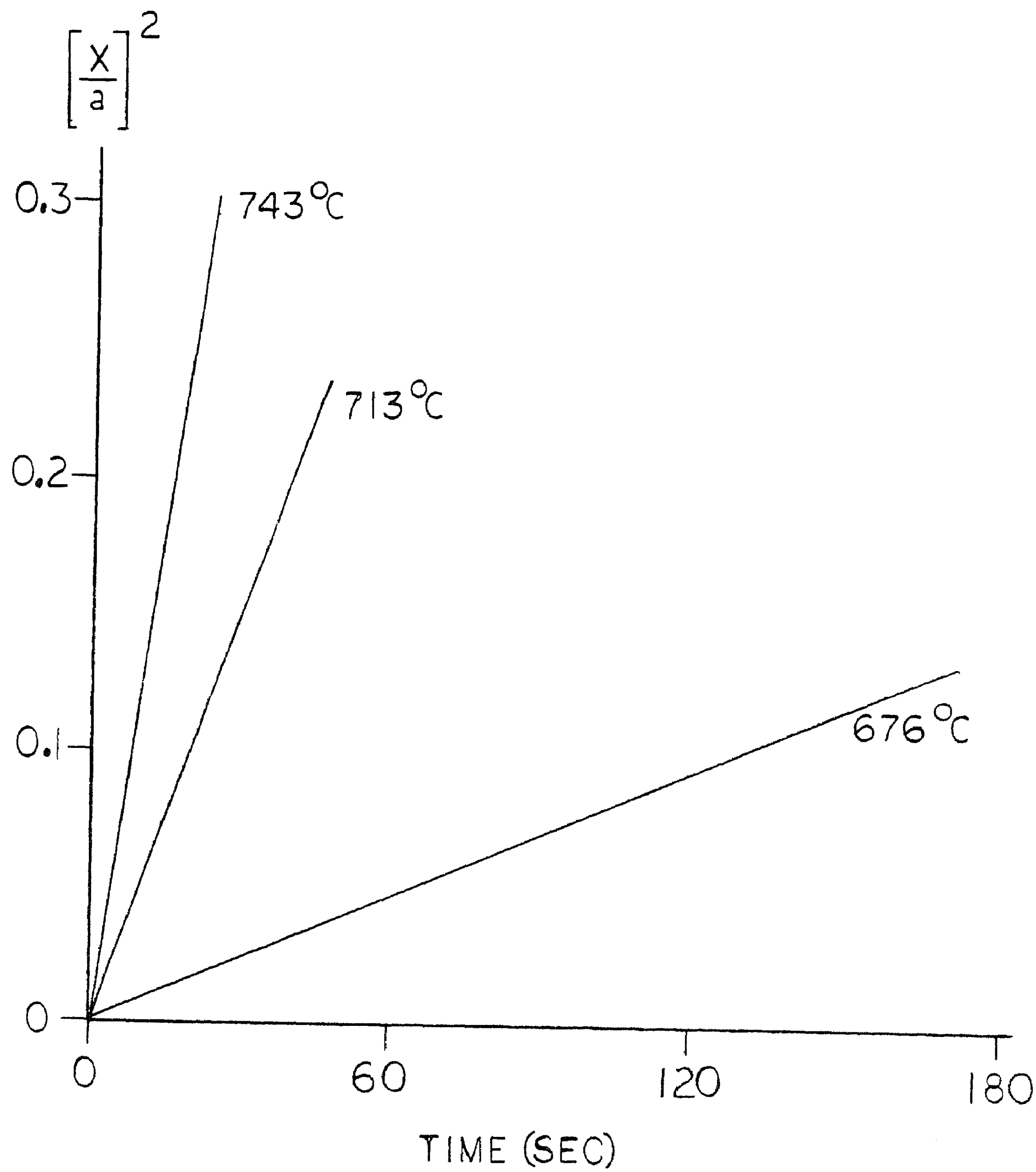

Figure 4. The experimental results confirmed the linear relationship of Frenkel's equation intersecting at the origin. Kuczynski along with Zaplatynskyj(13) confirmed Frenkel's colapsing theory, Equation 2, by heating capillary tubes and measuring the collapse of the internal diameter as a function of time.

Dillion, Matheson and Bradford(5) investigated the sintering of synthetic latex particles. Experimental results indicated that the coalescence process occurs by the same mechanism as was described by Frenkel equation.

Kuczynski, Neuville and Toner(3) performed the same type experiment as Kuczynski(2) using Poly(methy) Methacrylate (acrylic). Figure 5 presents the experimental results. They found for this polymer, Frenkel's equation(eq. 1) is inadequate. The following empirical equation was then correlated:

$$\left[\frac{x^2}{a^{1.02}}\right]^P = F(T) \quad t \qquad \text{(Equation 3)}$$

where F is a function of temperature only and P is the slope of the curve in Figure 5. Lontz(4) replots Figure 5 using $\frac{x}{a}$ for the Y axis (as opposed to $\frac{x^2}{a}$) versus time(Fig. 6). It is obvious from this graph that the y intersection of the linear curves tend to increase with temperature giving an indication of a time delay to the

Figure 5

NECK GROWTH OF PMMA SPHERES

$\frac{X^2}{a}$ vs TIME

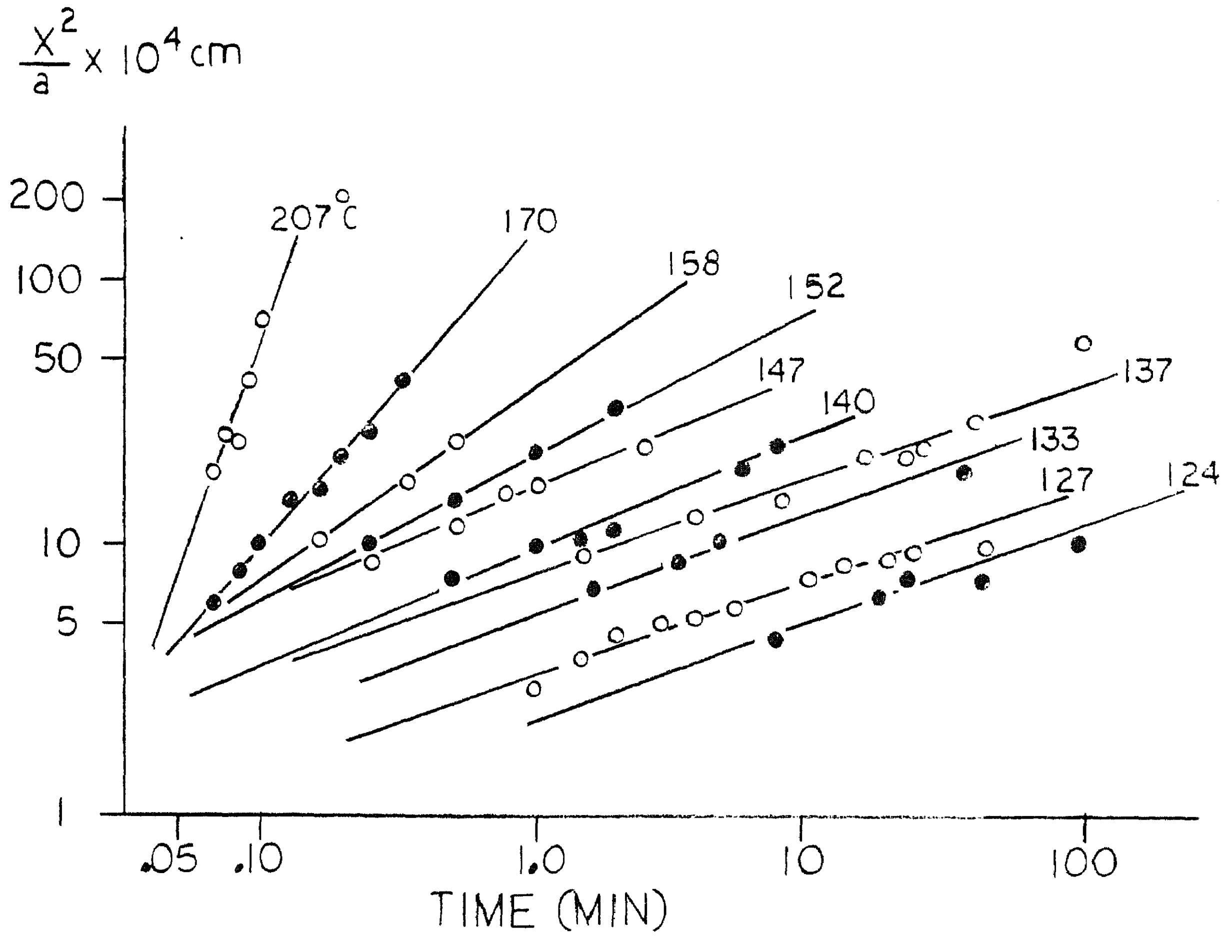

Figure 6

NECK GROWTH OF PMMA SPHERES

$\frac{X}{a}$ vs TIME

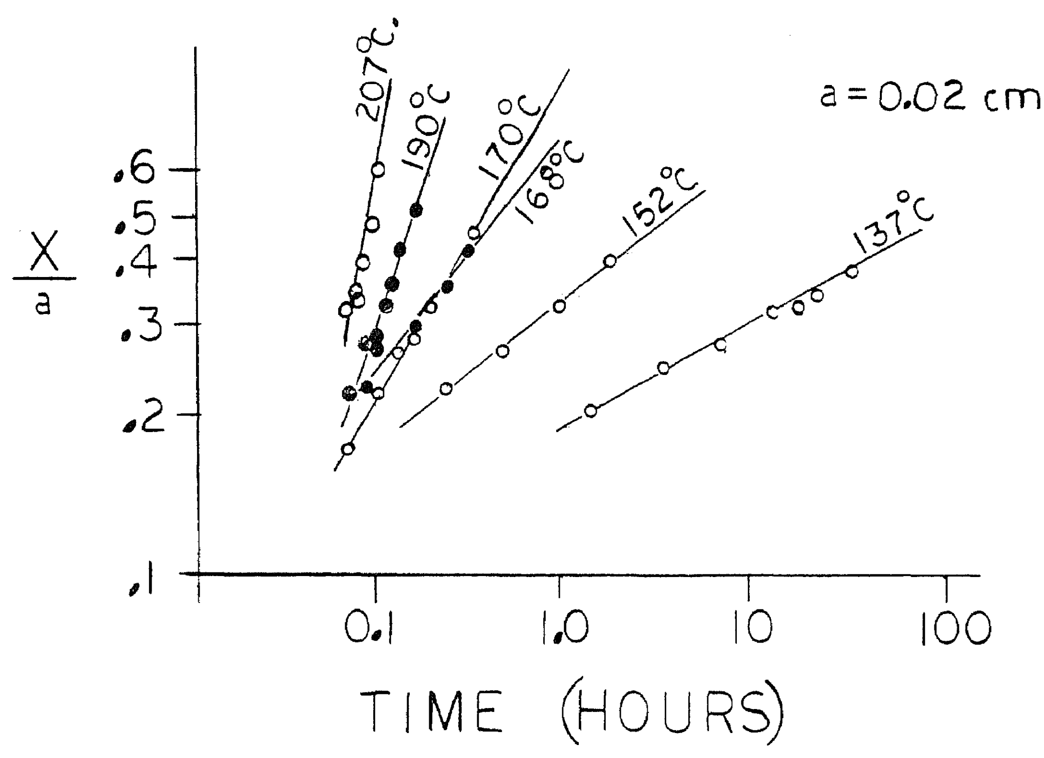

sintering process. This is not unexpected due to the transient temperature response of the spheres.

Shonhorn, Frisch and Kwei(10), studying the kinetics of wetting of surfaces by polymer melts, showed that polymers at high temperatures exhibited a shifted Frenkel curve, as is evident in the Kuczynski, Neuville and Toner's plots(Figure 5).

Lontz(4) developed a model of sintering between two viscoelastic spheres yielding the equation:

$$\frac{x^2}{a} = \frac{3t}{2\eta} \frac{1}{1 - \exp(-t/\lambda)} \qquad \text{(Equation 4)}$$

where the second right hand term is a correction factor to the Frenkel equation to account for viscoelastic effects. The term, λ ,is a relaxation time constant. The relaxation time constant is determined experimentally for each resin and temperature. Its significance can be better understood by examining the four element Maxwell-Voigt model(Figure 7) for a viscoelastic body.

The spring E_1 in Figure 7 act as the Hookean repsonse while the dashpot, η_3, corresponds to the Newtonian fluid response. The spring, E_2 , and dashpot, η_2, represent the

Figure 7

FOUR ELEMENT MAXWELL - VOIGHT MODEL

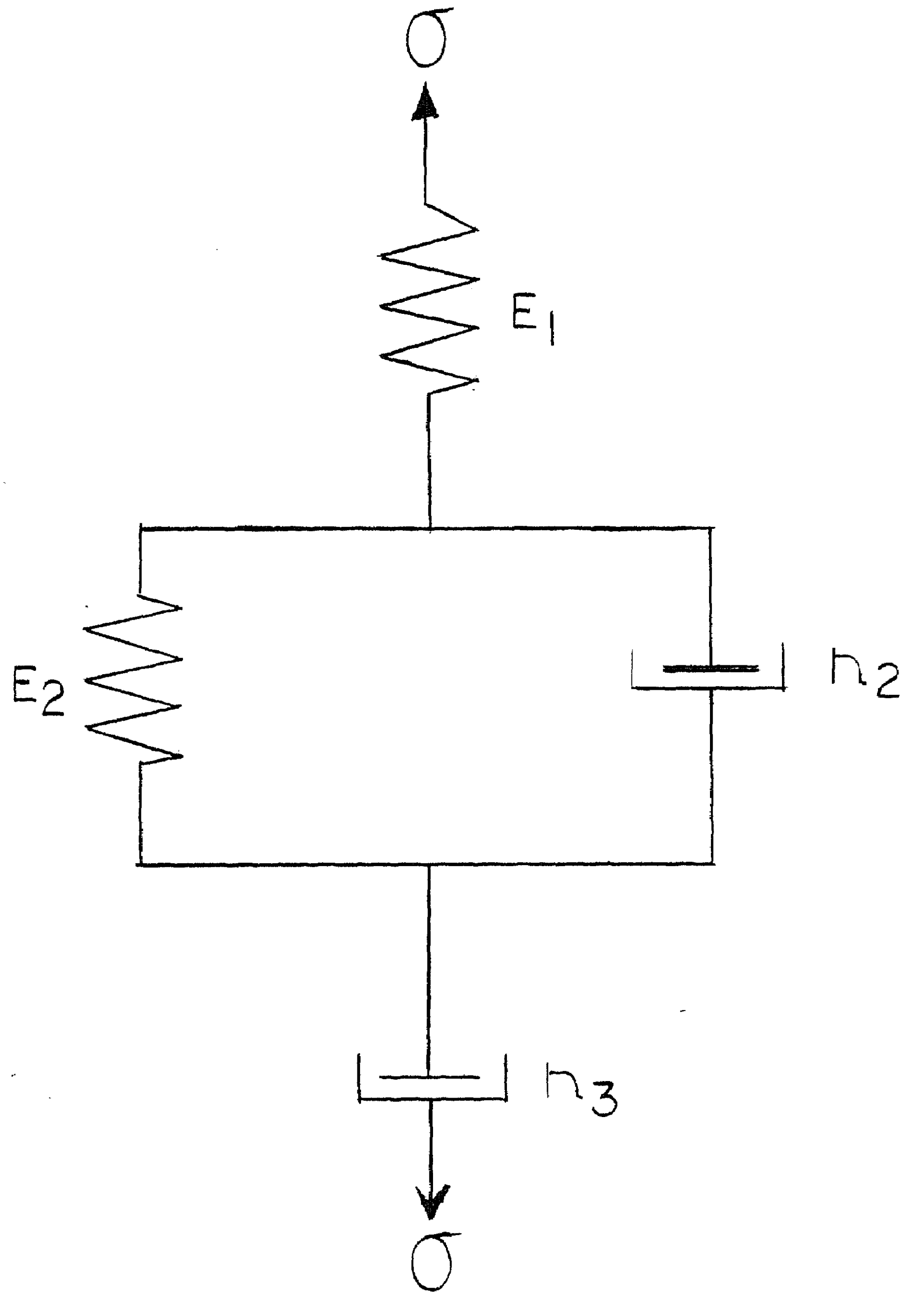

retarded elastic response of the polymer molecules. When the stress, σ , is applied, E_1 and η_3 react instantly while because of the physical arrangement, E_2 and η_2 have a delayed response. Together the system has a viscoelastic effect. The ratio of η_2 to E_2 is the relaxation time constant, λ ,or:

$$\lambda = \eta_2 / E_2 \qquad \text{(Equation 5)}$$

Narkis(8) also studied the sintering of closely packed Poly(methyl) Methacrylate spheres in a circulated air oven. Experimental results showing neck radius verus time for four temperatures are shown in Figure 8. The shapes of the curves were very similar to the theoretical curves given by Lontz's equation(Eq. 4)

An examination of these curves, show a non-linear portion is followed by a linear portion. The non-linear portion is due to the viscoelastic effect (E_2 and η_2 of our model) after which the relaxation term approaches unity reverting the Lontz equation to a shifted Frenkel equation (the linear portion). Note that the Kuczynski, Neuville and Toner(3) curves only showed the linear portion of the curves. They neglected to realize any relaxation effect but only stated that Frenkel's equation was inadequate. Also note, the viscoelastic effect is shortened as would be expected due to greater moleculer mobility as the sintering temperature is increasd.

Figure 8

SINTERING OF PMMA SPHERES BY NARKIS(8)

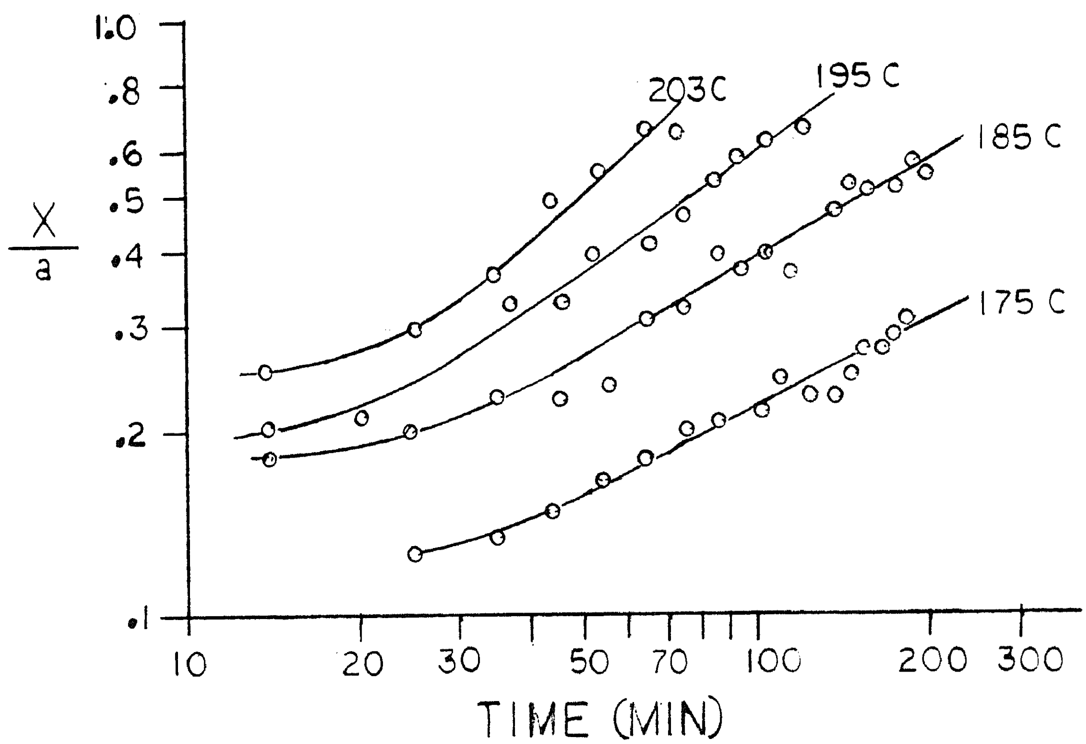

Steiner, Manson and Nippert(9), using the basic differential Frenkel equation, numerically integrated the equation using the exact value for the $\sin\theta$ rather than Frenkel's assumption of $\sin\theta = \theta$. (Only valid for small values of θ). Numerical results of $\frac{X^2}{a}$ versus time showed a better correlation to their experimental data for viscous sintering. A viscoelastic sintering equation which included a retardation time factor similar to that developed by Lontz was also derived.

Menges and associates(20) developed an isothermal growth correlation based on surface tension, neck curvatures and inner frictional forces. Theoretical results agreed with their experimental results.

Rosenzweig and Narkis(21) performed a study of dimensional changes of sintering particles. Based on the Frenkel's sintering model(Figure 9), the authors derived the following relationships of two sintering spheres:

$$X = (2aZ - Z^2)^{0.5} \qquad \text{(Eq 6)}$$

$$L = 2a - 2Z \qquad \text{(Eq 7)}$$

$$4a^3 - 3Z^2 a + Z^3 - 4a_o^3 = 0 \qquad \text{(Eq 8)}$$

Figure 9

GEOMETRY OF TWO SINTERING SPHERES

(FRENKEL'S MODEL)

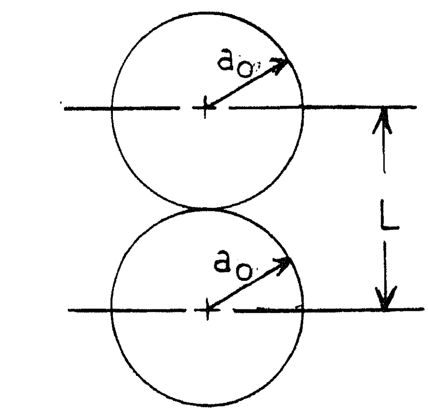

Initially - Two spheres with length L, between centers

a_o = initial radius of two spheres

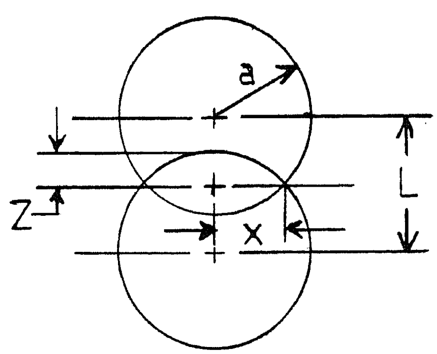

During sintering neck radius x, is formed as lenth L, decreases

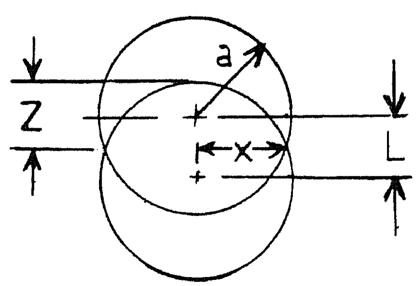

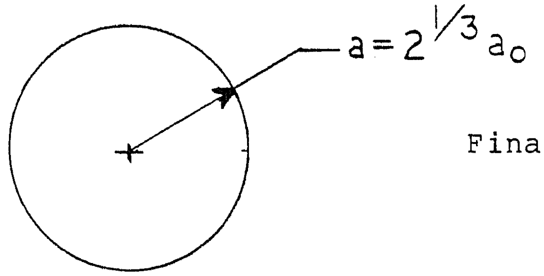

Final sintering results with sphere radius becoming equal to $2^{1/3} a_o$.

where: x = neck radius

a_o = original sphere radius

a = sphere radius during sintering

$2*Z$ = penetration depth of two sintering spheres

L = length between the centers of the two sintering spheres

These equations will be later used in this work to determine the density of the powdered material as a function of distance between centers of sintering spheres. The results were used to correlate the density of a group of spheres as a function of neck radius.

Thermal Conductivity

Progelhof, Throne, and Ruetsch(33) performed an in depth investigation of published articles studing the thermal conductivity of foamed, powdered or composite materials. In addition to the articles reviewed by Progelhof, Throne, and Ruetsch, references 34-46 were also reviewed. In most correlations evaluated, the values of k_c and k_d (where k_c = thermal conductivity of the continuous material and k_d = thermal conductivity of the discrete material) must be determined. In the case of rotomolding, until the material starts to stick to the mold, it is assumed that the polymeric material is the discrete phase that is surrounded by a continuous phase of air. Upon the commencement of the fusing process, the polymeric material is assumed to be the continous phase surrounding the discrete phase, air.

Figure 10 illustrates the Maxwell Model of thermal conductivity as reported by Progelhof, Throne and Ruetsch (35) of polyethylene and air. The top curve represents the predicted thermal conductivity with air as the discrete phase while the bottom curve represents polyethylene as the descrete phase. The dotted lines labled A', B' and C' represents possible routes where air originially the continuous phase changes over to the descrete phase as is expected to occur in the rotational molding process.

The original intent of this investigation was to use one of these equations to predict the thermal conductivity of the powdered material while in the pool. Using this value, new values as a function of temperature and neck growth would be estimated. However, in performing the thermal conductivity calculations, a great variance was found. Figure 11 shows six thermal conductivity estimate equations and the results using air as the discrete material and then as the continuous material. The results show a variance of two magnitudes. To avoid justifying one value over another, this investigation will use experimental data to determine the actual value. The experimental procedures are discussed latter.

Figure 10

MAXWELL'S MODEL FOR THERMAL CONDUCTIVITY

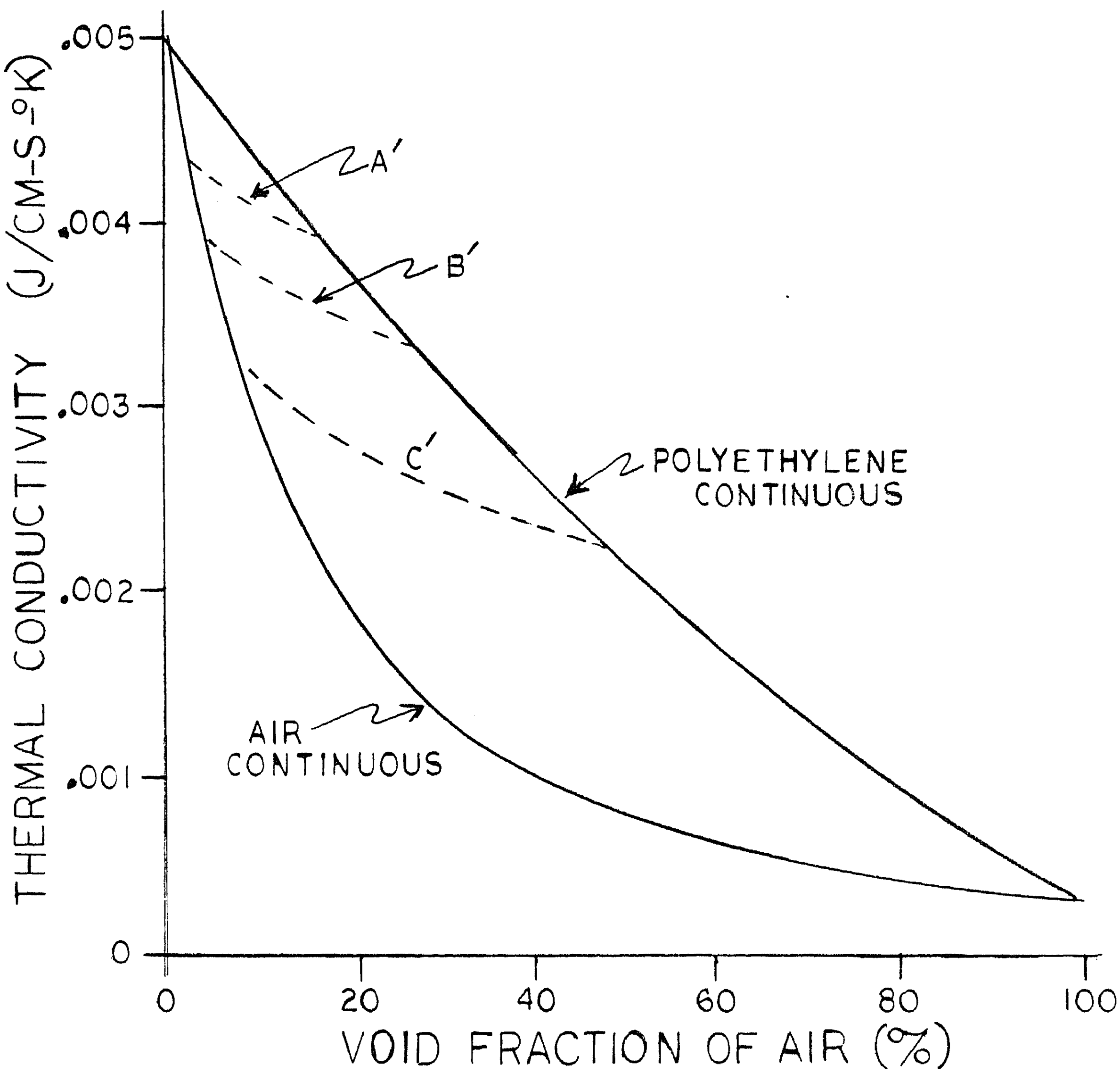

Figure 11

COMPARISON OF VARIOUS

VARIOUS COMPOSITE THERMAL CONDUCTIVITY EQUATIONS

	COMPUTED THERMAL CONDUCTIVITY (J/cm-sec-K)	
Descrete Material	Polyethylene	Air
Continuous Material	Air	Polyethylene
Fraction of Continuous Material	0.58	0.42
EQUATION		
Yagi - Kunni	9.90 E-05	3.24 E-04
Maxwell	4.98 E-04	2.52 E-03
Lewis and Nielson	2.76 E-03	1.10 E-02
Russel	1.08 E-03	2.66 E-03
Geometric Mean	1.39 E-03	1.39 E-03
Series	2.96 E-03	2.96 E-03

Thermal Conductivity of Polyethylene = 4.93 E-03 J/cm-s-K
Thermal Conductivity of Air = 2.42 E-04

NOTE: Equations used in the computations of the thermal conductivity taken from Reference 35.

III. STATEMENT OF THE PROBLEM

All previously published investigations of rotational molding were based upon models that had limited restrictions. One assumed constant physical and thermal properties, while the other assumes the material already distributed around the mold. Investigations dealing with sintering(densification) of particles all involved an isothermal process. In rotomolding, the "sintering" process starts with polymer powder being placed in a mold at ambient temperature. The mold is then heated as it is rotated in an oven. As the temperature of the polymer reaches the stick temperature, it begins to adhere to the mold wall. This process is continued until all powder has adhered and then begins to densify.

This dissertation is an investigation of the rotational molding process. It includes an analysis of the material flow in the pool and an investigation of the heating and densification process. It does not include the cooling portion of the cycle. A theoretical simulation model of the rotational molding process was then derived to predict pool depletion and densification times using temperature and time dependent properties. In lieu of justifying the use of one of the many composite thermal conductivity equations (reviewed earlier) over another, an experimental procedure was developed in conjuction with a small computer program for determining the actual powder thermal conductivity. In the conculsions, the theoretical results predicted by this new model are compared to the actual measured rotational molding pool depletion times and with the other previous simulation results. The densification times between the simulations developed are then compared with the earlier simulation results of Throne and Adhout.

IV. MASS FLOW IN ROTATIONAL MOLDING

In order to properly simulate the rotational molding process, an understanding of the mass flow within the mold cavity during that process is essential. Consider a simple cylindical mold cavity as shown in Figure 12 rotating in a clockwise direction. The angle theta (θ) is the included angle of the powdered material in the stationary zone of the pool. The angle phi (ϕ) is the angle that the stationary zone maintains as the mold rotates. This angle (ϕ) is a function of the material characteristics, the rotational speed, and the coeficent of friction of the mold surface. Based on Vanderbeck's experimental results, it has been shown that the angle (ϕ) remains constant during the depletion of the pool.

Consider a line segment A-B which begins at the center of the cord formed by the surface of the stationary pool of powdered material and ends at the mold surface. If the mold is rotated for a time interval(DT), the line segment is also rotated to the postion A'-B' shown in Figure 12. The area(volume) included by the two line segments and the mold surface is the amount of material that has entered the stationary pool leaving the free-falling zone during that time interval. This section is labled A-1.

Figure 12

ENTERING MASS FLOW IN ROTATIONAL MOLDING

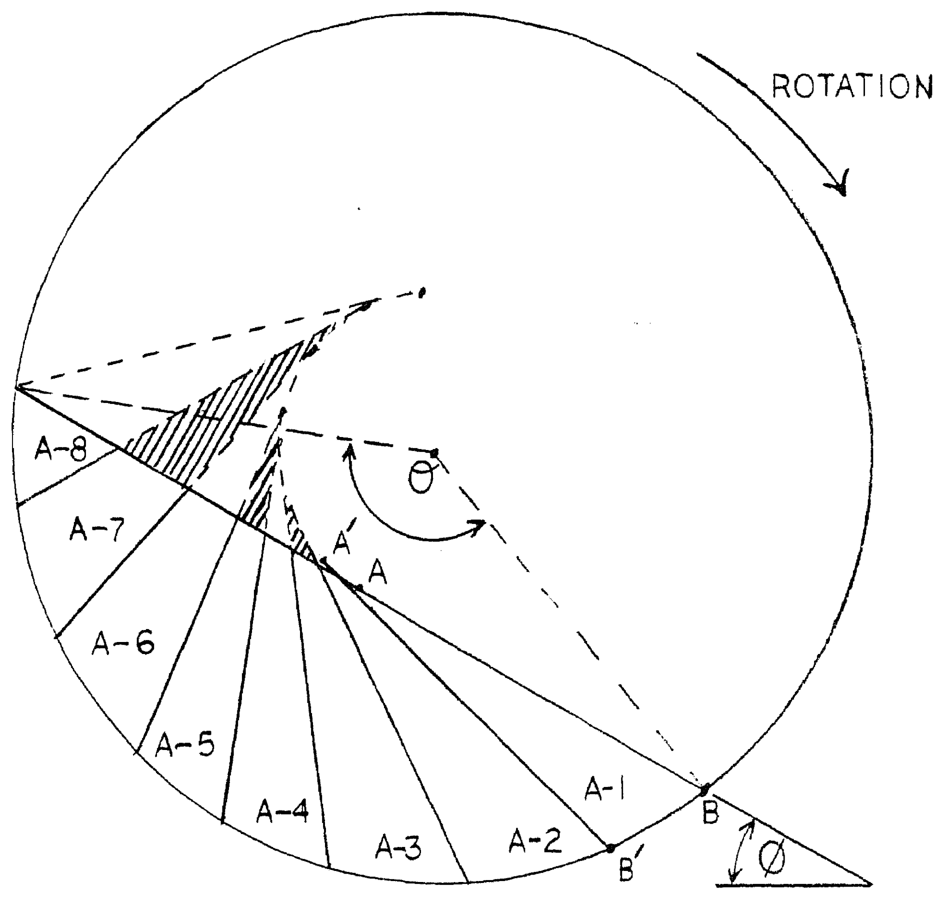

Allowing the mold to rotate for another time increment will move Area A-1 to the location of Area A-2 as shown in Figure 12. Note that the shift of A-1 has caused a portion of the area to protude past the surface line B-C of the stationary region. This outside area represents the amount of material of Area A-1 that has left the stationary pool and reentered the free-falling region during that time increment.

Rotating the mold by another time increment will move Area A-2 to the position of A-3. Again, a portion of the area, in the movement from A-2 to A-3, has exited Area A-2 of the stationary pool region and reentered the free fall zone during that time increment.

Continuing the rotation of the mold will cause the Area A-3 to move to A-4, then to A-5 and so on to A-8. After A-8 all material in the area that started at A-1 has completely exited the stationary pool. The amount of material that exits the stationary pool at each time interval for each area is equal to the amount of area passing through the pool surface Line B-C during that time increment.

From the preceding analysis, it is evident that the time length that the material remains in the pool depends on its location or position while entering the pool.

Material entering near the center surface of the pool (point A) remains in the pool for a short time duration while material entering near the mold surface remains longest in the pool.

The total mass leaving at each time interval is the amount that passes through line segment B-C in Figure 13 to join the free-falling powder. Moving line segment C-A in the opposite direction of the rotation for one time interval of rotation results in the postioning of that line labled C'-A' in Figure 13. The area bounded by line segments C-A, C'-A' and the mold surface is the material exiting the stationary pool in the next time interval. Continuing back at one time increment movement intervals, the areas shown are the areas leaving in the succeding time intervals. Some areas have a portion of their areas above the pool surface line meaning that this portion of material has not yet entered the stationary pool. Notice that the area shown leaving the stationary pool in the Figure is the same amount of area that had entered in Figure 12.

Figure 14 combines Figures 12 and 13 into a complete illustration of the mass flow within the stationary pool zone . In this figure an arc time length of eight time increments(intervals) were used. It can be seen that the material entering in the center(area labled 1) remains in

Figure 13

LEAVING MASS FLOW IN ROTATIONAL MOLDING

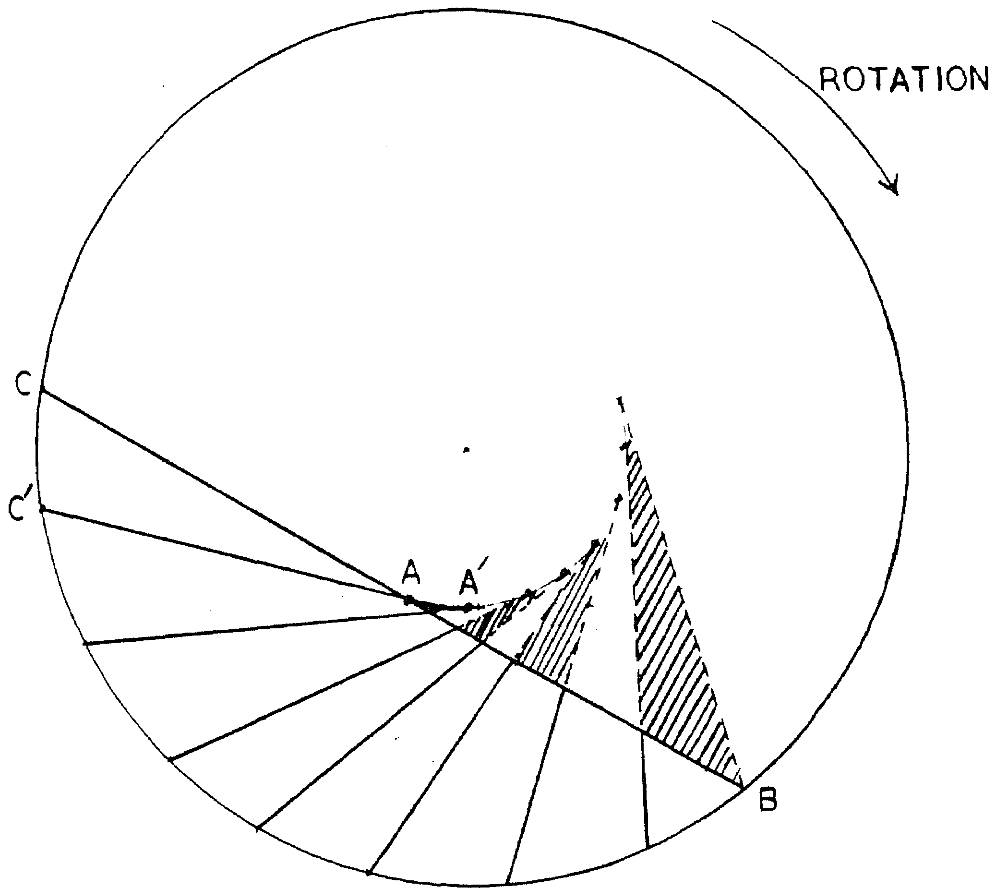

Figure 14

TOTAL MASS FLOW IN ROTATIONAL MOLDING

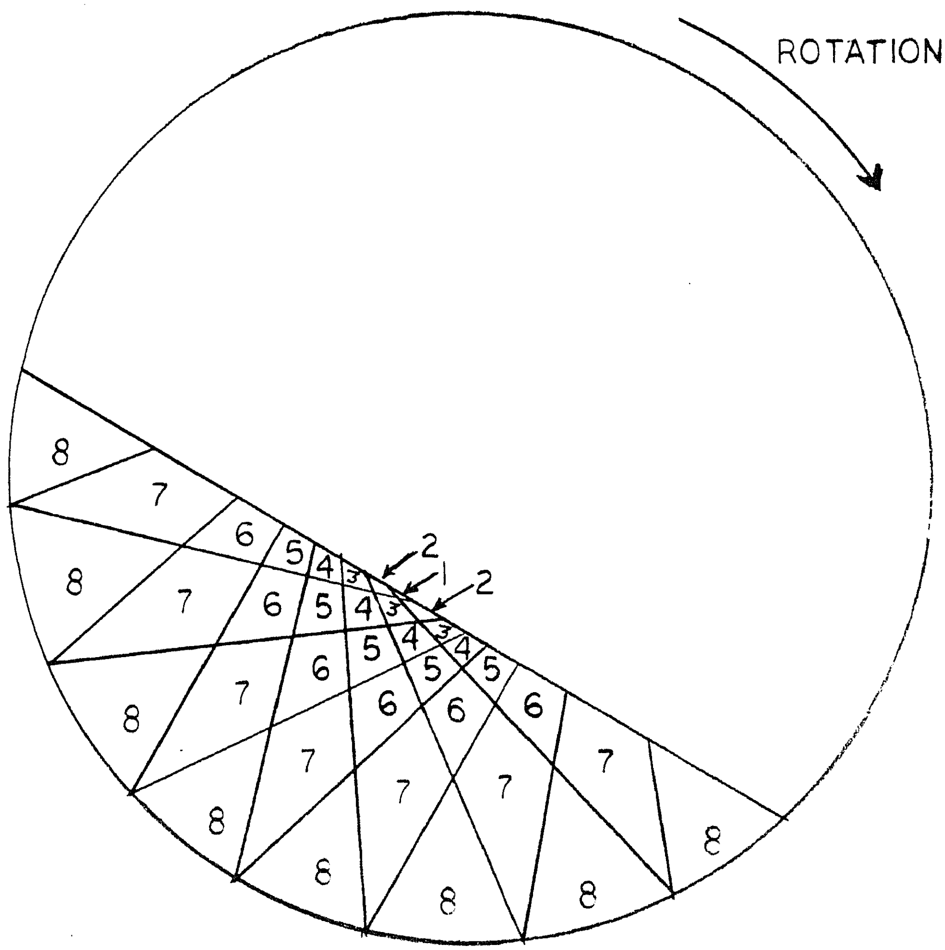

the pool for only one time increment while the areas labled 8 remain for all eight time increments. Those particles in between remain according to their relative position from the center.

It is assumed that after the material leaves the stationary pool, the material begins to fall down and mixes physically and thermally until it again rejoins the stationary pool and then repeats the cycle.

In addition to being rotated, the material is also being heated by the mold surface. When the mold reaches or exceeds the "stick temperature", the portion of material that is at or above that particular temperature will stick to mold wall, thus deminishing the amount of material in the pool. This process will continue until all material in the pool has left the pool by sticking to the mold surface.

V. ANALYSIS OF THE HEAT TRANSFER FOR SIMULATION ASSUMPTIONS

In the rotational molding process, the mass of material in the stationary pool is assumed to be heated by conduction from the mold surface. The time increment that an individual element is in contact with the mold surface is given by:

$$t(ms) = \theta / \omega \qquad \text{(Eq. 9)}$$

where, t(ms) = Contact time of an element with the mold surface.

θ = angle theta(Figure 13)

ω = angular velocity

Using typical values of an angle theta of 90 degrees, 7 RPM will result in a element contact time of 2.142 seconds.

During this contact time, the thermal penetration depth can be approximated by the results for a semi-infinite solid having a constant initial temperature and being subjected to sudden change in surface temperature:

$$T(x,t) = \operatorname{erf}\left\{\frac{X}{2 * SQR(\alpha * t)}\right\} *(\ Ti-Ts\ ) + Ts \qquad \text{(Eq. 10)}$$

where: T(x,t) = Temperature at time t, at a distance x from the surface

Ti = Original Initial temperature of the solid

Ts = New surface temperature

x = distance from surface

α = thermal diffusivity

t = time

Rearranging the above equation and solving for the distance, x will result in the equation:

$$x = 2 * SQR(\alpha *t)*erfc((T(x,t)-Ts)/(Ti-Ts)) \quad \text{(Eq. 11)}$$

The penetration depth will be at the position where T(x,t) = Ti. The inverse error function has the numeric value of 3.60. The equation reduces to :

$$x = 7.2 * SQR(\alpha *t) \quad \text{(Eq. 12)}$$

Using the numerical value of the thermal diffusivity of the High Density Polyethelyne powder as 1.7E-03 sq cm/sec, a contact time of 2.142 seconds will result in a penetration depth of 0.434 cm.

Since this penetration depth is very small compared to the depth of the pool, and that this penetration occurs only in the subareas adjacent to the mold surface, the computer simulation can use a rectangular system having the same number of columns as wedges in the actual system. This approximation will be in error when the pool is in the last phases of depletion. A comparison of the two systems is shown in Figure 15.

The rectangular system used in the computer simulation

Figure 15

COMPARISON BETWEEN THE ACTUAL ROTATIONAL MOLDING AND THE COMPUTER SIMULATION MODEL

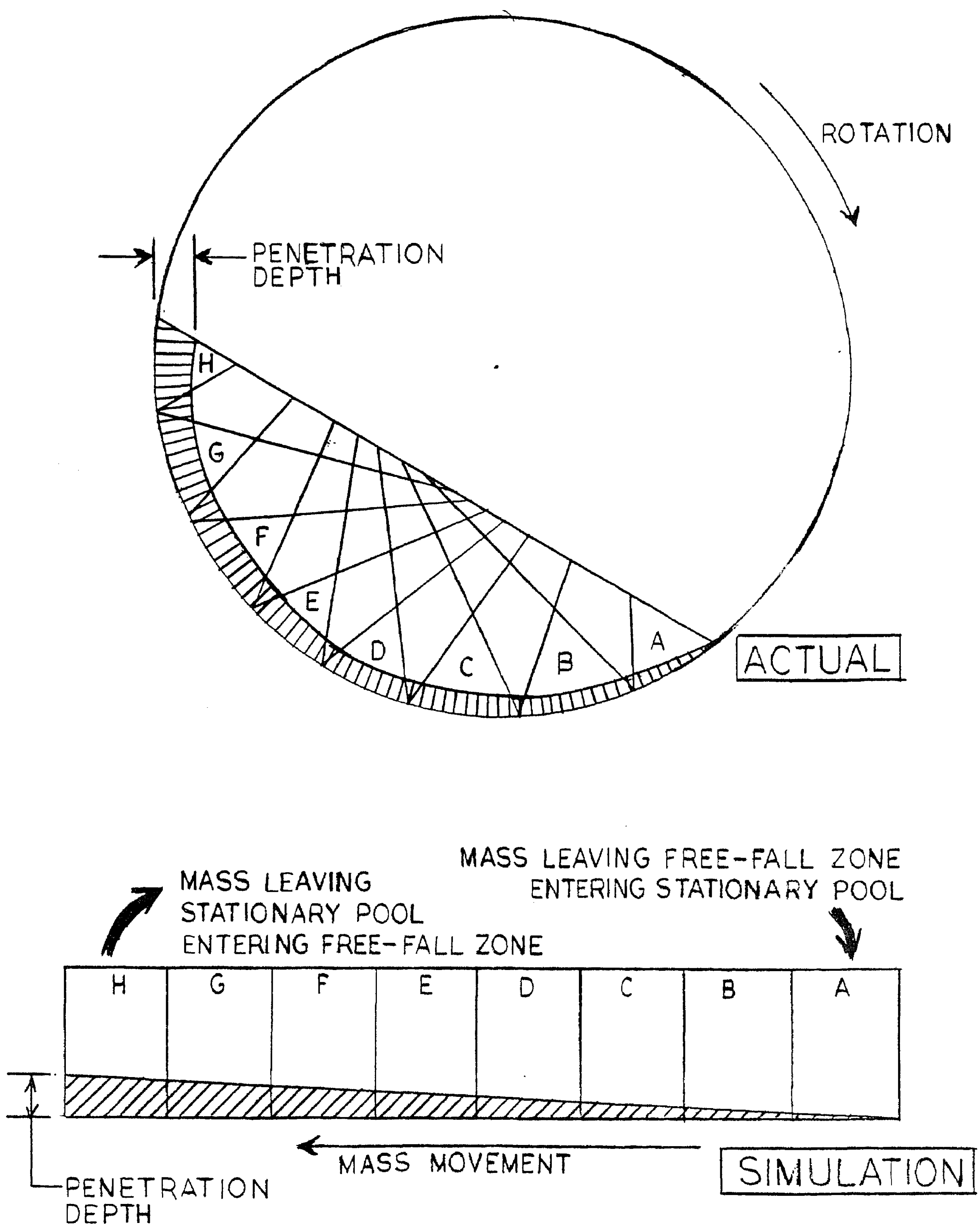

has a total area(or volume) equal to the area in the actual system and also a column width equal to the arc length of one wedge.

In this simulation, the material enters at position A in Figure 16 at a temperature equal to that of the free-falling powder region. The temperature profile for one time increment is then calculated. The material is then shifted over one position (labled B) simulating rotational movement and a new temperature profile is calculated for the next time interval using the old profile as its initial temperature.

This process is continued for all postions(columns A-H). After the last position (H),the material is assumed to leave the stationary pool and join the free-falling powder region. It is assumed in this phase of the model that all of the particles are thermally mixed. The average or equilibrium temperature of the powder in the free fall zone is computed by using a mass weighted average of the average temperature of the mass entering the free-falling region with the remaining material in this region, or:

$$\overline{T} = \frac{\overline{T_e} * M_e + \overline{T_{FF}} * (M_{FF} - M_L)}{M_{FF}} \qquad \text{(Eq. 13)}$$

where: $\overline{T}$ = new ave temperature of free falling region.

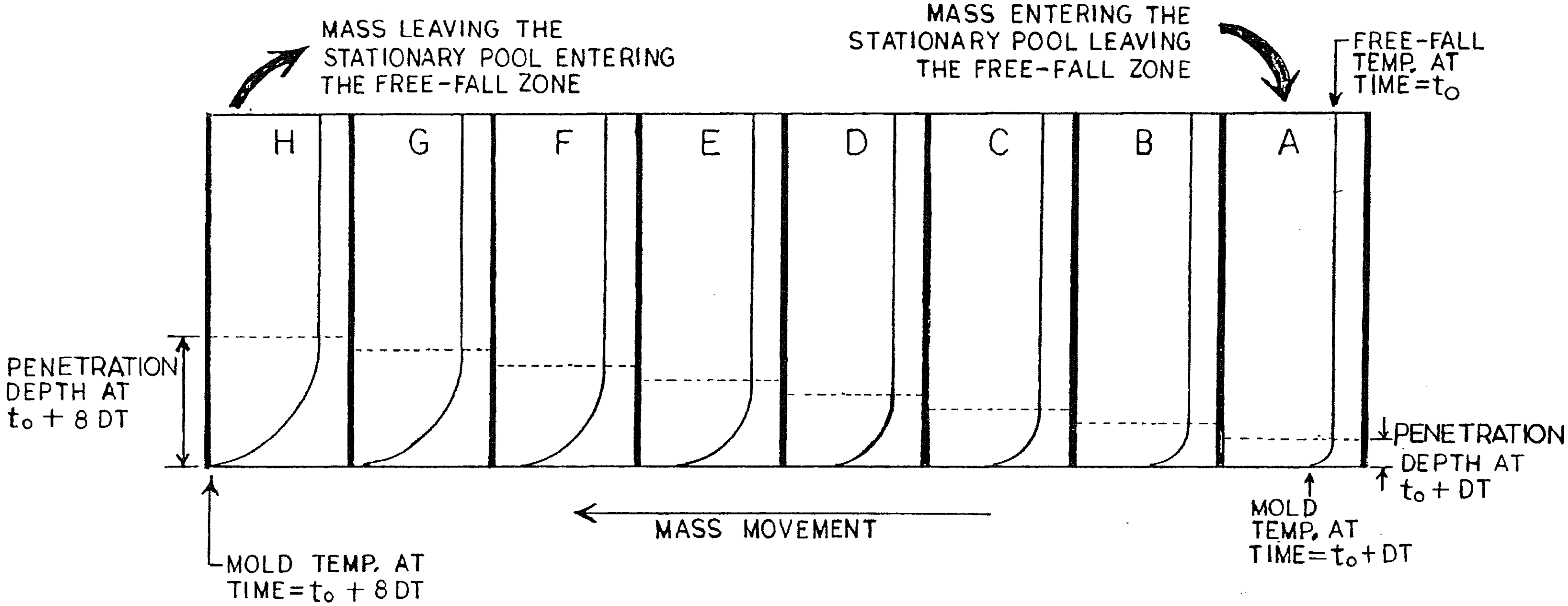

FIGURE 16

TEMPERATURE PROFILE DURING 8 TIME INTERVALS

$\overline{T_e}$ = new ave. temperature of mass entering

M_e = mass entering

$\overline{T_{FF}}$ = previous average temperature of free falling region

M_{FF} = previous amount of mass in free falling region

M_L = amount of mass leaving which is equal to the mass entering, M_e .

Simplifing:

$$\overline{T} = \overline{T_e} * \frac{M_e}{M_{FF}} + T_{FF} * \left[1 - \frac{M_e}{M_{FF}}\right] \qquad \text{(Eq. 14)}$$

The average temperature of the mass entering the free falling region, $\overline{T_e}$, is determined by the same mass weighted formula using the temperatures and mass within the penetration depth and that outside the penetration depth.

After the free falling region, the mass now re-enters the stationary pool at the present mixed mean free-falling temperature and the heating cycle described earlier is repeated.

When the polymer powder in contact with the mold surface attains the stick temperature, material above this temperature will adhere to the mold wall causing the powdered pool to become smaller in size. The simulation will still use the same amount of wedges (columns), however, the time increment (interval) will become smaller to compensate for the smaller contact time.

The cycle is repeated until all material has left the powdered pool and adheres to the mold.

VI. THEORETICAL MODEL USING NODAL ANALYSIS

In the theoretical analysis presented in this dissertation, a numerical method will be used. The geometry of the specimen is subdivided into small but finite subvolumes of thickness of ΔX. For each subvolume there is located a center nodal point which has been assigned a reference number, Figure 17. Note that the exterior subvolumes has a thickness of 1/2 ΔX with its node located at the surface.

In this actual transient heat transfer process, the temperature profile within a subvolume varies with position and time. However for this simplified model it was assumed that the temperature of each subvolume can be denoted by a nodal "mixed mean" or "equilibration" temperature. Thus the temperature within a node is assumed to be only a function of time. The mixed mean or equilibration temperature of the element is defined as the temperature the element will attain if all the internal energy of the element was distributed evenly throughout that element.

The temperature of each subvolume is assumed to be represented by the temperature of the node. It is further assumed that the rate of energy transfer between adjacent nodal points is approximated by the steady-state conduction

Figure 17

NODAL CONVENTION

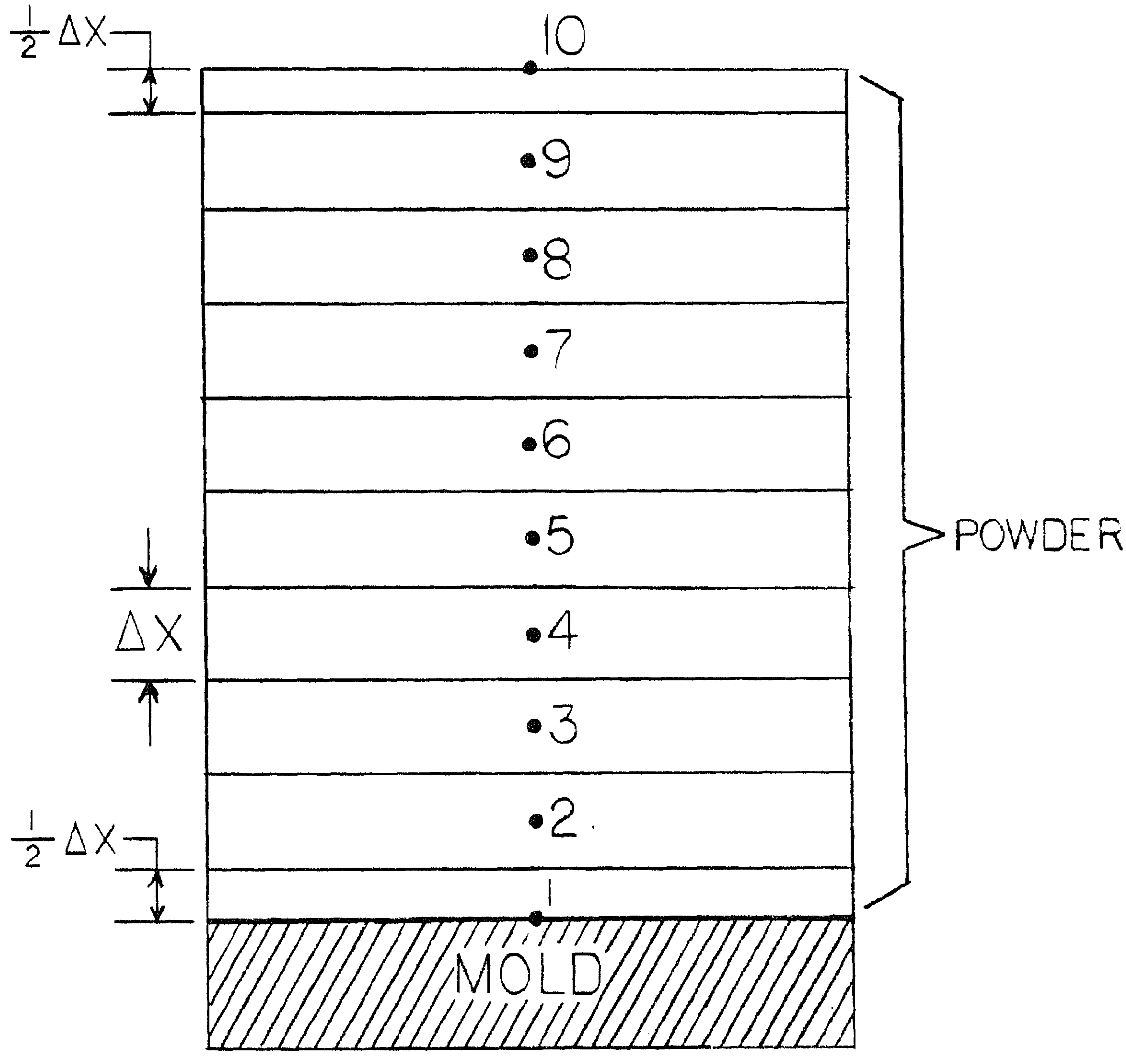

equation using the nodal temperature values as the descriptive temperature between the nodes. Thus in this model, a discontinuous temperature profile is being used to approximate the actual temperature profile (Figure 18). It is obvious that as the subvolumes become smaller, the approximate temperature profile will approach the actual temperature profile.

Writing an energy balance on node i results in the following equation:

$$q(in) - q(out) + q(generated) = q(stored) \qquad \text{(eq 15)}$$

Or:

$$\sum q_i + q(generated) = m_i C_i \frac{dT}{dt} \qquad \text{(eq 16)}$$

where: q_i = heat flow entering node i

m_i = mass of subvolume i

$\frac{dT}{dt}$ = the time derivative of temperature of subvolume i

The initial temperatures of all nodes were constant room temperature and the mold surface was subjected to a changing temperature. Because the temperature change will only occur within the penetration depth, nodal equations must then be made to include this depth. Temperatures of nodal volumes outside the penitration depth will not change, thus performing computations of these nodes are needless and a waste of valuable computer time.

Figure 18

APPROXIMATION OF THE TEMPERATURE PROFILE

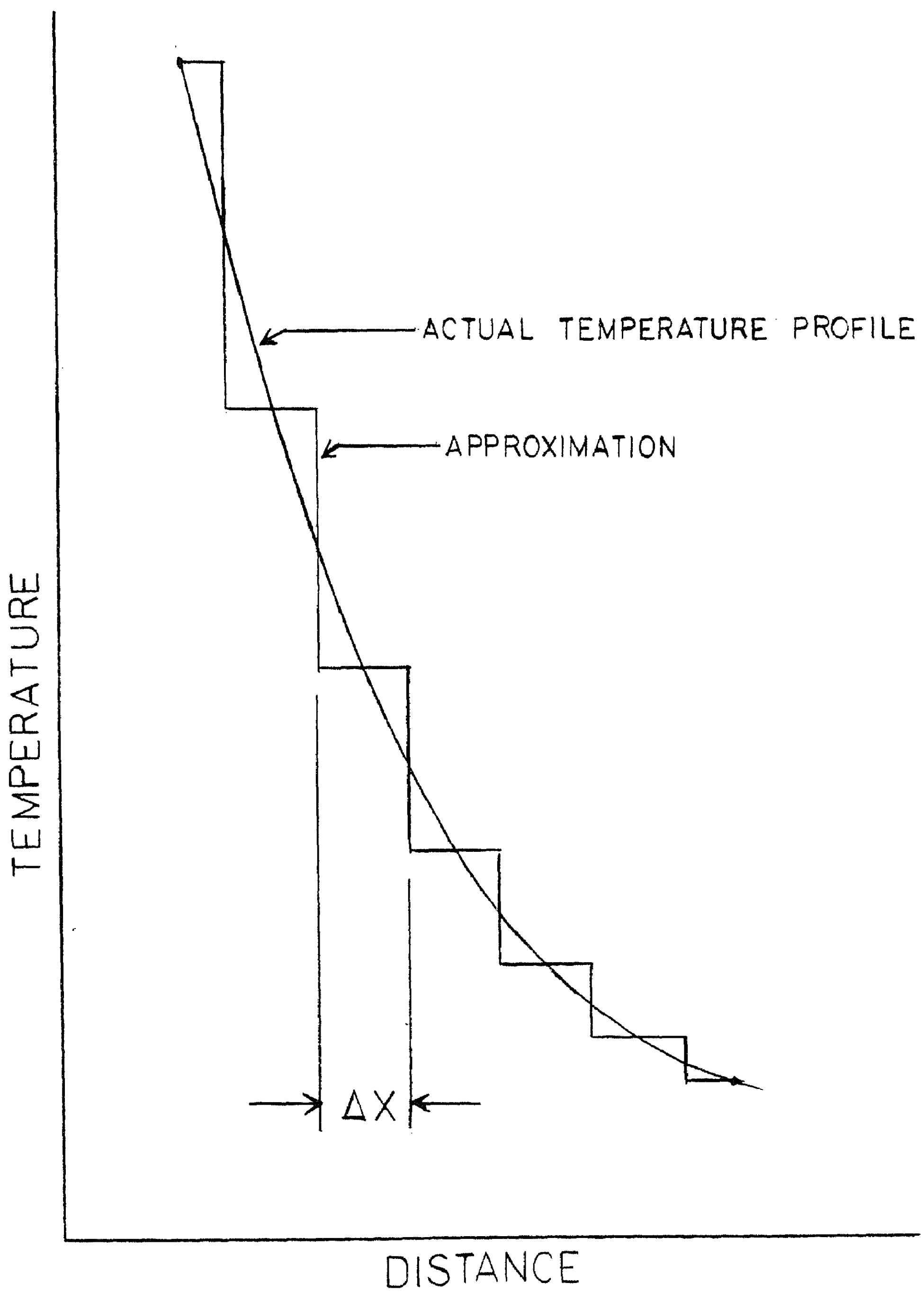

Figure 19 shows a typical stationary pool that is divided into eight wedges with each wedge divided into N nodal volumes. The nodal volumes have a fixed thickness such that the total distance extend slightly past the final penetration depth.

For this geometry, three types of nodal equations must be used. These equations are for: the surface nodes, the interior nodes and the final interior nodes outside the penetration depth.

The energy balance for the interior nodes of the column, Figure 19, is given by:

$$q(i-1:i) + q(i+1:i) = m_i C_i \frac{dT}{dt} \qquad \text{(eq 17)}$$

where: $q(i-1:i)$ = heat flow from node i-1 to node i

$$= k(i-1:i) \frac{A}{\Delta X} (T_{i-1} - T_i) \qquad \text{(eq 18)}$$

$k(i-1:i)$ = the average thermal conductivity between node i-1 and node i

$$= 1/2\ [k(i-1) + k(i)] \qquad \text{(eq 19)}$$

$q(i+1:i)$ = heat flow from node i+1 to node i

$$= k(i+1:i) \frac{A}{\Delta X} (T_{i+1} - T_i) \qquad \text{(eq 20)}$$

$k(i+1:i)$ = the average thermal conductivity between node i+1 and node i

$$= 1/2\ [k(i+1) + k(i)] \qquad \text{(eq 21)}$$

m_i = the mass of node i

$$= \rho\ A\ \Delta X \qquad \text{(eq 22)}$$

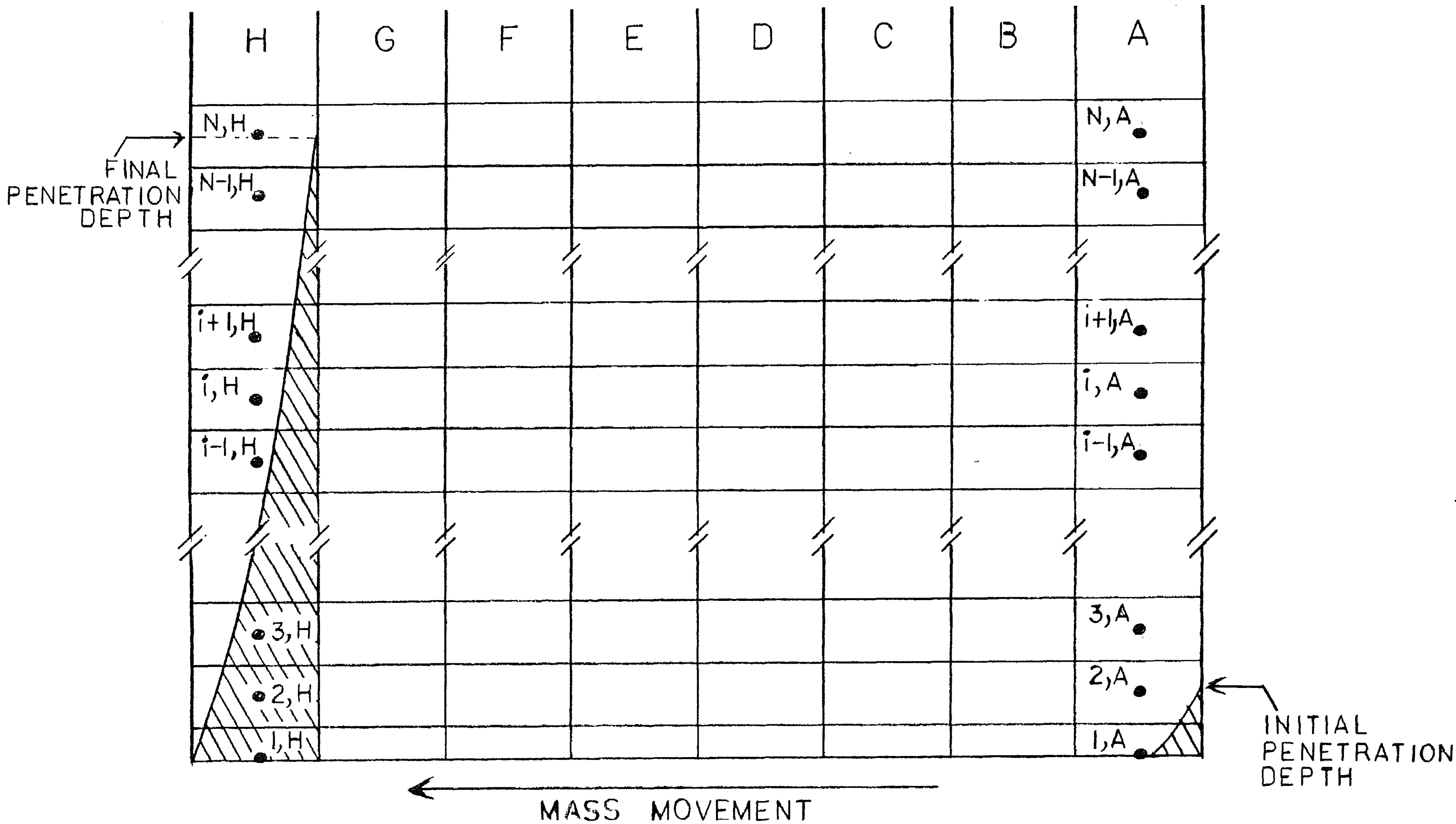

FIGURE 19

NODAL ASIGNMENTS FOR COMPUTER SIMULATION which results in the relationship:

$$k(i-1:i)\frac{A}{\Delta X}(T_{i-1}-T_i)+k(i+1:i)\frac{A}{\Delta X}(T_{i+1}-T_i)=\rho A \Delta X C\frac{dT}{dt} \quad \text{(eq 23)}$$

In this slab geometry, the cross-sectional area A is constant. Solving for the time rate of change of temperature:

$$\frac{dT}{dt}=\frac{k(i-1:i)}{\rho C \Delta X^2}(T_{i-1}-T_i)+\frac{k(i+1:i)}{\rho C \Delta X^2}(T_{i+1}-T_i) \quad \text{(eq 24)}$$

The surface node will be assigned the same temperature as the mold surface. Since the mold temperature changes as a function of time, then:

$$T(\text{surface node}) = T(\text{mold}) = T(t) \quad \text{(eq 25)}$$

The last interior node, which being outside the penetration depth, is always at a temperature of the pool temperature for that particular wedge, or:

$$T_{j,n} = T(\text{pool})_j \quad \text{(eq 26)}$$

Where: $T_{j,n}$ = temperature of node n in wedge j

$T(\text{pool})_j$ = pool temperature outside the penetration depth for wedge j

$= \overline{T}$

There are three basic methods of approximating the time derivative, the Pure Explicit or Euler's Method, the Pure Implicit Method, and the Implicit Crank-Nicolison Method.

Euler's Method estimates the temperature T' at the nodal point one time increment, $\Delta\theta$, later by computing the time derivative of the present temperature T, multiplying it by the time increment between T and T', and then adding this to the present temperature T, or:

$$T' = T + \left.\frac{dT}{dt}\right|_{t} \Delta\theta \qquad \text{(eq 27)}$$

This is shown graphically in Figure 20.

The Pure Implicit Method estimates the future nodal temperature T' in a similar fashion as the Euler's Method. But instead of using the time derivative of the present temperature T, it uses the derivative of the future temperature T', or:

$$T' = T + \left.\frac{dT}{dt}\right|_{t'} \Delta\theta \qquad \text{(eq 28)}$$

This is shown in Figure 21.

In the Implicit Crank-Nicolson Method, the arithmetic mean value of the derivatives at the beginning and at the end of the time interval is used to determine the future tmeperature. Or:

$$T' = T + \left[\frac{\left.\frac{dT}{dt}\right|_{t} + \left.\frac{dT}{dt}\right|_{t'}}{2}\right] \Delta\theta \qquad \text{(eq 29)}$$

This is shown in Figure 22.

Figure 20

EULER'S METHOD OF APPROXIMATION

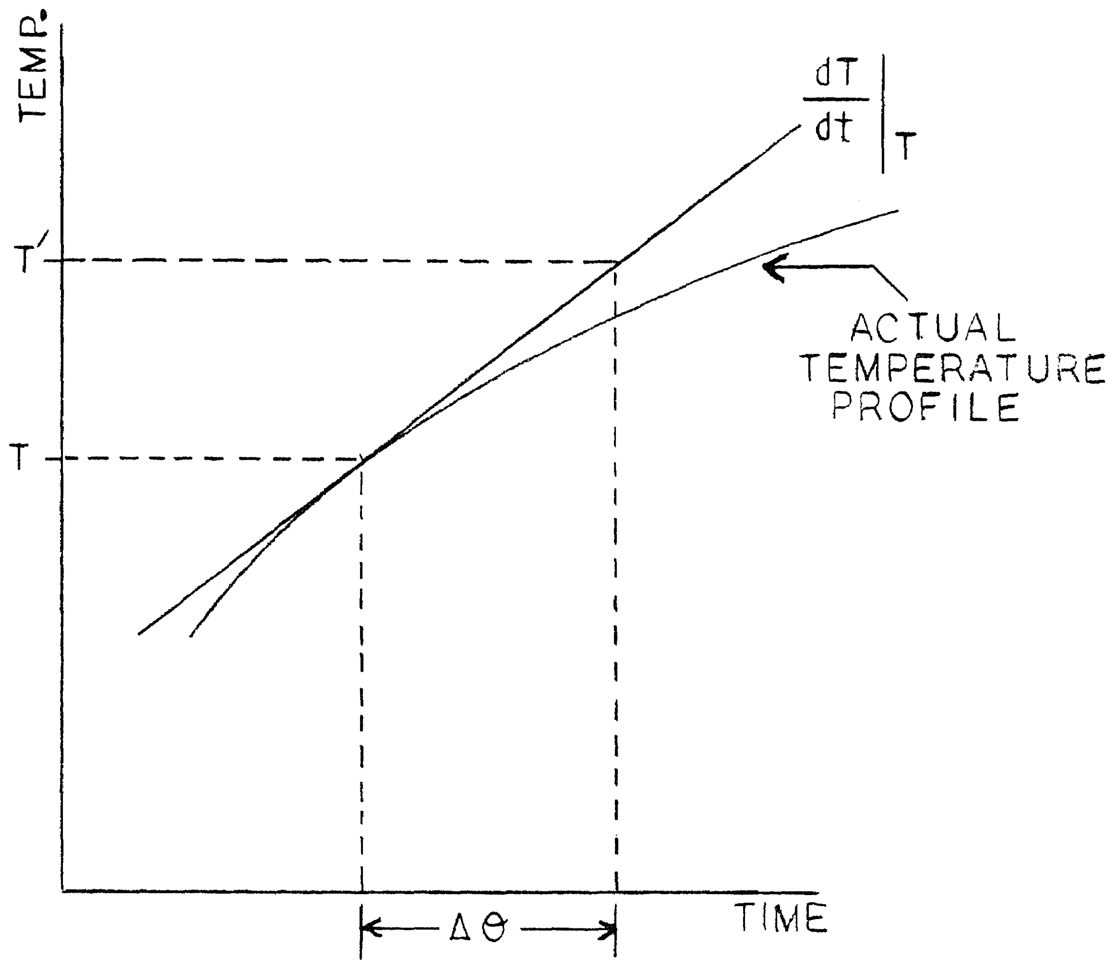

Figure 21

THE PURE IMPLICIT METHOD OF APPROXIMATION

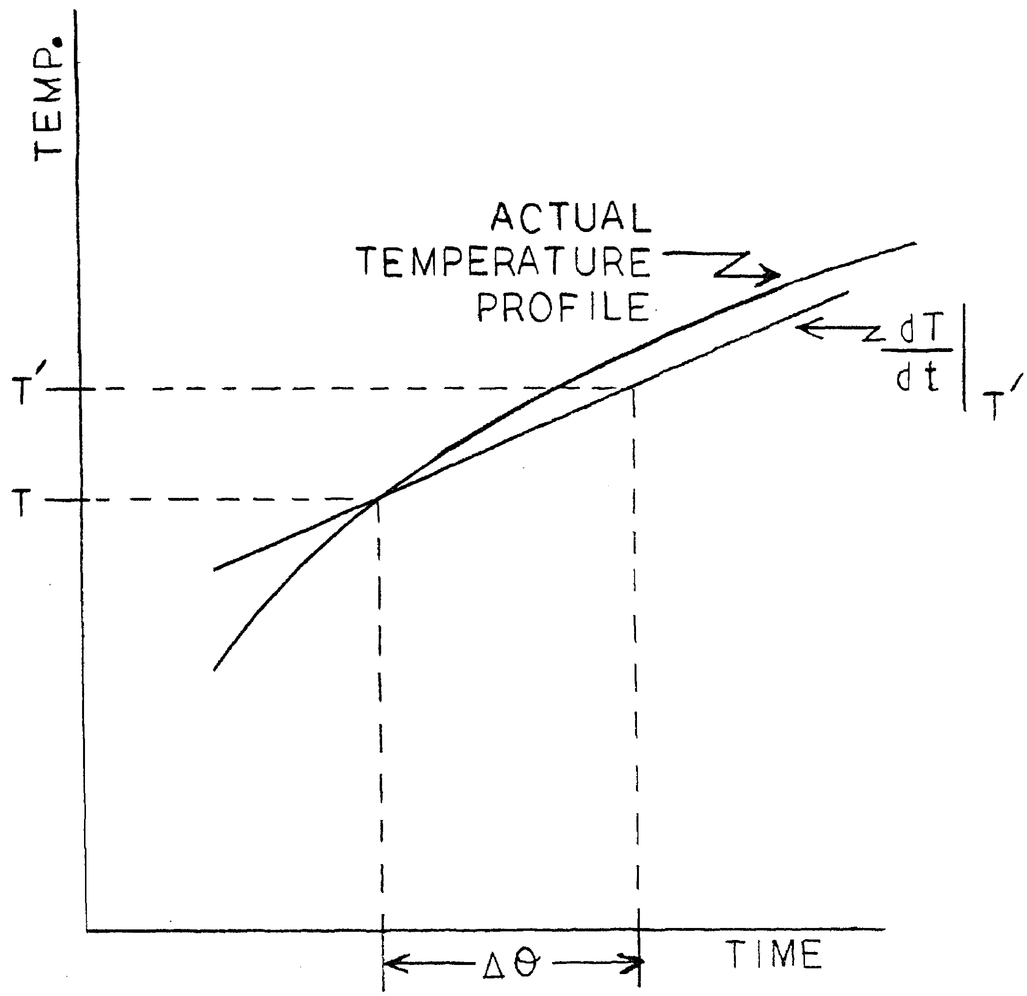

Figure 22

THE CRANK-NICOLSON METHOD OF APPROXIMATION

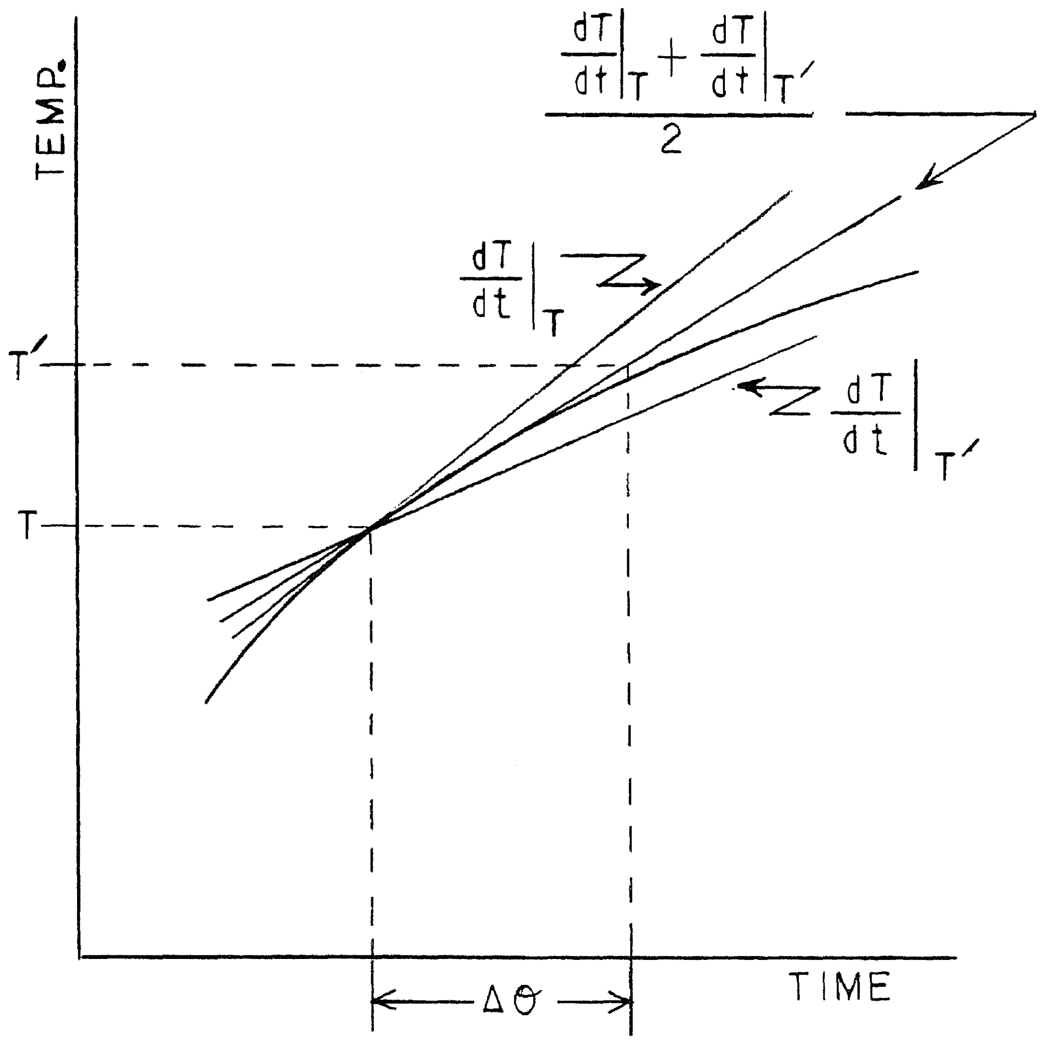

If the Pure Implicit or the Implicit Crank-Nicolson Method is used to approximate the time derivative, the result will be a set of N simultaneous equations with N unknowns. This would require the computer to solve a tri-diagonal matrix for each time increment for each column.

Euler's Method, however, results in a set of N equations with one unknown per nodal energy balance equation. Consequenty, the future temperature T' can be found directly by solving a simple algebraic equation. Therefore, in this dissertation, Euler's Method of approximation was used.

Substituting for the time derivative for an interior nodal equation results in:

$$\frac{T_i' - T_i}{\Delta\theta} = \frac{k(i-1:i)}{\rho C \Delta X^2}(T_{i-1} - T_i) + \frac{k(i+1:i)}{\rho C \Delta X^2}(T_{i+1} - T_i) \qquad \text{(eq 30)}$$

Solving for the future temperature T':

$$T_i' = T_i\left(1 - \frac{\Delta\theta}{\rho C \Delta X^2}\{k(i-1:i) + k(i+1:i)\}\right) + \frac{\Delta\theta}{\rho C \Delta X^2}\{k(i-1:i)T_{i-1} + k(i+1:i)T_{i+1}\} \qquad \text{(eq 31)}$$

In the use of the Euler's Method of approximation, it must be noted that the equations become unstable when the expression $\frac{1-K\Delta\theta}{\rho C \Delta X^2}\Sigma k$ becomes negative (K is some constant).

Often the k's, K, ρ, C and ΔX are predetermined. Therefore it is necessary to compute the value of $\Delta\theta$ such that the value of the expression is greater than or equal to zero. Or:

$$1-\frac{K\Delta\theta\Sigma k}{\rho C\Delta X^2} \geq 0.0 \qquad \text{(eq 32)}$$

Or:

$$\frac{K\Delta\theta\Sigma k}{\rho C\Delta X^2} \leq 1.0 \qquad \text{(eq 33)}$$

Solving for $\Delta\theta$:

$$\Delta\theta \leq \frac{\rho C\Delta X^2}{K\ \Sigma k} \qquad \text{(eq 34)}$$

Usually the maximum allowable value of will be used, or:

$$\Delta\theta_{MAX} = \frac{\rho C\Delta X^2}{K\ \Sigma k} \qquad \text{(eq 35)}$$

If the values of ρ , C, and k are not constant, the minimum values of ρ and C and the maximum value of k must be used to determine the stability constants.

Since the nodal thickness, ΔX in the simulation developed, becomes smaller as the material densifies, the maximum time increment ($\Delta\theta$) will be recalculated at each iteration assuring that all nodal equations remain stable.

The second simulation model developed includes the effect of convection heating by oven air. The exterior surface nodal equation of the mold is given by:

$$T_{eM}' = T_{eM} + \left[1 - \frac{2\ \Delta\theta}{\rho_M\ C_M\ \Delta X_M}\ \left(\frac{k_M}{\Delta X_M} + H_A\right)\right] + \frac{2\ \Delta\theta}{\rho_M\ C_M\ \Delta X_M}\ \left[\frac{k_M}{\Delta X_M} * T_{IM} + H_A * T_{OVEN}\right] \qquad \text{(eq 36)}$$

where: T'_{eM} = Future temperature of the external mold surface one time increment ($\Delta\theta$) latter.

T_{eM} = Present temperature of the external mold surface.

ρ_M = Density of the mold material

K_M = Thermal Conductivity of mold material

C_M = Specific heat of mold material

ΔX_M = Mold thickness

H_A = Coefficient of Convection of the air in the oven

Toven = Oven temperature

T_{IM} = Temperature of mold's internal surface

The maximum allowable time increment for this nodal equation is:

$$\Delta\theta_{MAX} = \frac{\rho_M\ C_M\ \Delta X_M}{2\left(\frac{K_M}{\Delta X_M} + H_A\right)} \qquad \text{(eq 37)}$$

The mold's internal surface nodal temperature equation is:

$$T_{IM}' = \left[1 - \frac{2\ \Delta\theta\ k_M}{\rho_M\ C_M\ \Delta X_M^2}\right] T_{IM} + \frac{2\ \Delta\theta\ K_M}{\rho_M\ C_M\ \Delta X_M^2} * T_{eM} \qquad \text{(eq 38)}$$

where: T'_{IM} = Future temperature of the internal mold surface one time increment ($\Delta\theta$) later.

T_{IM} = Present temperature of the internal mold surface.

The maximum allowable time increment for this nodal equation is:

$$\Delta\theta_{MAX} = \frac{\rho_M \, C_M \, \Delta X_M^2}{2 \, K_M} \qquad \text{(eq 39)}$$

When using more than one type of nodal equation, the minimum $\Delta\theta_{MAX}$ must be the largest time increment used in the numerical analysis. This will assure stability for all equations.

The temperature of the first node of the powdered material now becomes equal of T_{IM} .

The equations developed in this chapter were used to predict the powder temperatures during the rotational molding process.

VII. INVESTIGATION INTO THE DENSIFICATION PROCESS

To accurately simulate the rotational molding process from powder rotation to the formation of molten mass, the powder densification process must be understood. Experimental studies were performed to determine the basic densification phenomena and the results were used to describe the densification in the simulation model.

Because the individual powder particles used in rotational molding have such irregular shape (see Figure 23), it becomes very difficult to obtain experimental observational data that can be used to describe the densification process . Thus, it becomes necessary to experiment with a much simpler particle geometry and then hypothesize how the process occurs with much more complex geometry. However, problems still occur in attempting to freeze the densification process at a particular time frame while the material is in an actual rotational mold. The solution was to model the rotational mold in an environment with a flat plate apparatus, Figure 24. The powdered material was heated through the base plate and at a particular instant of time the heating process was stopped by removing the plate from the heater and placing the plate on dry ice.

FIGURE 23

TYPICAL ROTATIONAL MOLDING MATERIAL DURING DENSIFICATION

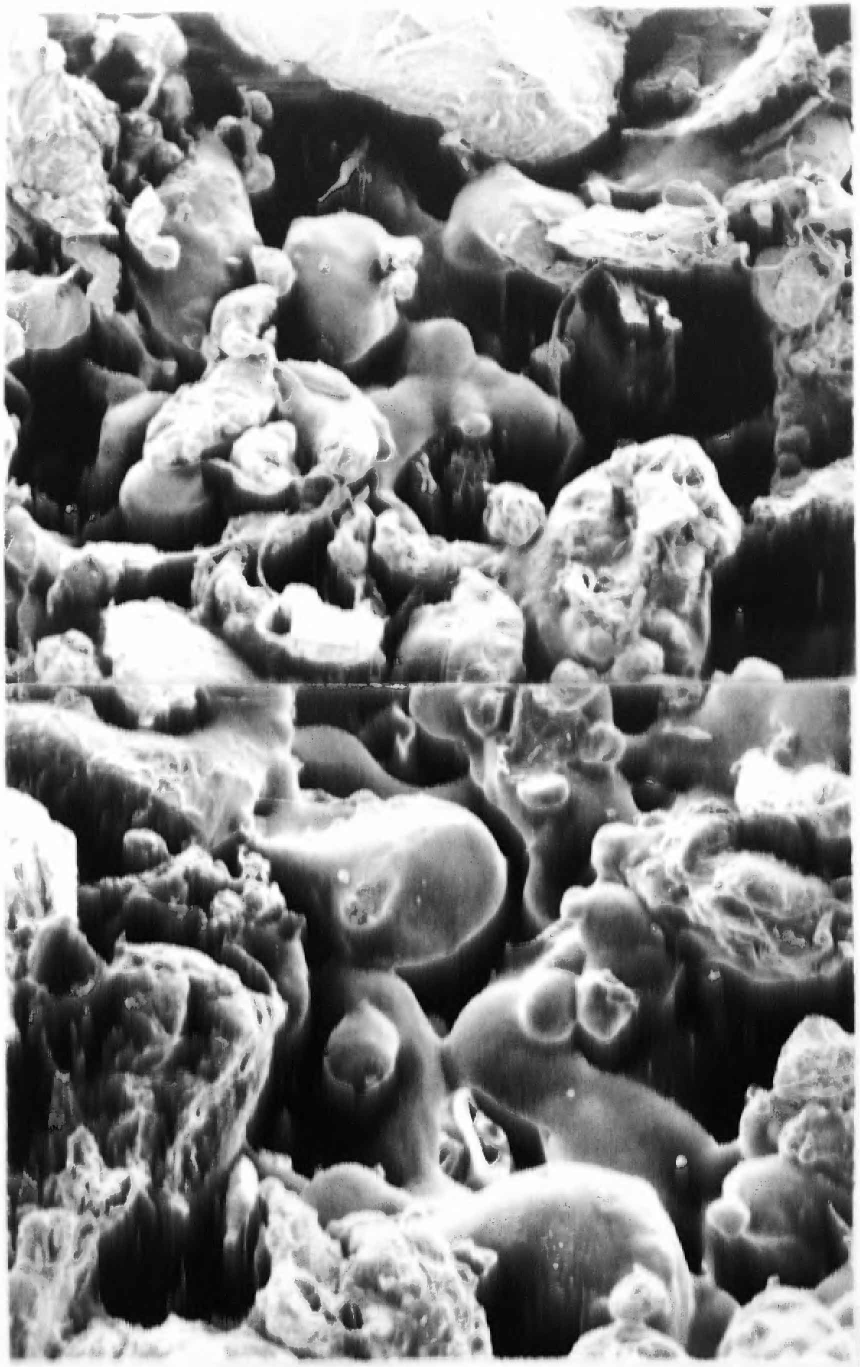

Figure 24

FLAT PLATE APPARATUS USED IN DENSIFICATION STUDY

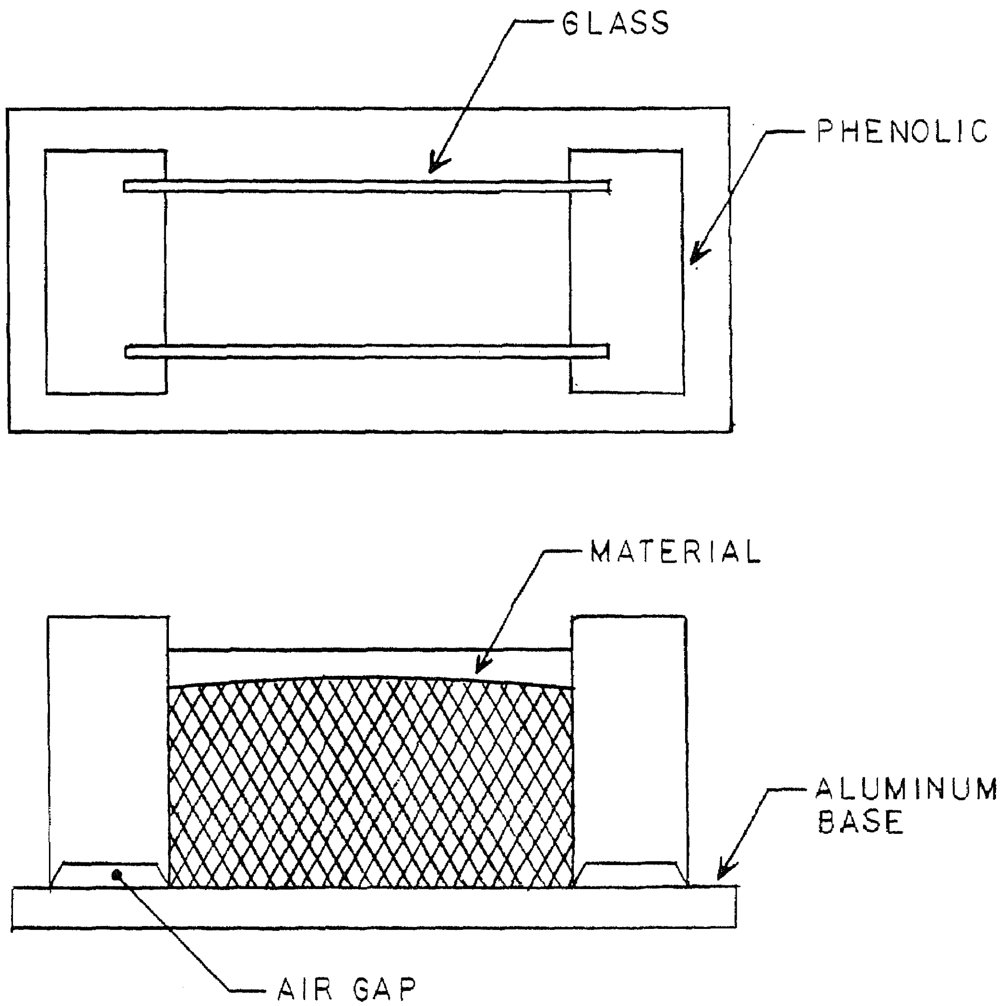

Figure 25 compares a photo of a rotational molded part of DuPont acrylic microspheres made in the uniaxial rotational mold in the NJIT laboratory and a photo of a part molded on the flat plate apparatus. Both molding processes were conducted under similar temperature time histories. (material data listed in Appendix C) Notice the similarities; both have a totaly densified region, a region with slight necking, and a region where spheres are attached but no appreciable or noticeable radius at the points of contact. Hence, the flat plate apparatus is a viable means of analyzing and understanding the densification process in rotational molding.

An analysis of the densification process was performed after a review of a flat plate experiment using significantly larger spheres illustrating a non-necking densification process. This experiment involved using one-eighth diameter High Density Polyethylene(HDPE) spheres (Appendix B for data) packed in a body centered cubic array using an apparatus shown in Figure 24. This apparatus was heated through its base, simulating the non-isothermal heating that occurs in the rotational molding process.

As energy was applied to the base plate , the lower portion of the bottom spheres became less viscous and was forced down by the weight of the spheres above. The less

FIGURE 25

COMPARISON BETWEEN ROTATIONAL MOLDING AND FLAT PLATE MOLDING OF ACRYLIC MICROSPHERES

TOP

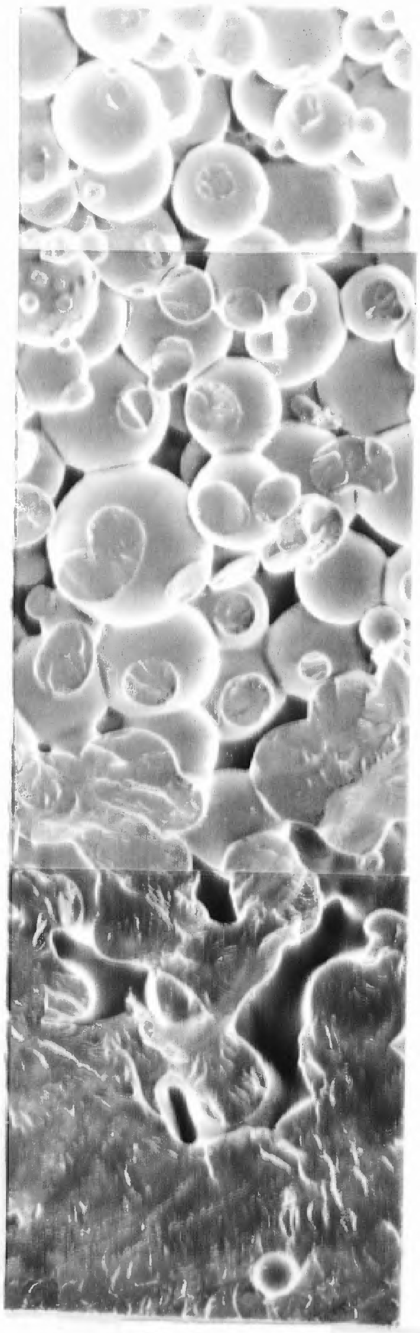

HOT PLATE

FLAT PLATE MOLDED

TOP

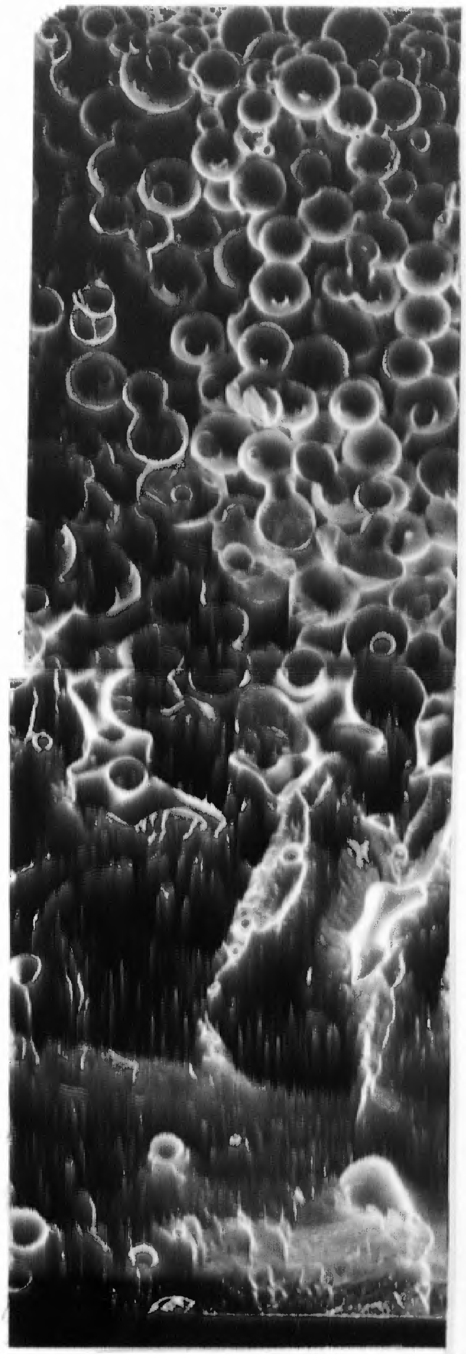

HOT PLATE

ROTATIONAL MOLDED

viscous material flowed between the spheres, filling the voids(Figure 26a-c).

The upper portion of the bottom layer next became soft allowing the pressure of the harder spheres above to deform the lower level spheres(Figure 26d). The final shape of a bottom layer spheres appeared to be flat on the bottom due to the flat plate and dimpled on the top due to the more viscous upper level spheres. With continued heating of the plate, the interior spheres deformed next. As seen in the bottom layer analysis, the lower portion of the more viscous upper layer retained its spherical shape while the lower layer was deformed (Figure 27-a).

As the upper portion of the interior sphere increases in temperature, the harder, more viscous next upper layer spheres deformed the interior sphere below(Fig. 27a-d). The final shape is spherical in the lower region and dimpled on top (Figure 27e). Duplication of the experiments using one-eighth diameter acrylic spheres produced the same results as those obtained with the HDPE spheres.

The experimental results indicated a different densification process that was described in the literature survey. Unlike sintering, the one-eighth diameter spheres

Figure 26

THE MELTING OF BOTTOM LAYER SPHERES

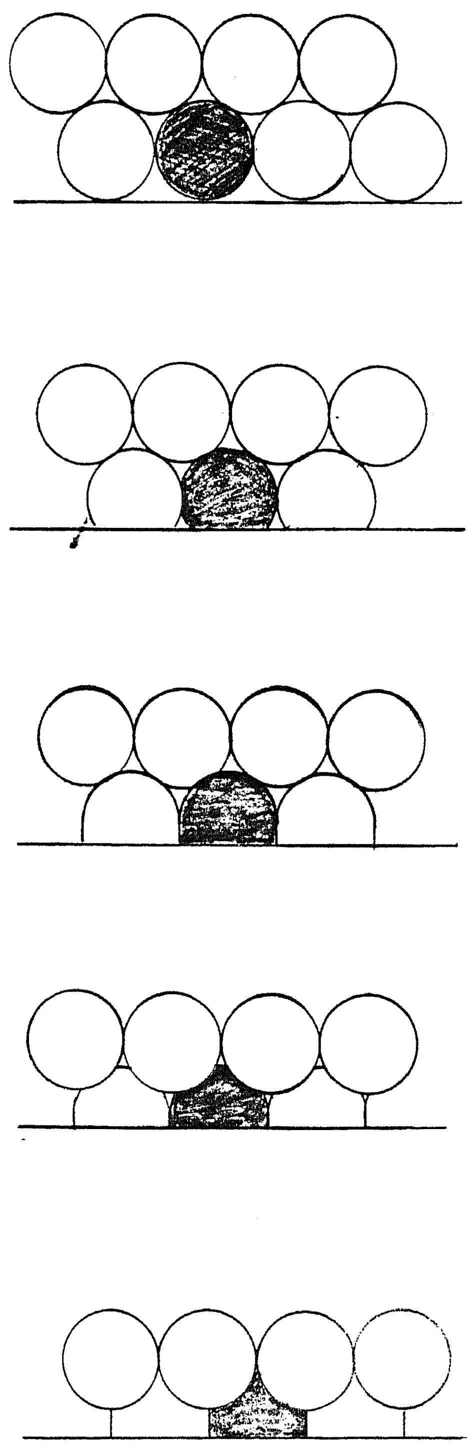

(a) Original set-up

(b) As heat in applied, the lower portion of the bottom spheres become less viscous (melts) and is forced down by the weight above.

(c) The displaced material begins to fill the voids

(d) The heat continues and causes the upper portion of the bottom layer to become soft allowing the pressure of the more viscous, harder spheres to deform the lower level spheres.

(e) The final shape is flat on the bottom(caused by the plate) and dimpled on top (caused by the harder upper level spheres)

Figure 27

THE MELTING OF MIDDLE LAYER SPHERES

(a)

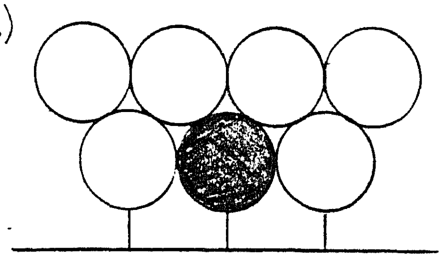

As was seen in the Bottom Layer Analysis, the lower portion of the middle layer retains its spherical shape during melting because it is more viscous(harder) than the layer below causing the lower level to be deformed by the spheres above it.

(b)

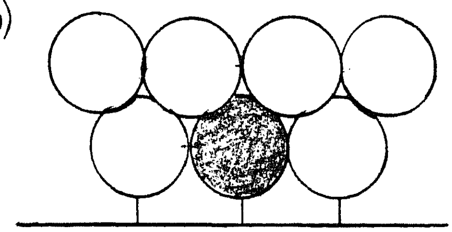

As the upper portion of the sphere increases in temperature, it allows the harder, more viscous upper layer spheres to deform it.

(c)

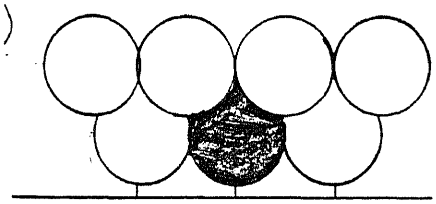

(d)

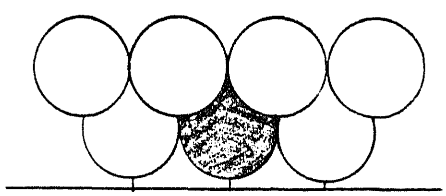

(e)

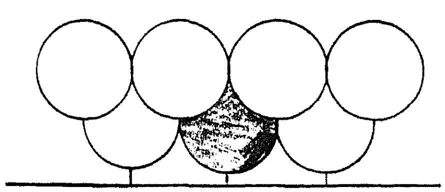

The final shape is spherical on the bottom and dimpled on top.

showed no necking but rather filled the voids between the individual spheres by viscous flow.

The spheres used is this experiment were approximately one hundred times greater in size than normal rotational material. The only useful conclusions that were drawn from this study was that material flow caused by lower viscosity may also be a significant factor in the mechanism that occurs in the densification process of rotational molding.

The next set of experiments were performed with the DuPont acrylic microspheres using the Flat Plate apparatus. Because the size distribution of the microspheres was very close to that of a rotational molding grade polyethylene powder, the results obtained using the microspheres gave considerable insight into the actual densification mechanism.

Several experiments were conducted terminating the densification process at different time intervals. The specimens were then mounted and photographed with a Scanning Electronic Microscope. The temperature - time profiles used in these experiments were identical to those used by Vanderbeck(30) in his experiments. A direct comparison between results of the computer simulation developed in a latter section in this dissertation using a model of the densification process observed here and the actual experiments results of Vanderbeck.

Figure 28 shows the photographs of six simulated rotomolding experimental runs of the acrylic microspheres that were frozen at various time frames. Though difficult to see in the photographs, all the spheres have adhered together at the points of contact and the densification process was initiated.

As the temperature rises, the spheres nearer to the heat source began the necking process by sintering. With increasing time and mold temperature, neck radius of the spheres near the high temperature surface continue to increase. In addition, the necking process starts to occur with the interior spheres.

The latter photographs show that as the neck growth reaches a maximum of between 10% and 20%, there appears to be a dramatic change occuring. Necking is overcome by viscous flow from melting. This process continues until all the spheres have lost their individuality and have melted into one homogenous part. This drastic change is a characteristic of a material where by the temperature causes the material to flow faster than the slow viscous flow of the sintering process. This temperature at which material flow overcomes the sintering process will be referred to as the melt interface temperature (Tm).

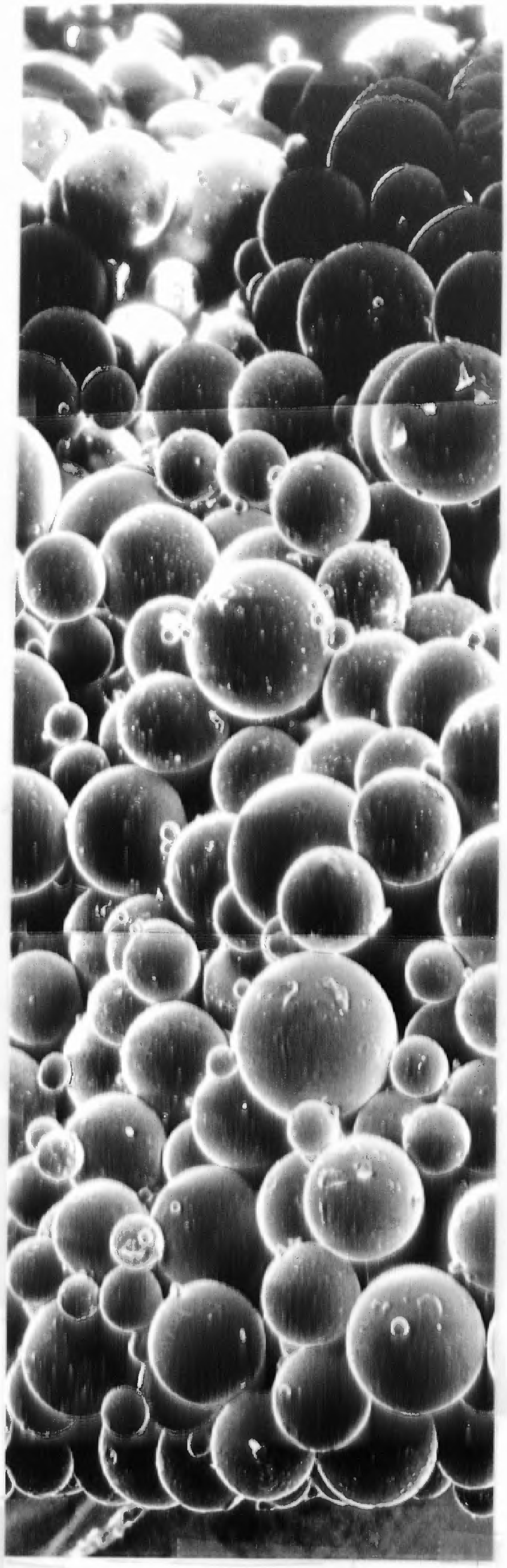

HOT PLATE

FIGURE 28

SCANNING ELECTRONIC MICROSCOPE PHOTOGRAPHS OF ACRYLIC MICROSPHERES FOR VARIOUS TIME INTERVALS

8 MINUTES

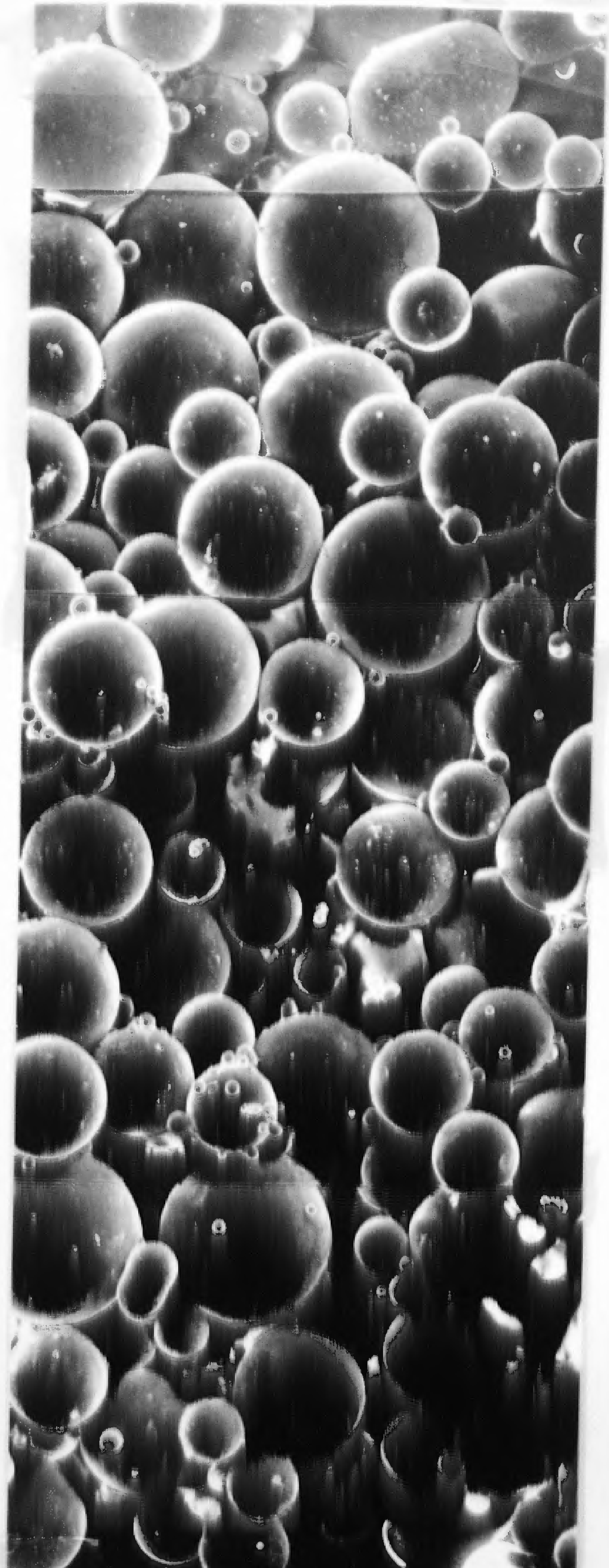

10 MINUTES

HOT PLATE

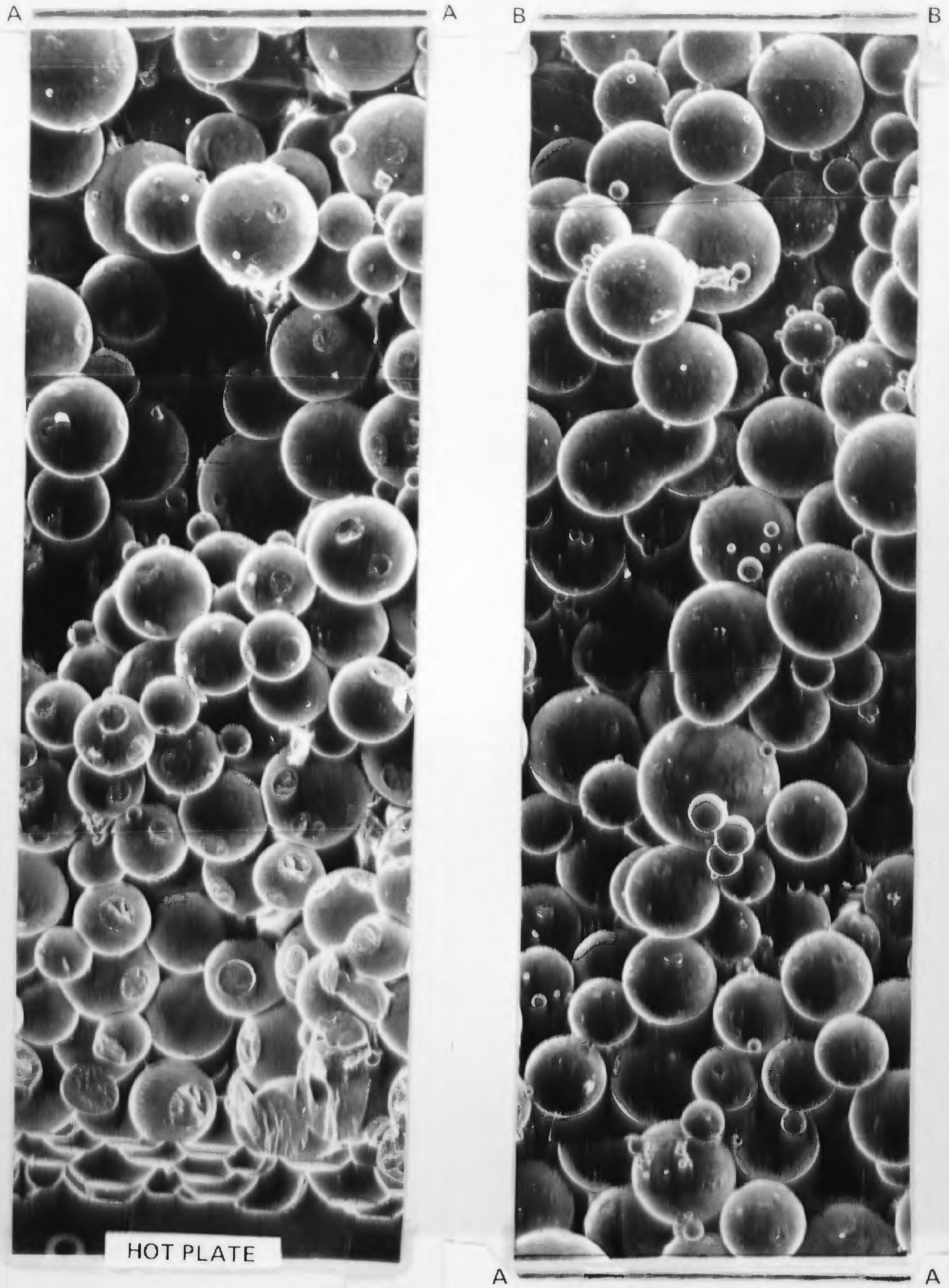

12 MINUTES

TOP

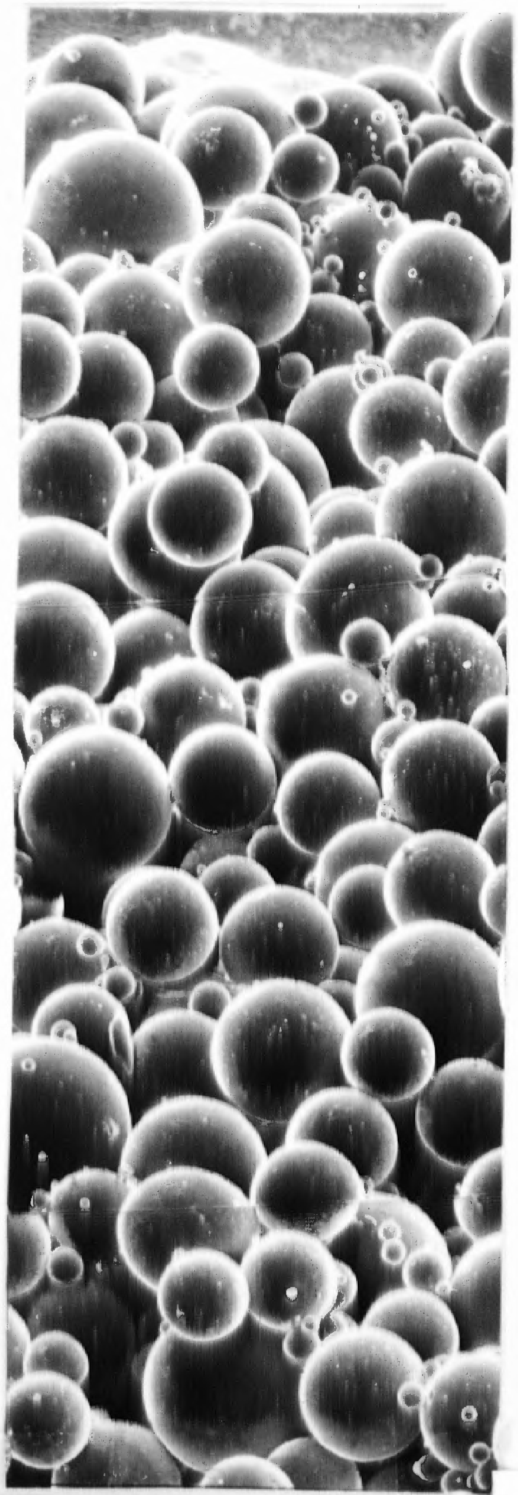

12 MINUTES (CONTINUED)

HOT PLATE

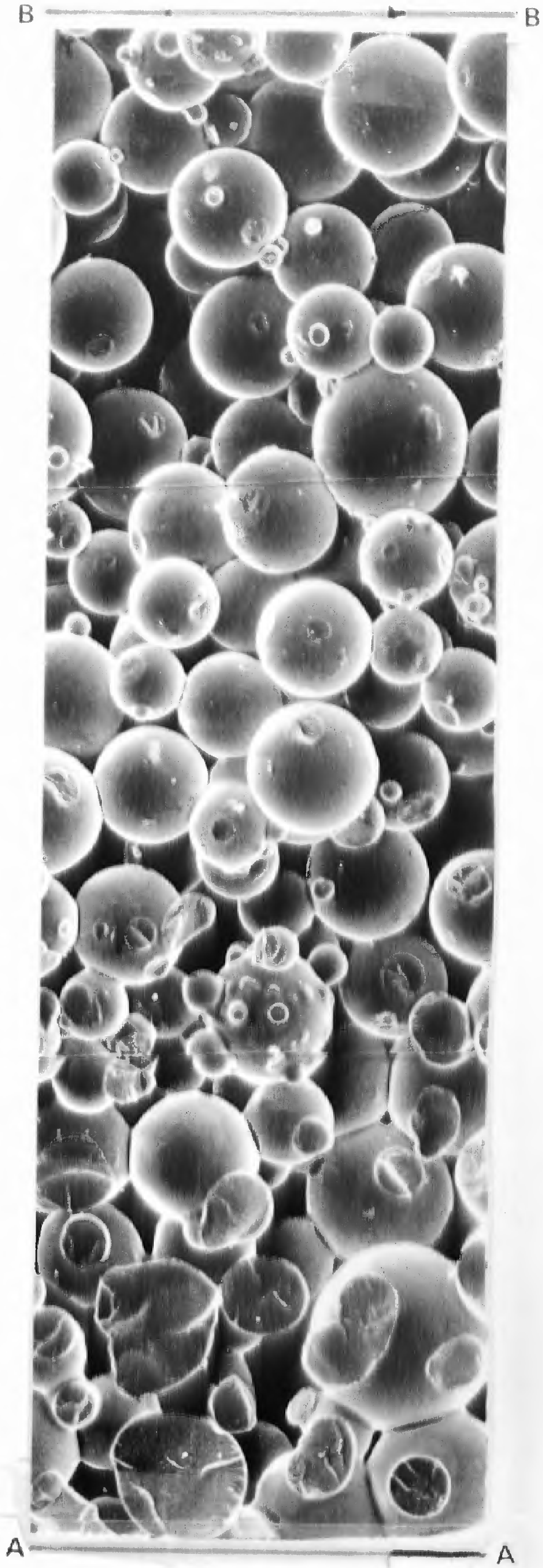

16 MINUTES

C — C

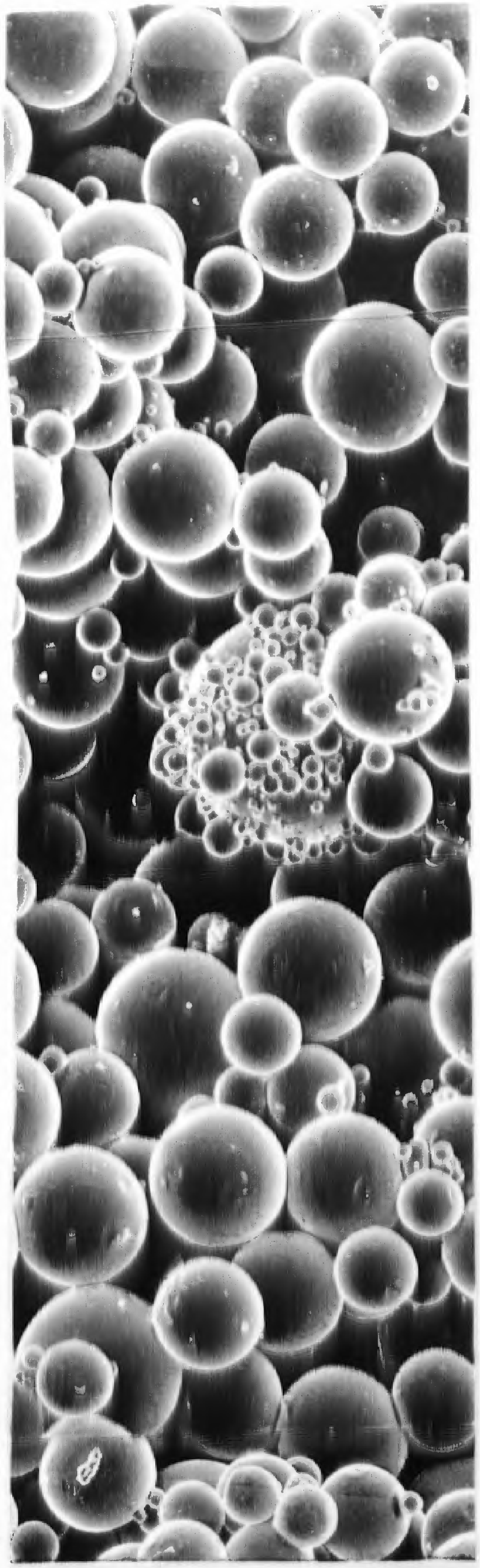

B — B

TOP

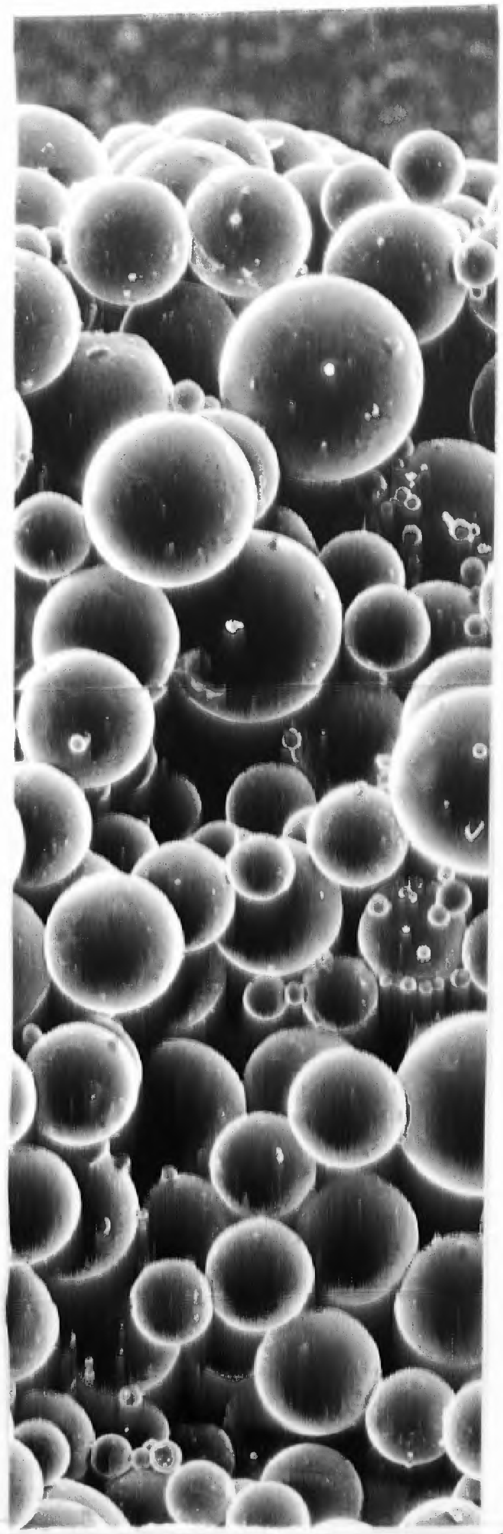

C — C

16 MINUTES (CONTINUED)

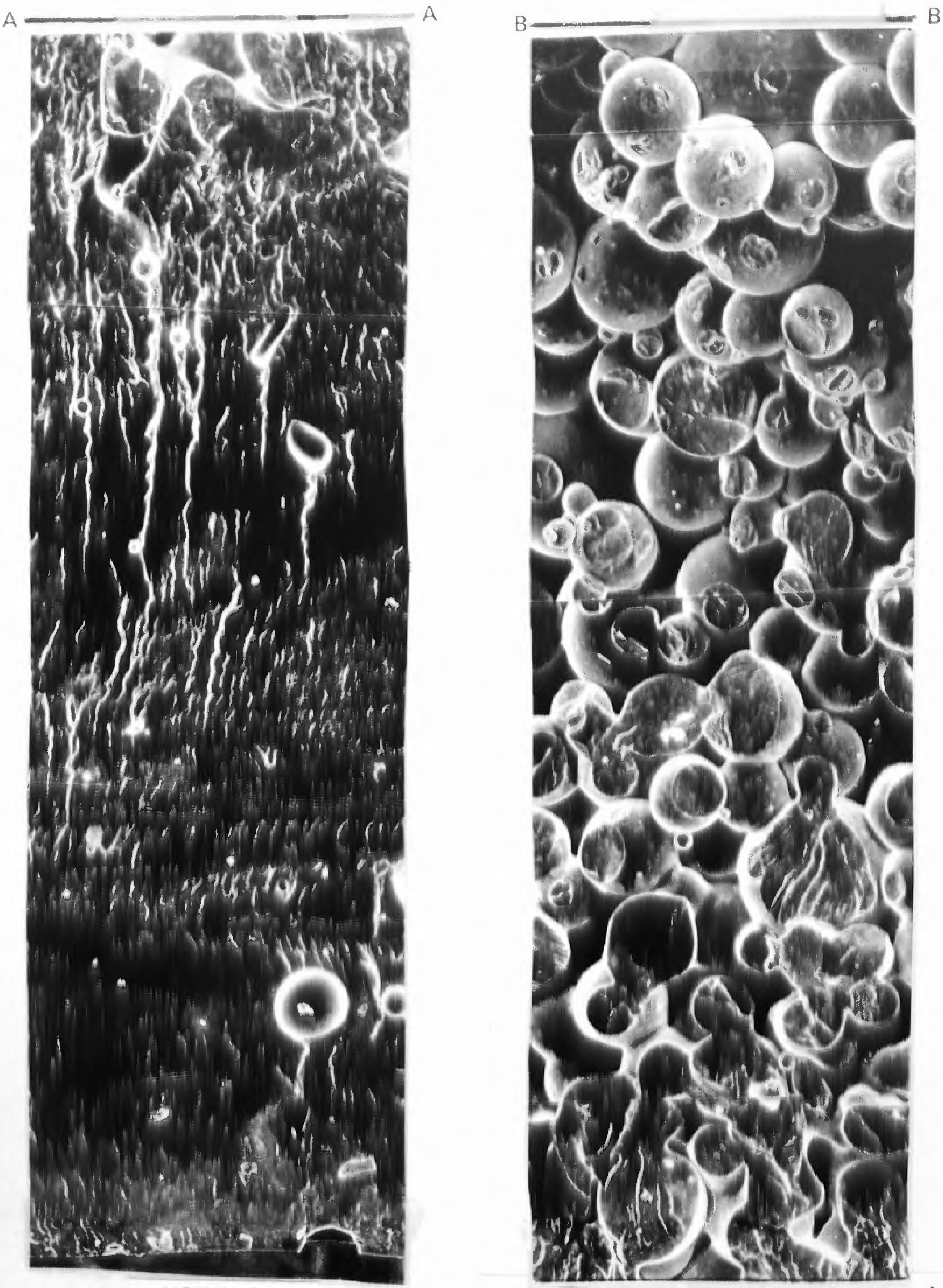

HOT PLATE

20 MINUTES

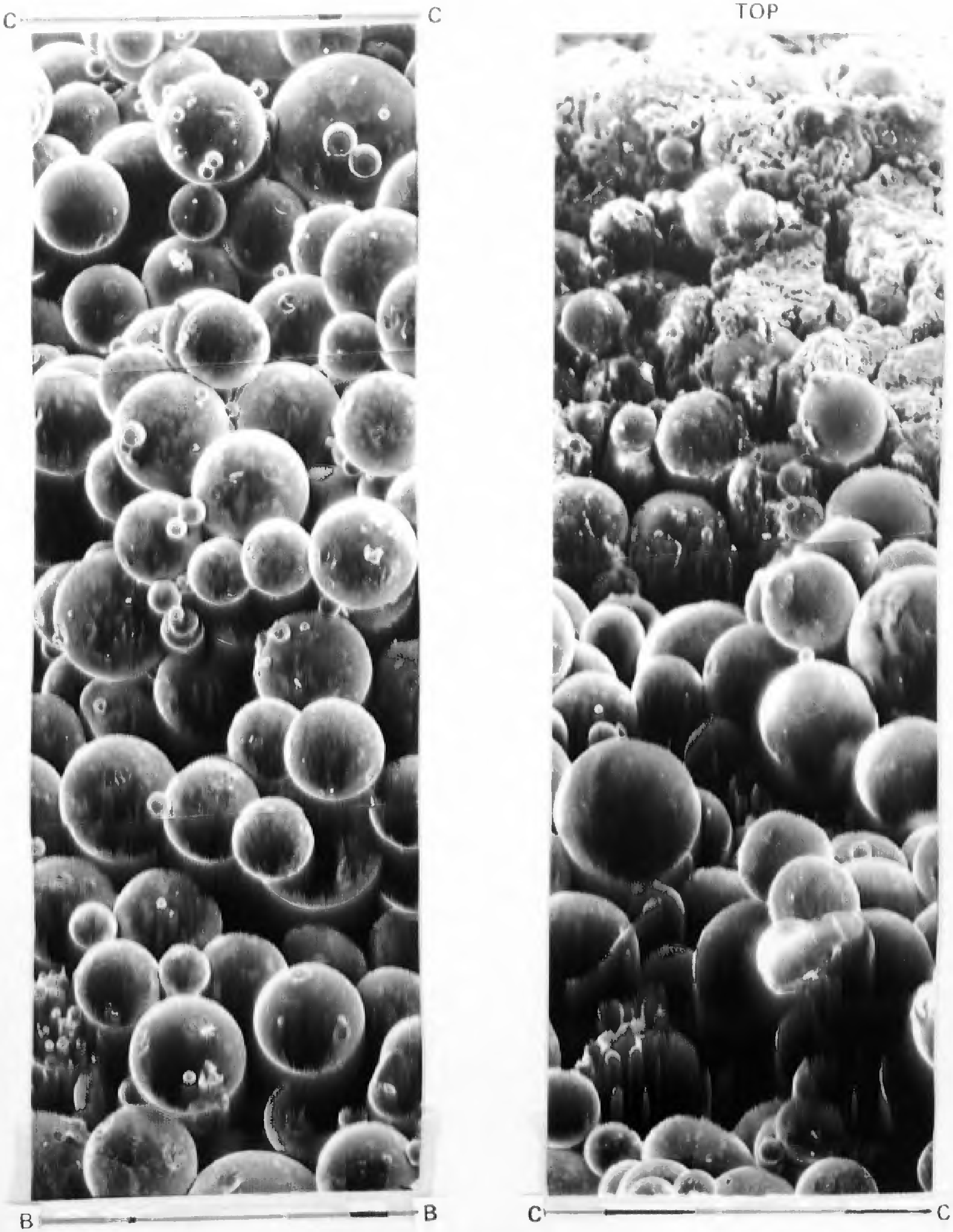

20 MINUTES (CONTINUED)

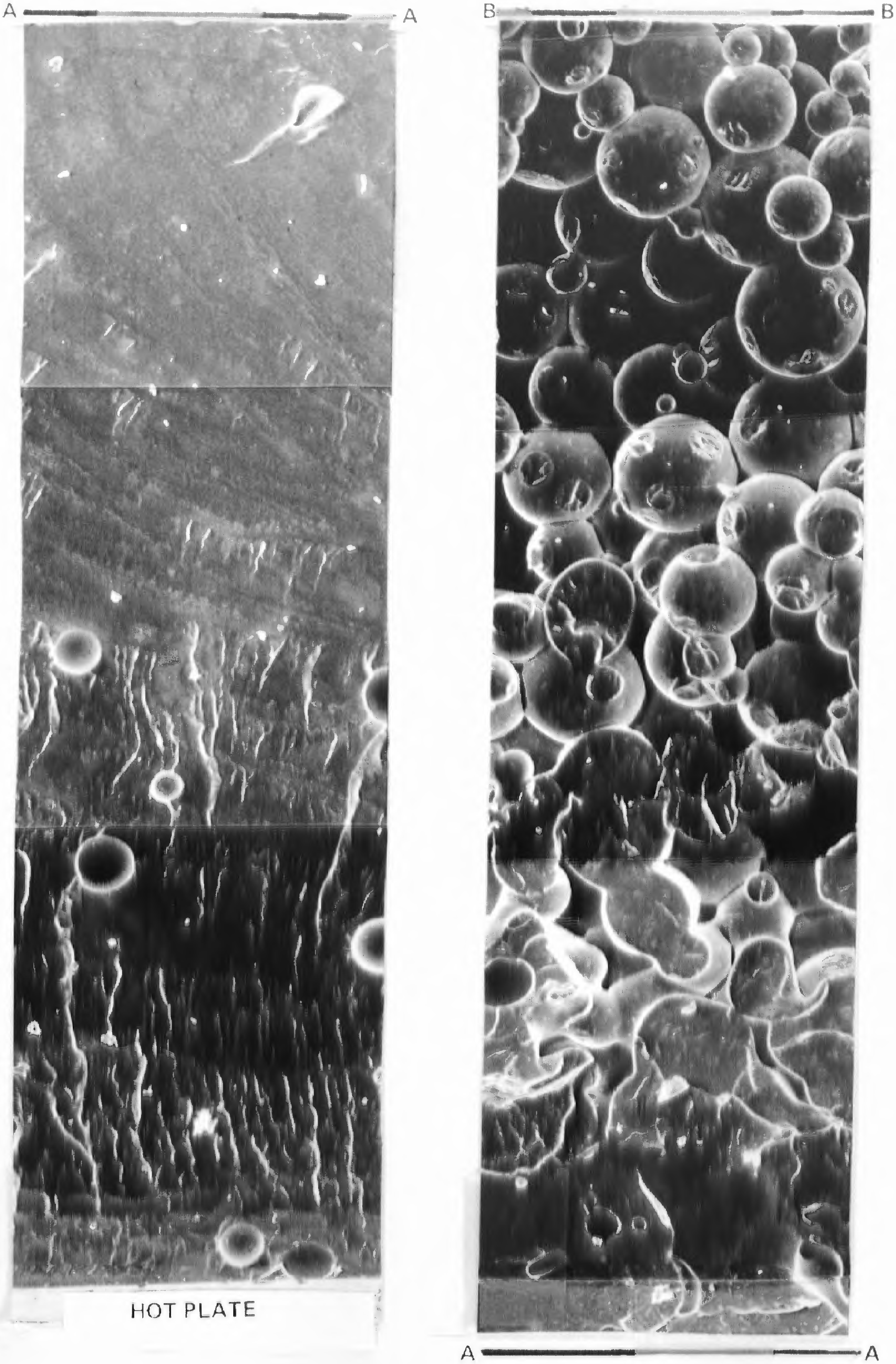

24 MINUTES

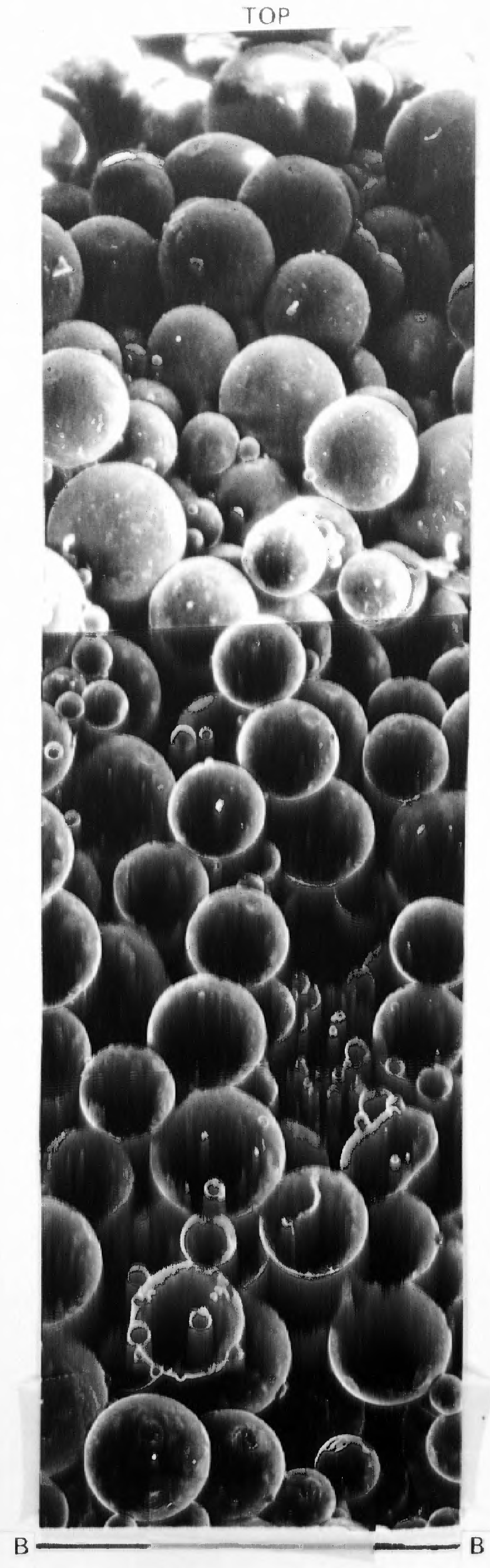

24 MINUTES (CONTINUED)

VIII. DETERMINATION OF THE PHYSICAL PROPERTIES

As discussed previously, the simulation model will use nodal analysis in which the average neck size for a representative particle will be computed at each node as a function of time. The value of the thermal conductivity of each nodal subvolume at any particular time will be a direct function of the neck size within the nodal volume at that instant of time. The equation used to estimate the instantaneous thermal conductivity showing the effect of necking due to sintering is:

$$K_{Ei} = K_P + \left[\frac{X_i}{a}\right]^N (K_S - K_P) \qquad \text{(eq 40)}$$

where: K_{Ei} = thermal conductivity at node i

K_P = thermal conductivity of initial powder

K_S = thermal conductivity of the solid polymer

X_i = neck radius of node i

a = original sphere radius

N = power law exponent (value = 1)

Even though the actual polyethylene powdered material is not spherical, the value of the original sphere radius, a, is the average sift size radius.

The thermal conductivity of the powdered material(K_P) was to be initially be determined using the equations mentioned earlier in the literature survey for predicting the thermal conductivity of composite system. Figure 11 compared the results of using various composite material equations for determining thermal conductivity based on the material data in Appendix A. The calculated values of equivalent thermal conductivities(K_{Ei}) can be seen to vary greatly. Therefore it becomes necessary to experimentally determine, with use of a simple computer simulation, the actual thermal conductivity of the powder. The experiment and the subsequent determination of the powder thermal conductivity will be described in the next chapter.

The neck size for each node is calculated in the computer simulation by adding the calculated change in neck size during that time increment to the previous neck size of the node. Using Frenkel's Equation:

$$X = \left[\frac{3 a t \gamma}{2 \eta}\right]^{0.5} \qquad \text{(eq 1)}$$

and differentiating eq. 1 with respect to time will give the change of neck radius as a function of time, or:

$$\frac{\partial X}{\partial t} = \left[\frac{3\ a\ \gamma}{8\ \eta\ t}\right]^{0.5} \qquad \text{(eq 41)}$$

Converting the equation to a small finite change in time (Δt), the change in neck radius for a time Δt is :

$$\Delta X = \left[\frac{3\ a\ \gamma}{8\ \eta\ t}\right]^{0.5} \Delta t \qquad \text{(eq 42)}$$

When the neck radius exceeds 50% of the sphere radius, Frenkel states that the collapse of the bubble formed is:

$$r_o - r = \frac{\gamma}{2\eta} t \qquad \text{(eq 2)}$$

differenting with respect to time:

$$\frac{\partial r}{\partial t} = -\frac{\gamma}{2\eta} \qquad \text{(eq 43)}$$

for a small finite change in time:

$$\Delta r = -\frac{\gamma}{2\eta} \Delta t \qquad \text{(eq 44)}$$

since the negative change in bubble radius(Δr) is equal to the increase of neck radius, the change in sphere radius above 50% necking is:

$$\Delta X = \frac{\gamma}{2\eta} \Delta t \qquad \text{(eq 45)}$$

As the temperature of a node exceeds the melt temperature, material flow overcomes necking in the densification process. Hence, the neck radius for that particular node instentaniously becomes equal to the radius of the spheres. In other words, the material has completely densified into a homogenious part for that nodal subvolume.

Density is computed in the similar manner as to that of thermal conductivity. The origial powder density was found by experimentally by weighing a volume of the polyethylene material and comparing it to the same volume of water. The density measured for the polyethelyne powder is listed in Appendix A. The density at the complete melt is that of the solid polymer. Density and other physical data of the base resin was supplied by the manufacturer.

The intermediate density is a assumed to be linearly proportional to the distance between the centers of two sintering spheres as was shown in Figure 9. As length L decreases, the density increases proportionaly. Using Frenkel's model, the length L can be correlated to the neck radius, x, thus allowing a direct coorelation of density to neck radius. Figure 29 is a plot of length L vs neck radius using equations 6 through 8 and solving them simutaneously with a = 0.0125 cm. The curve between 0% and 40% neck radius/ sphere radius ratio can be approximated with a straight line fit with only a 2.5% variance. Therefore, it is possible to state that density is proportional to neck radius, or:

$$\rho_{Ei} = \rho_P + \frac{x_i}{a} (\rho_s - \rho_p) \qquad \text{(eq 46)}$$

where:

ρ_{Ei} = Equivalent density at node i

ρ_P = initial powder density

ρ_s = density of solid polymer

x_i = neck radius at node i

a = sphere radius

Figure 29

LENGTH, L VS. NECK RADIUS, X

FOR FRENKEL'S SINTERING MODEL

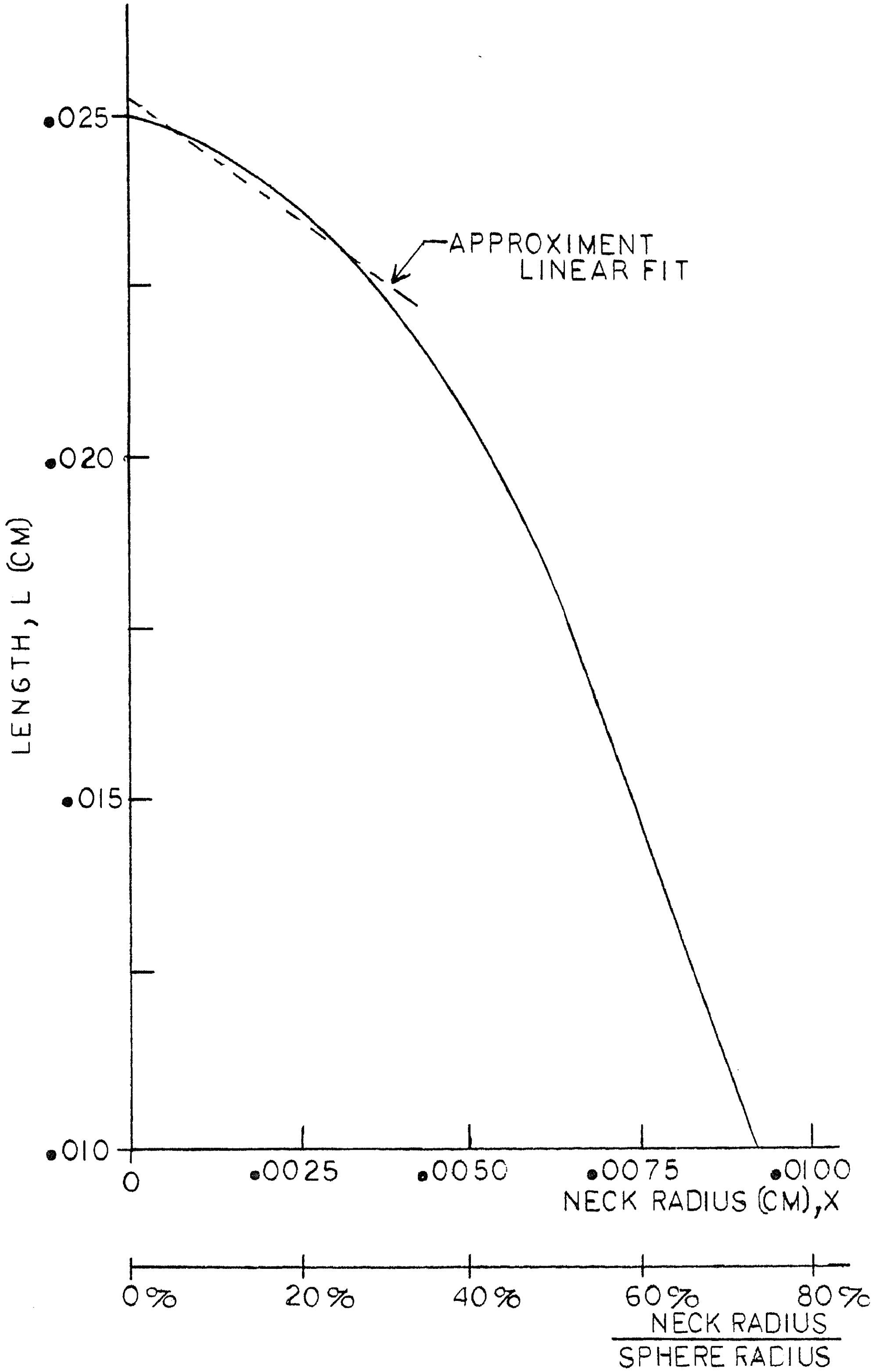

Because of the density change, the distance between nodes in the simulation also changes. The distance between node i and node i-1 is one half the thickness of node i added to the half the thickness of node i-1. These distances are a function of their relative nodal densities. Therefore the nodal distance between node i and node i-1 is proportional to the ratio of the original density to the new average density between node i and node i-1, or:

$$Dx_{i,i-1} = \frac{\rho_p}{(\rho_{E_i} + \rho_{E_{i-1}})*\frac{1}{2}} * Dx \qquad \text{(eq 47)}$$

where: $Dx_{i,i-1}$ = Nodal distance between node i and node i-1

ρ_p = Density of original powdered material

ρ_{E_i} = Equivalent density at node i

$\rho_{E_{i-1}}$ = Equivalent density at node i-1

Dx = original nodal distance

Since specific heat is energy per amount of mass to raise the temperature of the mass one degree, the specific heat of the powder is assumed equal to that of the solid since the mass of air in the powder is neglible. Hence the specific heat remains constant in the simulation developed.

IX. DETERMINATION OF INITIAL THERMAL CONDUCTIVITY

Since the consistency of the thermal conductivity equations of composite materials vary too greatly, it becomes necessary to determine the conductivity of the initial state of the polymeric powder by a combination of an experiment and a computer simulation. The experiment will entail heating the powder and measuring temperature-time histories at specific locations while the computer program will simulate the experiment in an attempt to duplicate the temperature - time histories and thus determining the thermal diffusivity which includes the thermal conductivity.

The experimental set-up used in shown in Figure 30. The apparatus consists of a cardboard tube 3.25 inches long, 3.375 inches inner diameter with a 0.25 inch wall thickness. The tube is beveled at the bottom to minimize heat transfer up the tube wall. Aluminum foil was then epoxied to the beveled edge, bottom of the tube, to contain the powdered material.

Six thermocouples were positioned as shown in Figure 30. To maintain their correct height level, sewing thread was positioned through the tube at the different levels.

Figure 30

THERMAL CONDUCTIVITY EXPERIMENTAL SET-UP

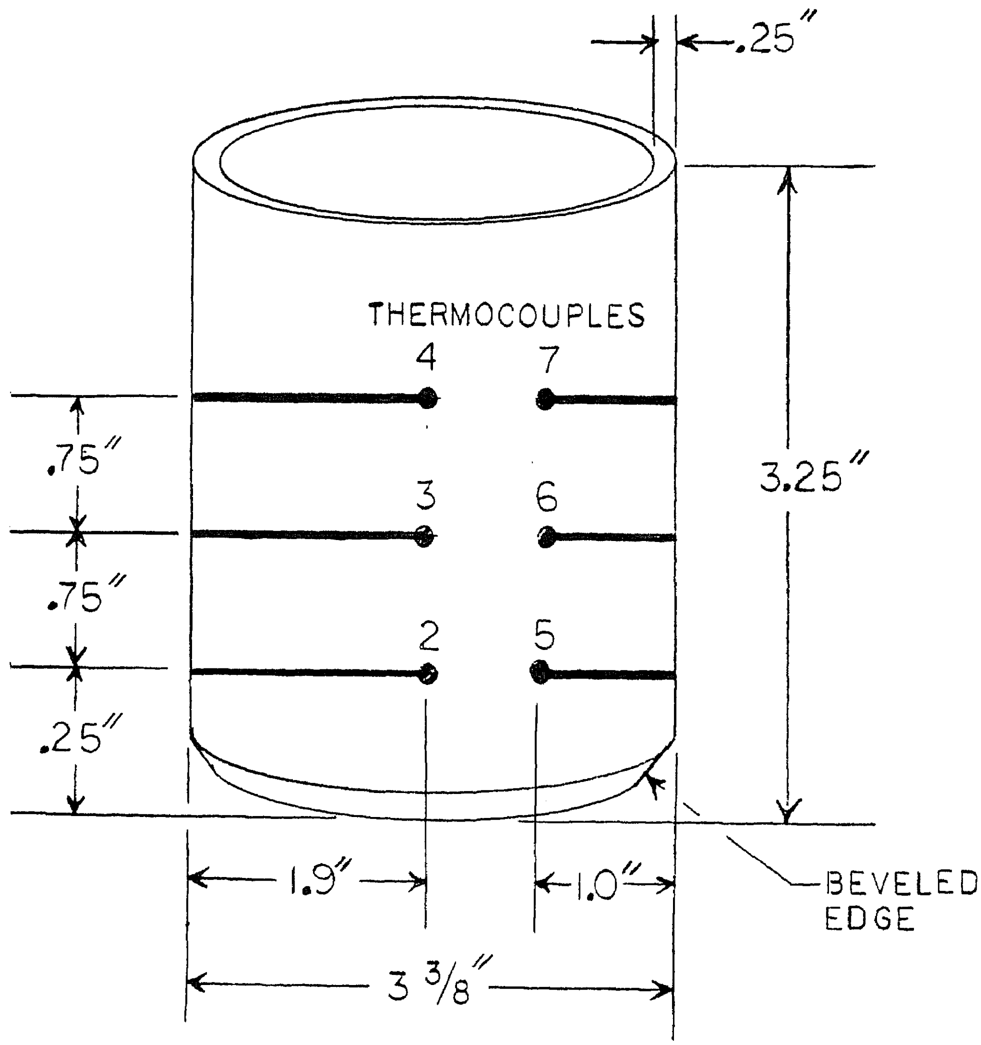

The thermocouple was then wrapped along the taught thread. The experimental proceedure used in these experiments were as follows:

1. The tube with the powdered material was placed on a hot plate and is heated slowly.

2. The temperature at each thermocouple location was then recorded every two minutes for seventy minutes.

3. This data was then used in a computer simulation to determine the thermal conductivity of the powdered material.

Since the experiment was conducted with six thermocouples, the computer simulation can estimate six average thermal conductivities (actually diffusivity) for each experimental run. They are the diffusivities from position 2 to 3, 2 to 4, 3 to 4, 5 to 6, 5 to 7 and 6 to 7. Using two consecutive runs at the same heating rate, twelve estimates of the diffusivity were made.

The computer program used was a simple flat plate simulation having a nodal geometry as is shown in Figure 31. The simulation allowed input of an actual measured temperature - time history at node 1 and predicted the temperature - time history of one of the other two thermocouples located at node i in the simulation. In chosing the correct diffusivity in the simulation, the predicted temperature - time history duplicated the actual.

Figure 31

NODAL GEOMETRY

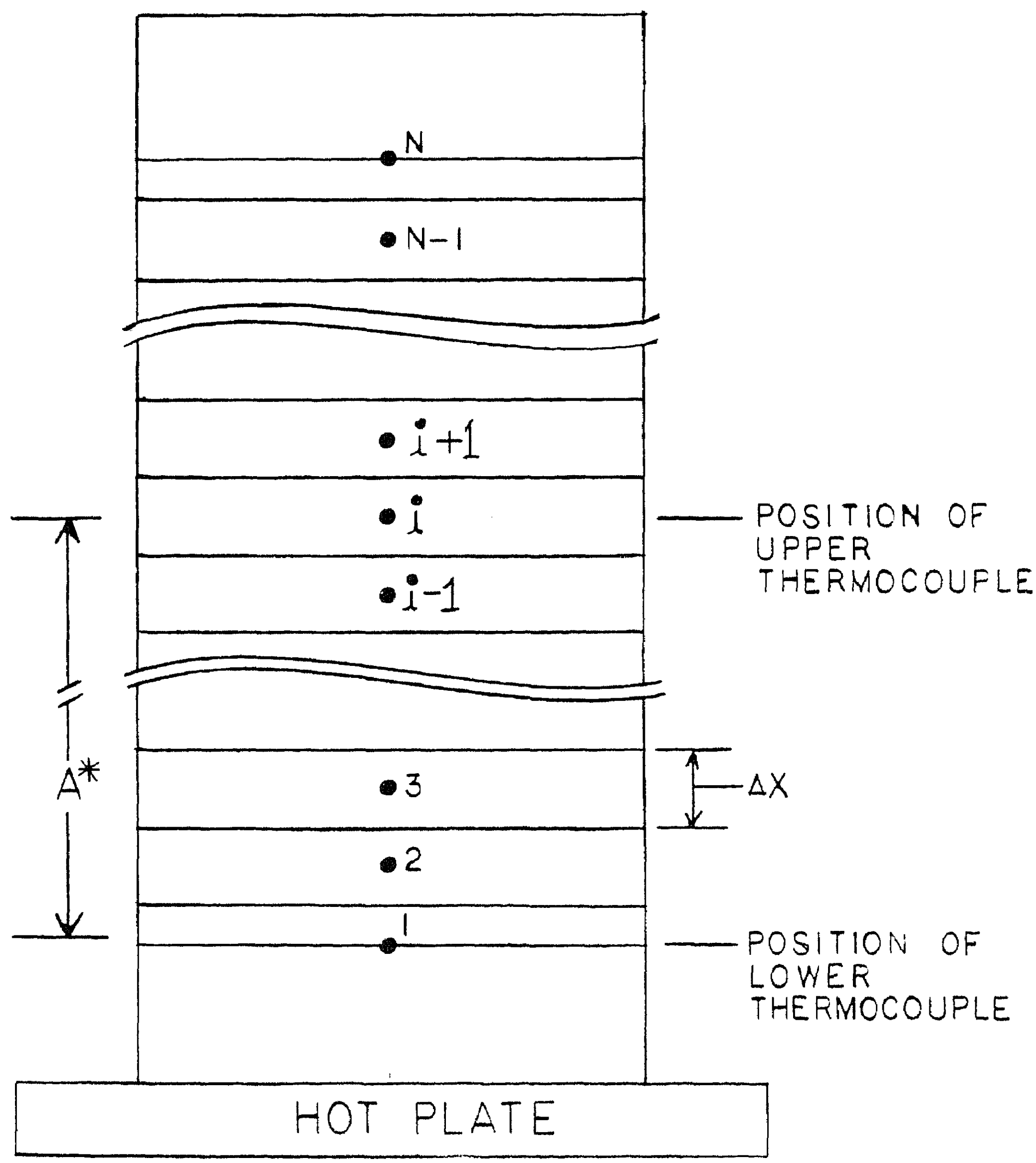

A* = DISTANCE BETWEEN THE TWO THERMOCOUPLES USED IN THE SIMULATION

Six predictions of diffusivities per experimental run were obtained in using the simulation. They included predicted diffusivities between positions stated in the previous paragraph. The method of selecting the correct diffusivity was through trial and error. If the diffusivity used was too low, the predicted temperature time history was lower than the actual. If the diffusivity used was too high, the predicted history was higher.

The extra nodes from i+1 to n were added to negate end effects. A technique to check that this assumption was valid was to perform the simulation with more nodes. If the predicted temperature time history at node i was unchanged then node i was uneffected by the end effects. In the actual experiment, end effects were negated by adding an additional quantity of powder, approximately one and a half inches above the last thermocouple.

There is essentially one nodal equation used in the flat plate simulation. For the internal nodes(node 2 to node n-1), the equation is:

$$T_j' = T_j * \left[1 - 2\, \frac{DT * AL}{DX^2} \right] + \frac{DT * AL}{DX^2} * \left[T_{j-1} + T_{j+1} \right] \qquad \text{(eq. 48)}$$

where T_j' = the temperature of node j one time increment(DT) latter.

T_j = the present temperature of node j

T_{j-1} = the present temperature of node j-1

T_{j+1} = the present temperature of node j+1

DT = time increment

AL = thermal diffusivity = $k/\rho C_p$

k = thermal conductivity

C_p = specific heat

ρ = density

The last node n is assumed adiabatic. The equation for this node is the same as equation 41 except T_{n+1} will have the same value as T_{n-1} , or:

$$T_n' = T_n * \left[1 - 2 \frac{DT * AL}{DX^2} \right] + 2 \frac{DT * AL}{DX^2} * T_{n-1} \qquad \text{(Eq 49)}$$

The computer simulation performs the following steps:

1 - Sets values for nodal distance(DX) and diffusivity(AL) and then determines the maximum time increment.

2 - Reduces the time increment to a division of a one minute interval so that temperatures will be calculated for each minute.

3 - Sets all nodes to the initial temperatures.

4 - Increments time by one time increment and sets node 1 to the temperature of the lower thermocouple at that time.

5 - Calculates the new nodal temperature for node 2 through node n.

6 - If the time is at a minute interval, then print the predicted temperature of the other thermocouple.

7 - Change the old nodal temperature values to the new predicted values.

8 - Go back to step 4 until the simulation is over.

To check the validity of this simulation, results of a trail simulation are compared to the Heisler Charts in Figure 32. Note the exact fit proving the simulation.

In the performance of this simulation, if the temperature time history of node i is identical to the experiment, the correct diffusivity must be ajusted accordingly and the simulation repeated. An example of the simulation - experiment matching for the Phillips Petroleum polyethylene(Appendix A) is shown in Figure 33.

Figure 34 shows the values of the diffusivity found with the corresponding thermal conductivity. This spread in values will be used in the rotational molding simulation to determine the effects in molding time. Appendix D lists the computer program used in this flat plate simulation.

Figure 32

COMPARISON BETWEEN SIMULATION AND HEISLER CHARTS

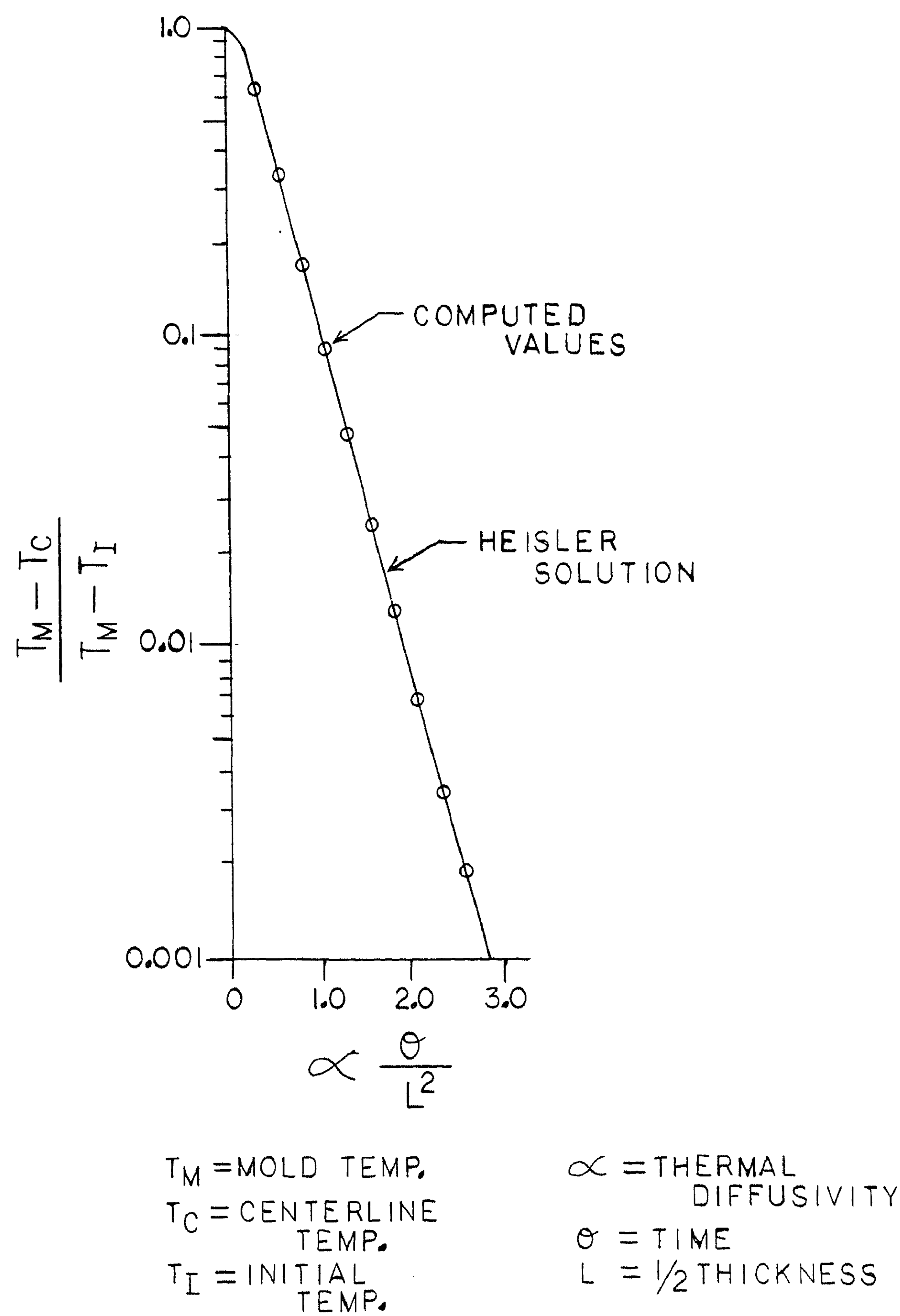

Figure 33

COMPARISON BETWEEN MEASURED AND COMPUTER PREDICTED TEMPERATURES

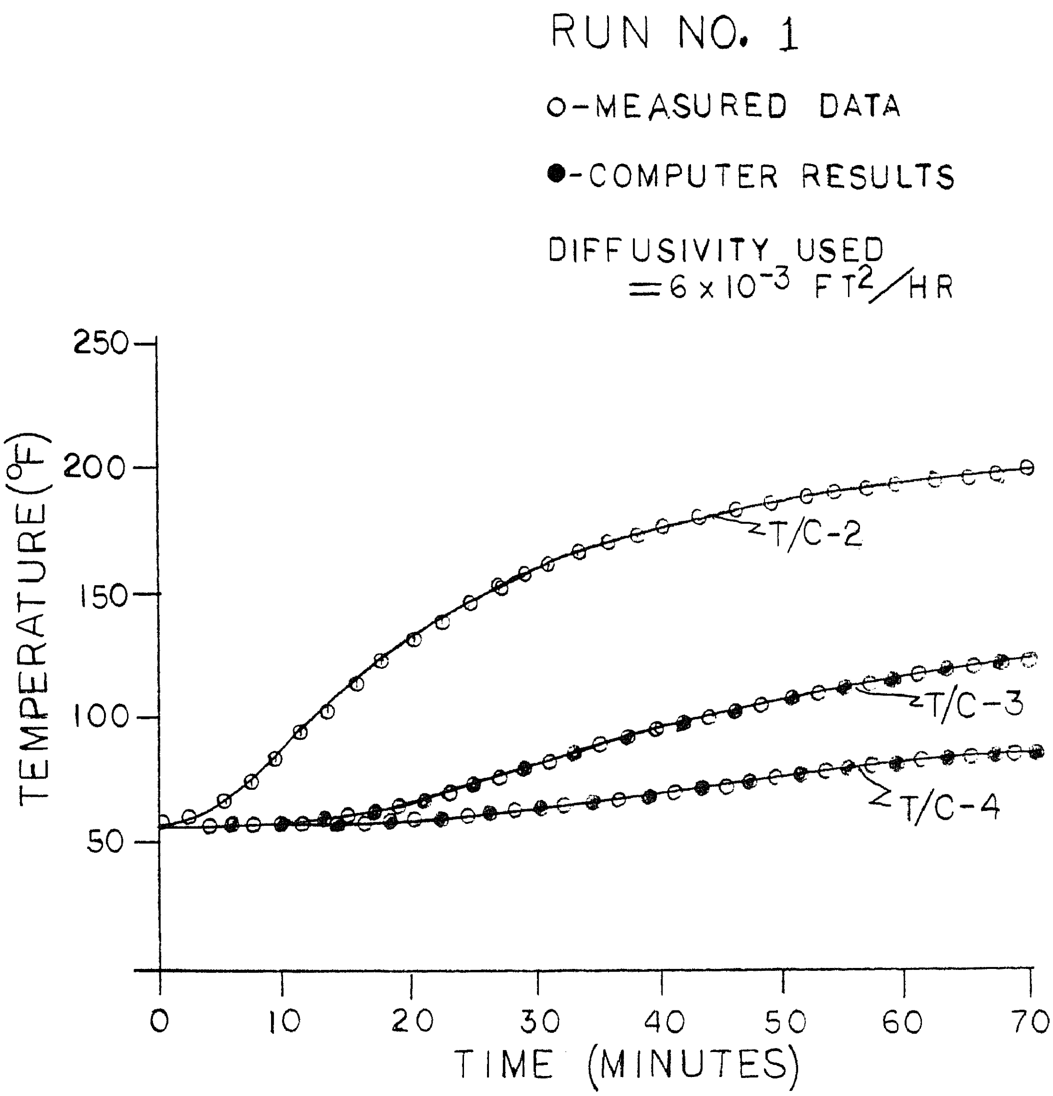

FIGURE 34

EXPERIMENTALLY AND COMPUTER SIMULATED DETERMINATION OF THERMAL CONDUCTIVITY

Run No.	Thermo-couples	Diffusivity (Ft2/Hr)	Diffusivity (Cm2/sec)	Thermal Conductivity (B/hr-ft-F)	Thermal Conductivity (J/cm-s-K)
1	2 - 3	6.0E-03	1.55E-03	0.105	1.82E-03
	2 - 4	6.0E-03	1.55E-03	0.105	1.82E-03
	3 - 4	6.0E-03	1.55E-03	0.105	1.82E-03
	5 - 6	7.5E-03	1.94E-03	0.131	2.27E-03
	5 - 7	6.5E-03	1.68E-03	0.113	1.96E-03
	6 - 7	7.5E-03	1.94E-03	0.131	2.27E-03
2	2 - 3	6.0E-03	1.55E-03	0.105	1.82E-03
	2 - 4	6.0E-03	1.55E-03	0.105	1.82E-03
	3 - 4	6.0E-03	1.55E-03	0.105	1.82E-03
	5 - 6	5.0E-03	1.29E-03	0.087	1.51E-03
	5 - 7	7.0E-03	1.81E-03	0.122	2.11E-03
	6 - 7	9.5E-03	2.45E-03	0.160	2.77E-03

Average Thermal Conductivity = .155 B/Hr-ft-F
Standard Deviation = 0.020 B/Hr-ft-F

NOTE: Thermal Conductivity calculated computed diffusivity using a density of 31.8 lb/ft3 and a specific heat of 0.55 B/lb-F (Appendix A).

X. THE COMPUTER SIMULATION FOR ROTATIONAL MOLDING

The rotational molding computer simulation (Appendix F) consists of the main program named ROTOTP, supported by the following subroutines: PRINT and CONST, and functions: VIS, SU, RHO, RADX, COND, and CP. The main program ROTOTP performs the simulation, PRINT is the printing routine and CONST computes the constants used in the nodal temperature equations. In addition CONST compute the neck growth for each node during every time increment. The functions VIS, SU, RHO, COND, and CP computes the viscosity, surface tension, density, thermal conductivity and specific heat respectively for each node. Function RADX computes the distance between adjacent nodes based on the density at those nodes.

The main program is divided into ten parts as is labeled in the program listing. Preceding Section I is a glossary of all variables used in the main programs. Section I initializes all the variables and sets all program flags. The variables include: the mold stick temperature(SS), the complete melt temperature(SM), the printing interval(PT), the number of wedges(NC), the material radius(RAD), the initial temperature(IT), the mold radius(RO), the radius from the center of the mold to the surface of the stationary pool material(RI), acceleration due to gravity(G), rotational speed of the mold(RPM), the angle of response(BA), and the coefficients used in the mold temperature-time history equation(A, B, and YY).

Section II performs initial computations using the initial values in Section I. They include computation of the pool angle theta(TH), cross-sectional area of stationary pool(AA), radial mold velocity(W), maximum penetration thickness(AD), maximum time increment(DT), the nodal distance(DX), and the number of nodes per column(N). This section then sets each node to the initial temperature and each nodal neck radius to zero. Then all major values are printed.

Section III begins the iteration process. The mold temperature(MT) based on time is determined. For each iteration the maximum time increment(DT) and time increment used(TS) is determined using the maximum diffusivity and the minimum nodal distance(all usually located at the surface node). Cross sectional areas(AT and AS), penetration thickness(AD) and free-fall time(TF) is also calculated for each iteration.

Section IV computes the nodal temperatures and nodal neck size at each nodal subvolume. The values C1, C2, C3, DB, and DA in the temperature equation and the new neck size is determined in the subroutine CONST. The program also checks each node to determine if its temperature is equal to or has exceeded the complete melt temperature(SM). When reached, the nodal neck radius becomes equal to the orginal radius of the material simulating full densification of the material.

Section V controls the printing of nodal temperatures and neck sizes. The printing time interval(PT) was selected in Section I. In addition, the temperature and neck size are printed at the point in time when there is no material remaining in the stationary pool and when all material has completely densified. At the end of the simulation, the neck size of each node location is printed showing the amount of neck growth that occured before complete melt had overcome the sintering process.

If mold sticking has not yet occured in the simulation, the program enters Section VI where it calculates the new free-fall section's average temperature for the next time interval. It calculates the temperature energy of the last column of the stationary pool that enters the free-fall zone during the next time interval and adds it to that remaining in the pool after a portion of it re-enters the stationary pool.

The program then rotates the stationary pool nodes over one column distance simulating one time increment of travel. For example, the values of the nodes in the next to the last column move over to the last column. The nodal values in the second to the last column are shifted to the next to the last column and so on.

Next, the nodes in the first column are then initialized to the temperature of the material that had just exited from the free-fall zone and re-entered the stationary pool. The computer simulation then returns to Section IV and begins another iteration process for the next time interval.

If there is material sticking to the mold, the program by-passes Section VI and goes on to Section VII where it determines the amount of material in the last column that will stick to the mold wall and the amount that enters the free-fall zone during the next time interval.

This routine then sets up new nodal columns to simulate the stuck material. Since the time interval(TS) decreases as the cross-section of the stationary pool decreases, the simulation maintains, for each stuck column, its width(DC), position in the mold(PS), the number of nodes(N3), its height(H2), the distance between the last two nodes of the column(H3), and the nodal neck sizes (ANECK). It must be noted that the stuck height(H2) is very seldom an integer of the nodal distance(DX), therefore all nodal distances are the length DX except between the last two nodes which has a distance larger than DX making up the extra distance.

This section then calculates the energy of the material in the stationary pool column not sticking but entering the free-fall zone.

Section VIII simulates the rotation of the mold when sticking has occured. The stationary pool and then the stuck material is rotated one column width in the same manner described in the discussion of Section VI. The values of the stuck column's width(DC), number of nodes(N3), height(H2), and the distance between the last two nodes(H3) is also shifted along with the column. The position(PS) is updated to reflect its new position in the mold.

Section IX checks if the rotation causes any of the stuck material to re-enter the stationary pool. If no re-entering occurs, the computer simulation goes to Section X. If re-entering occurs, the simulation determines the portion of column width(EN) that re-enters the pool as well as the portion remaining outside(OT).

The portion of the column remaining outside(OT) is combined to the adjacent column to make one equivalent column having a combined average nodal temperatures with a width equal to OT plus the width of the adjacent column.

The nodal temperatures and neck size of the stationary pool's first column is assigned the same values as the re-entering material(EN). Since the nodal distance of the last two nodes is usually larger than the normal nodal distance(DX), the last node is replaced by two nodes. The next to the last node will have the same neck size and temperature as the last node of the stuck material re-entering the pool. The remaining material is to be combined with the re-entering powder from the free fall zone to form an equivalent node. Additional nodal subvolumes are added representing the re-entering powder from the free fall zone adding an additional height equal to the penetration thickness.

If there is not enough mass in the stationary pool to allow adding the height of a penetration thickness, then fewer subvolumes are used having an equivalent cross sectional area equal to that of the remaining pool material. The last node will then be modeled as an adiabatic edge. The temperatures and neck radius nodal values of these added subvolumes are equal to that of the re-entering material from the free-fall zone.

Section X calculates the new angle theta(TH) based on the amount of material in the stationary pool zone. The program then returns to Section III and starts the iteration again for the next time increment.

When the amount of material in the stationary pool becomes zero, angle theta (TH) becomes zero. Therefore, the rotational simulation portion of this program is no longer needed making this simulation a simple one-dimensional heat transfer simulation having the number of columns equal to that of the number of columns of stuck material. The simulation then consists of the iteration process in Sections III and IV until the temperature of the last nodes reaches or exceeeds the complete melt temperature(SM). At that point, the simulation calls SUBROUTINE PRINT and then terminates the simulation by printing the neck size of each node height level at the point when complete melt had overcome the sintering process.

XI. COMPUTER SIMULATION WITH OVEN CONVECTION

To simulate heating by oven convection in rotational molding, a few significant modifications were made to the original nodal model and to the computer program earlier developed (as listed in Appendix F.).

The original model assumed a temperature-time relationship which was described by a polynomial equation for the mold's internal surface, NODE 1, that is in direct contact with the powdered material. The temperature values of the other nodes are then calculated during each iteration based on the temperature time history of NODE 1.

With oven convection, two additional nodes are used in the model accounting of the effect of the mold itself and the resistance between the heated air and the mold's surface. Figure 35 shows the position of these extra nodes. The node labled A in the figure represents the oven air and has a temperature value equal to the oven temperature, or:

$$T(A) = T(OVEN)$$

NODE B represents the exterior surface of the mold. Its nodal temperature equation (eq 36) is listed in Chapter VI. NODE 1 represents the interior surface of the mold having equation 38 as its nodal temperature equation. The

Figure 35

OVEN CONVECTION SURFACE NODAL CONVENTION

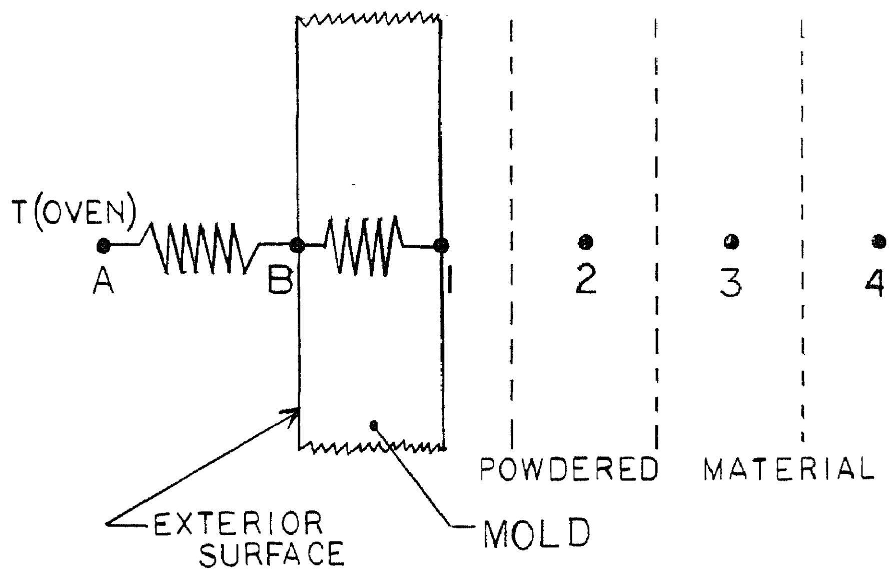

distance between NODE B and NODE 1 is equal to the thickness of the mold.

With the additional nodal equations, there are two additional stability equations, each having a maximum allowable time increment. The computer simulation calculates for each iteration the three maximum time increments and then allows the time increment used to be no greater than the minimum value of the three.

The future temperature values of NODE B and NODE1 as well as the remaining nodes are computed for each iteration using the nodal temperature equations developed. Appendix H is the listing of the Rotational Molding Simulation having oven convection.

XII. DISCUSSION OF RESULTS

Using the computer simulation program earlier developed, a number of runs were performed in order to predict pool depletion and total densification times with variations in temperature-time histories, rotational speeds, material amount, and thermal properties of the powdered material. The results of the rotomolding simulations as well as results of the Vanderbeck and Throne/Ahdout simulations are compared in Table 2 to the actual experimental results performed by Vanderbeck(30). The simulations reported in Table 2 used the polynominal temperature-time equations discussed earilier.

Section I of Table 2 compares each simulation at various power input levels having 50 grams of powdered material in the mold cavity. The different power inputs correspond to a particular mold temperature-time history as described by Vanderbeck(30). Results show a 40% to 55% error in the Vanderbeck simulation, a -3.6% to -10.2% error in the Throne/Ahdout simulation and a -2.1% to -11.1% error in the Rotational Mold Simulation developed here.

In Section II and III, the thermal diffusivity of the powder used in Section I was decreased by 20% and increased by 20% respectively. Simulations using the 500 watt and

TABLE 2

POOL DEPLETION TIMES

	POWER INPUT (WATTS)	RPM	MATERIAL AMOUNT (GRMS)	RI	ACTUAL TIME (SEC)	VANDERBECK PREDICTED (SEC)	VANDERBECK % ERROR	ROTOMOLD SIMULATION THERMAL DIFFUSIVITY (CM2/SEC)	ROTOMOLD SIMULATION PREDICTED (SEC)	ROTOMOLD SIMULATION % ERROR	THRONE/AHDOUT SIMULATION PREDICTED (SEC)	THRONE/AHDOUT SIMULATION % ERROR
I	500	7	50.0	4.796	383	553	44	1.70E-03	375	-2.1	369	-3.6
	600	7	50.0	4.796	335	470	40	1.70E-03	315	-5.9	310	-7.4
	700	7	50.0	4.796	300	439	46	1.70E-03	276	-7.9	278	-7.3
	800	7	50.0	4.796	274	411	55	1.70E-03	244	-11.1	246	-10.2
II	500	7	50.0	4.796	383	---	---	1.36E-03	378	-1.2	376	-1.8
	800	7	50.0	4.796	274	---	---	1.36E-03	247	-9.9	246	-10.2
III	500	7	50.0	4.796	383	---	---	2.04E-03	372	-3.0	363	-5.2
	800	7	50.0	4.796	274	---	---	2.04E-03	240	-12.4	239	-12.8
IV	800	10	50.0	4.796	277	392	42	1.70E-03	235	-15.1	246	-11.2
	800	15	50.0	4.796	275	368	34	1.70E-03	229	-16.7	246	-10.5
	800	20	50.0	4.796	267	354	33	1.70E-03	227	-15.0	246	-7.8
	800	25	50.0	4.796	268	340	27	1.70E-03	225	-16.0	246	-8.2
V	700	10	50.0	4.796	302	424	40	1.70E-03	268	-11.2	278	-7.9
	700	15	50.0	4.796	302	403	34	1.70E-03	262	-13.2	278	-7.9
	700	20	50.0	4.796	303	388	28	1.70E-03	259	-14.5	278	-8.2
	700	25	50.0	4.796	292	373	28	1.70E-03	258	-11.6	278	-4.8
VI	500	7	84.5	1.361	508	655	29	1.70E-03	508	0	737	45.1
	600	7	84.5	1.361	437	573	31	1.70E-03	459	5.0	647	48.1
	700	7	84.5	1.361	399	516	29	1.70E-03	424	6.2	596	49.4
	800	7	84.5	1.361	366	486	33	1.70E-03	392	7.1	546	49.1

For Temperature Equation Used: $T = At + Bt^2 + IT$

IT = 20 C

Watts	A	B
500	18.2	-0.324
600	22.0	-0.430
700	25.0	-0.531
800	29.0	-0.711

800 watt temperature-time histories resulted in the predicted pool depletion times shown for both the Throne/Ahdout and the Rotational Mold Simulations. For the 20% change, the Rotomolding Simulation showed a change between 0.8% and 1.6% while the Throne/Ahdout Flat Plate simulation resulted in a 1.6% to 3.3% change.

Section IV and V in Table 2 show the results of varying the rotational speed of the mold. The Vanderbeck simulation yielded a difference of 27% to 42% between the predicted and actual experimental results. Because the Throne/Ahdout simulation is a flat plate analysis with no rotational parameter, the pool depletion times are constant for power input reguardless of the actual rotational speed. The Throne/Ahdout simulation produced a 4.8% to 11.2% difference between actual and experimental results. The Rotational Mold Simulation had a 11.2% to 16.7% difference.

Note that the Rotational Mold Simulation developed here predicts a time difference of 10 seconds between the 10 RPM and 25 RPM pool depletion times of the 800 watt power input while the actual experimental difference was 9 seconds. For the 700 watt power input, the predicted and actual experimental time differences were identical with 10 seconds.

Section VI is the actual and predicted pool depletion time results of a mold containing 84.5 grams of powder. The Throne/Ahdout has a difference ranging from 45.1% to 49.1%. The Rotomold Simulation produced a 0.0% to 7.1% difference.

Table 3 is a comparison of pool depletion and total densification times with the Rotomold and Throne/Ahdout simulation containing a 50 gram charge using oven convection coefficients in lieu of the polynomial temperature equations. Using a typical oven temperature of 371 degrees Centigrade, an aluminum mold thickness of 0.655 cm yielded results showing a close agreement between the two simulation for typical air convection coefficients.

The previous comparison of the 50 gram charge simulations show that the Rotomold Simulation developed here and the Throne/Ahdout Simulation will predict pool depletion and total densification times within a satisfactory tolerance. The Vanderbeck Simulation however, showed between 27% and 57% error. It also showed at those power inputs an insensitivity to changes in thermal conductivity.

It is confusing however, that for the 50 gram charge simulations, the Throne/Ahdout Simulation which is a flat plate simulation with no rotation or thermal mixing has as

TABLE 3

DEPLETION AND DENSIFICATION TIMES

Convection Coefficient (B/Hr-Ft2-F)	(J/sec-cm2-K)	Ribe Simulation (sec) Depletion	Densification	Throne/Ahdout Simulation (sec) Depletion	Densification
2	1.1356E-03	442	577	431	572
4	2.2712E-03	241	300	232	295
6	3.4068E-03	174	208	167	204
8	4.5424E-03	141	162	134	158
10	5.6780E-03	126	135	125	135

Material Stick Temperature (deg C) = 110
Material Melt Temperature (deg C) = 138
Oven Air Temperature (deg C) = 371.0
Amount of material in mold (grams) = 50.0

Properties of Aluminum Mold

Thermal Conductivity (J/cm-sec-K) = 2.025
Density (Kg/Cm3) = 2.707E-03
Specific Heat (J/Kg-K) = 8.7085E-02
Thermal Diffusivity (Cm2/sec) = 8.588

good as or even better results then the Rotational Mold Simulation developed. It would seem logical that the flat plate simulation temperature profile would show a maximum temperature at the mold's surface dropping rapidly to a minimun temperature at the inner surface. The difference between the minimum and maximum temperature would then increase with time causing a dramatic increase in predicted pool depletion and densification time for the powdered material. The flat plate simulation did not predict this. In fact, its predictions for the temperature profiles were very close to the Rotomold Simulation.

This seeming discrepency can be explained. In the Vanderbeck experiments, the pool depletion times for 500 through 800 watts are shown(Table 3) equivalent to an oven convection coefficient of approximently 1.137E-03 to 2.271E-03 J/Sec-cm2-K (2.0 to 4.0 B/hr-ft2-F). The ratio of the convection coefficient to the thermal conductivity of the powder divided by the thickness(h/(k/L)) determines the temperature profile. Krieth (55) states that if the ratio, h/(k/L) is less than 0.1 then the temperature throughout the material can be assumed constant for transcient thermal analysis. In other words, the heat input is so slow that it allows the material to distribute its internal energy evenly.

Pre-distributing 50 grams of powdered material around the mold will result in a material height of 0.4 cm, the ratio, h/(k/L) varies between 0.22 and 0.46. Although these values are not below 0.1, they are close enough to produce similar results. In addition, because these ratios are low, a 20% change in either direction of the thermal conductivity (as was reported in Section II and III of Table 2) would produce very little change in the pool depletion and total densification times.

With 80 grams of material charge, the material height (the value L) becomes 1.67 cm increasing the ratio four fold. Section VI of Table 2 shows the dramatic change in prediction times of the Throne/Ahdout simulation as compared to the actual results. The error now increases to a range of 45% to 49%.

By increasing the thermal conductivity, Table 4 shows again the limitation of the Throne/Ahdout simulation. Notice that as the conductivity, k, becomes smaller (making h/(k/l) larger), the deviation between the Rotational Molding Simulation and the Throne/Ahdout Simulation becomes extremely large.

Similar results are found if the value of the coefficient of convection becomes large as may occur in

TABLE 4

DEPLETION AND DENSIFICATION TIMES AS A FUNCTION OF THERMAL CONDUCTIVITY

Thermal Conductivity (J/Cm-sec-K)	Thermal Diffusivity (cm2/sec)	Ribe Simulation (sec)		Throne/Ahdout Simulation) (sec)	
		Depletion	Densif.	Depletion	Densif.
1.99E-02	1.7E-02	95	84	116	113
1.99E-03	1.7E-03	126	126	135	135
1.99E-04	1.7E-04	154	245	200	258
1.99E-05	1.7E-05	215	873	418	919

Material Stick Temperature (deg C) = 110
Material Melt Temperature (deg C) = 138
Oven Air Temperature (deg C) = 371.0
Amount of material in mold (grams) = 50.0
Oven Convection Coefficient (J/cm2-sec-K) = 5.678E-03

Properties of Aluminum Mold

Thermal Conductivity (J/cm-sec-K) = 2.025
Density (Kg/Cm3) = 2.707E-03
Specific Heat (J/Kg-K) = 8.7085E-02
Thermal Diffusivity (Cm2/sec) = 8.588

radiant and forced Fluid heating of the mold. Table 5 illustrates the effect of changing convection coefficients by factors of magnitude. Again, high errors (19% to 34%) occur in the prediction of the pool depletion and densification times.

In summary, the Throne/Ahdout Simulation is accurate only when using certain combinations of the simulation parameters, otherwize large errors will occur in pool depletion and total densification predictions. The Rotational Molding Simulation developed in this dissertation does predict accurate times for the pool depletion and densification as was verified by the experimental results of Van der Beck(30). It models closely the material flow, mold heating of the powdered material, rotation of the stationary pool and material melted to the mold wall, and the thermal and physical mixing during the free-fall zone.

TABLE 5

DEPLETION AND DENSIFICATION TIMES

AS A FUNCTION OF CONVECTION COEFFICIENT

Convection Coefficient (J/Cm2-S-K)	Depletion Times (sec) Ribe Sim.	T/A Sim.	% Diff.	Densification Times Ribe Sim.	T/A Sim.	% Diff.
3.407E-03	331	445	34	355	468	32
3.407E-02	122	151	24	137	178	30
3.407E-01	101	121	20	109	130	19
3.407	99	118	19	105	125	19

Material Stick Temperature (deg C) = 110
Material Melt Temperature (deg C) = 138
Oven Air Temperature (deg C) = 371.0
Amount of material in mold (grams) = 80.0
Thermal Diffusivity (Cm2/sec) = 1.7E-03

Properties of Aluminum Mold

Thermal Conductivity (J/cm-sec-K) = 2.025
Density (Kg/Cm3) = 2.707E-03
Specific Heat (J/Kg-K) = 8.7085E-02
Thermal Diffusivity (Cm2/sec) = 8.588

NOTE: T/A = Throne/Adhout

XIII. CONCLUSIONS AND REMARKS

This dissertation has presented an investigation of the densification process in rotational molding of a thermoplastic powder in a cylindrical cavity.

First, a thorough literature survey was performed to review past works of rotational molding analysis, as well as the study of sintering, the effects of temperature on viscosity and surface tension for polymeric material, a review of thermal conductivity equations of composite materials and a review of other areas that would assist in the analysis of the densification process in rotational molding.

Next, an in depth study of the mass flow in a rotating cylinder together with an analysis of the heat transfer during rotational molding were performed to attain the understanding necessary to model the densification process.

The densification process in rotational molding was then modeled mathematically using Nodal Analysis. Nodal temperature equations were derived for typical oven convection heating and a special case where the mold's temperature-time history is known. The special case was modeled to provide a comparison and validation of the simulation developed with previous experimental research.

The research for this dissertation included an exhaustive investigation and analysis into the densification process (neck formation) by use of Scanning Electronic Microscope(SEM) photography. Because of the large depth-of-field of the SEM, photographs which were almost impossible to obtain before, allow the analysis to be performed. Based on this analysis, the intermediate physical property correlations needed in the nodal temperature equations were derived.

Lacking an agreement between results of published composite thermal conductivity equations, a hybrid experimental procedure coupled with a computer simulation was devised to determine the actual initial thermal conductivity of the powdered polymeric material.

Finally, a computer program was written to simulate the heating and densification during the rotational molding process. Results showed agreement with actual rotational molding experimental findings. In addition, results of other simulations were compared showing their shortcomings.

It is important to include in this summary a discussion of one logistical drawback in the use of this simulation; that being the amount of computer time required.

Because of the intricate modeling, the simulation will require from 800 to 6000 seconds of computer time. This equates to a maximum of $650.00 per simulation when used on a Control Data Corp. mainframe system(CDC 6500).

If, because of cost, the use of the Rotational Molding Simulation becomes prohibitive, modifications to the Throne/Ahdout Simulation will improve its accuracy. A complete examination and modification to the Throne/Ahdout Simulation is beyond the scope of work for this dissertation. However let it be noted that the major modification would encompass a thermal mixing routine to simulate the free fall thermal/physical mixing zone for the powdered material that has a temperature below the stick temperature.

Since miminal computer cost was not an original requirement, this dissertation has performed and completed all its objectives. It has investigated the heating and densification portion of the rotational molding process. Included, was an analysis of the heat transfer, mass flow and neck formation colmenating into a valid and proven simulation.

APPENDIX A

NOMINAL PHYSICAL PROPERTIES OF MARLEX LX470 (POLYETHYLENE)

PROPERTY[1]	ASTM	Metric Units	Value
Density	D1505	g/cm3	0.943
Melt Index	D1238	g/10 min	3.0
Flow Index, CIL, 190C 10.4 MPa[2]		g/10 min	3.0
Brittleness Temperature	D746	Deg. C	-118
Specific Heat @ 90C(ref 58)		cal/g-C	0.55
ROTATIONAL MOLDED PROPERTIES[3]			
ESCR, Condition A, F50	D1693	h	200
Tensile Strength at Yield 2"(50.8 mm) per min.	D638 Type IV Spec	MPa	22.1
Elongation 2"(50.8 mm) per min.	D638 TYPE IV Spec	%	350
Flexural Modulus	D790	MPa	965
Impact ARM Standard[4] at -28.9 deg C		J	68

[1] Physical properties reported herein were determined on compression molded speciments prepared in accordance with Procedure C of ASTM D1928 (Ref 57).

[2] Data obtained using a gas extrusion plastometer based on design by Canadian Industries, Ltd., with a die having an orifice diameter of 0.49 mm and a land length of 4.48mm.

[3] Physical properties are based on parts molded at optimum conditions (Ref 57).

[4] Ten pound dart with 0.5 inch point in center of 0.125 inch thick unsupported 3.5 inch diameter area.

APPENDIX A (continued)

U. S. STANDARD SIEVE SIZE DISTRIBUTION OF MARLEX LX470

Size	Inches	mm	Percent of material stopped by sieve
30	0.0232	0.590	0.0007
35	0.0197	0.500	4.40
40	0.0164	0.420	16.41
45	0.0138	0.350	20.81
50	0.0117	0.297	19.19
60	0.0088	0.250	5.96
80	0.0070	0.177	18.10
100	0.0059	0.149	7.78
120	0.0049	0.125	3.56
170	0.0035	0.088	2.32
200	0.0029	0.074	1.05
230	0.0025	0.063	0.27
270	0.0021	0.055	0.11
PAN	----	---	0.14
			100.00 %

Measured Specific Gravity of Powder = 0.5096
Specific Gravity of Resin = 0.9430

Void Fraction of Air = 45.96%

APPENDIX B

PHYSICAL PLASTIC PROPERTIES OF ONE-EIGHT DIAMETER SPHERES MADE OF POLYETHYLENE AND ACRYLIC

PROPERTY	UNITS	POLY-ETHYLENE	ACRYLIC
Impact Strength, Notched Izod	Ft-lb/in	1 - 10	0.4 - 0.6
Tensile Strength	PSI x 1000	2.5 - 5	7.9
Tensile Modulus	PSI x 1000	85 -160	350 - 450
Thermal Conductivity	Cal/cm2/sec/ C/cm x 10000	8	4 - 6
Specific Gravity		0.94 - 0.96	1.18 - 1.19
Elongation	%	5 - 10	2 - 10
Flexural Strength	PSI x 1000	2 - 3	14 - 16
Flexural Modulus	PSI x 1000	90 - 150	350 - 450

APPENDIX C

PHYSICAL PROPERTIES OF MICROSPHERES COMMERICALLY NAMED "ELVACITE" ACRYLIC RESINS 2021 by DuPont

Density(resin) 1.196 Kg/M3
Glass Transition Temperature 100 Deg C
Tukon Hardness, Knoop No. 20
Tensile Strength (23 Deg C., 50% RH) 106 MPa 15kPsi
Elongation at Break (23 Deg C., 50% RH) 4%

U. S. STANDARD SIEVE SIZE DISTRIBUTION

Sieve Size	Inches	mm	Percent of material stopped by sieve
30	0.0232	0.590	0.48
35	0.0197	0.500	0.16
40	0.0164	0.420	0.18
45	0.0138	0.350	0.27
50	0.0117	0.297	3.26
60	0.0088	0.250	18.87
80	0.0070	0.177	65.58
100	0.0059	0.149	4.83
120	0.0049	0.125	3.28
170	0.0035	0.088	1.92
200	0.0029	0.074	0.92
230	0.0025	0.063	0.10
270	0.0021	0.055	0.08
PAN	----	---	0.07
			100.00 %

Measured Specific Gravity of Powder = 0.730
Specific Gravity of Resin = 1.196

Void Fraction of Air = 38.96%

APPENDIX D

FLAT PLATE SIMULATION

```
90 REM SLAB TEMPERATURE TIME HISTORY SIMULATION
95 DIM T(30),TN(30),TT(15),TP(15)
97 OPEN1,4,2
100 AL=6.200E-03:REM FT2/HR
105 PRINT#1,"AL = ";AL
110 AL=AL*0.04 :REM IN2/SEC
120 DX=0.09375   :N=17  :REM DX IN INCHES
125 TM=0.0  :NN=0
130 TS=DX©2/(2*AL)
140 M=INT(60/TS)+1
150 DT=60/M
160 FORJJ=1TO11:READ TT(JJ):NEXTJJ
170 FORJJ=1TO11: READ TP(JJ):NEXTJJ
180 FORI=1TON:T(I)=TP(1):NEXTI
200 TM=TM+DT:NN=NN+1
210 GOSUB 1000
220 T(N+1)=T(N-1)
230 FOR I=2TON
240 TN(I)=T(I)*(1-2*DT*AL/DX©2)+DT*AL/DX©2*(T(I-1)+T(I+1))
245 IFTN(I)<T(I)THEN STOP
250 NEXTI
260 FORI=2TON:T(I)=TN(I):NEXTI
265 PRINTTM;T(9)
270 IF INT(NN/M)=NN/M THEN PRINT#1,TM;TM/60,T(1),T(9),T(16)
280 IF TM/60>60 THEN  PRINT#1:CLOSE1:STOP
290 GOTO200
1000 REM SUBROUTINE TO DETERMINE 1ST NODE TEMPERATURE
1010 FOR JJ=2TO11
1020 IF(TM/60 <TT(JJ)) THEN 1030
1025 NEXTJJ
1030 RA=(TM/60 -TT(JJ-1))/(TT(JJ)-TT(JJ-1))
1035 IFRA=0THEN T(1)=TP(JJ-1):RETURN
1040 T(1)=TP(JJ-1)+RA*(TP(JJ)-TP(JJ-1))
1050 RETURN
2000 DATA 0,2,5,10,15,20,30,40,50,60,100
2010 DATA 64,67,86,127,153,171,195,210,220,227,227
```

APPENDIX E

FLOW DIAGRAM FOR THE ROTATIONAL MOLDING SIMULATION

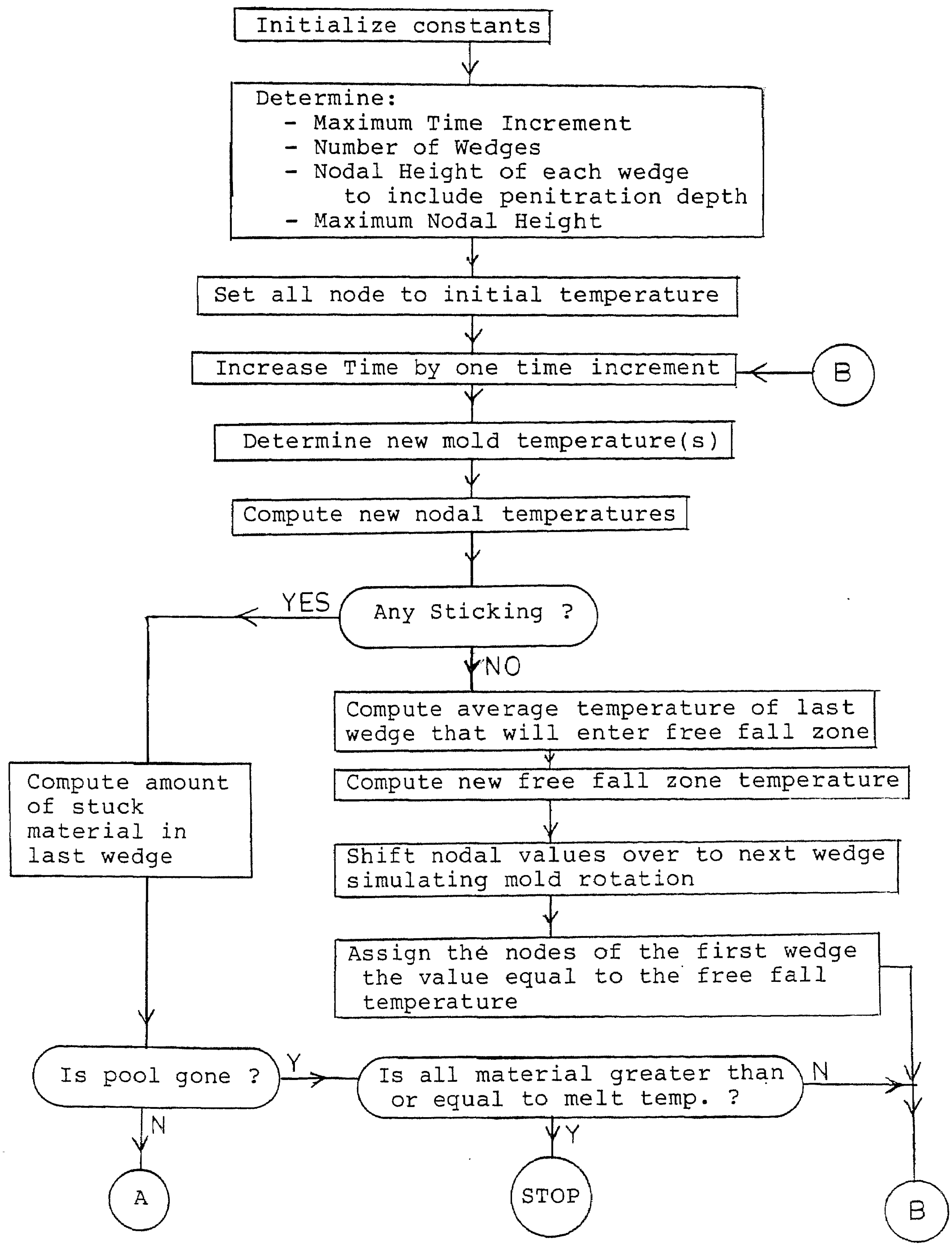

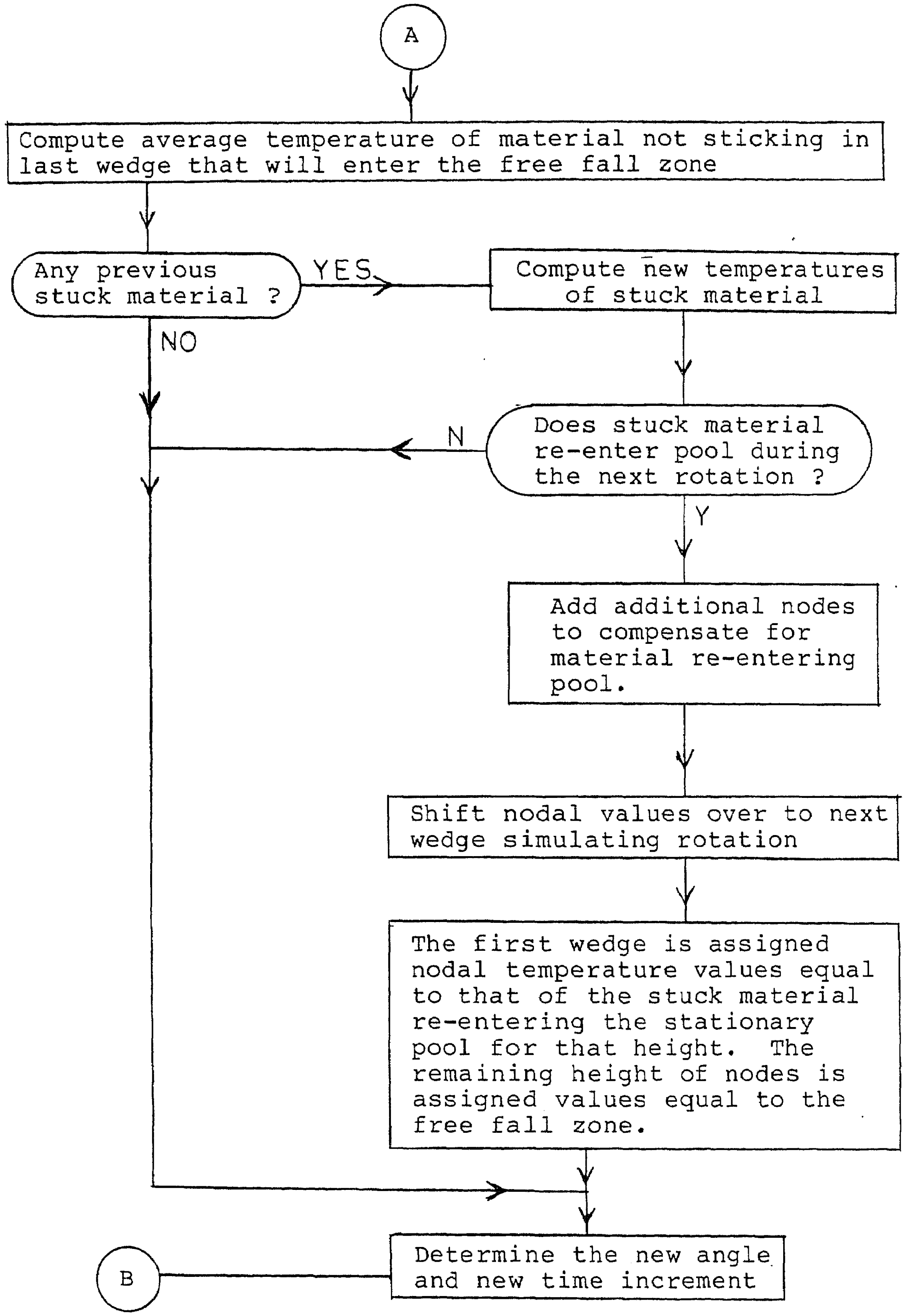
A
Compute average temperature of material not sticking in last wedge that will enter the free fall zone
Any previous stuck material ?
YES
NO
Compute new temperatures of stuck material
Does stuck material re-enter pool during the next rotation ?
N
Y
Add additional nodes to compensate for material re-entering pool.
Shift nodal values over to next wedge simulating rotation
The first wedge is assigned nodal temperature values equal to that of the stuck material re-entering the stationary pool for that height. The remaining height of nodes is assigned values equal to the free fall zone.
Determine the new angle and new time increment
B

APPENDIX F

ROTATIONAL MOLDING SIMULATION

```
      PROGRAM R485(INPUT,OUTPUT,TAPE5=INPUT,TAPE6=OUTPUT,TAPE8)
      DIMENSION TN(100),T(200,100),DC(200),PS(200),N3(200),H3(200)
     C ,H2(200),ANECK(200,100),BNECK(100),ANEK(100)
      COMMON SS,SM,AL,AM,DX,N,TM,AA,AT,AD,TH,DL,N2,CT,NC,N3,RAD,TS
      COMMON TAIR,BMT,MT
      INTEGER CT,KL
      REAL H,H3,H2,K,M,IT,HT,LT,MT,H1,MTN
      DATA ANECK,BNECK/20000*0.0,100*0.0/
C
C     GLOSSARY
C
C          A COEFFIEIENT IN TEMPERATURE EQUATION
C          AA  TOTAL CROSS SECTIONAL POOL AREA (CM2)
C          AD  PENITRATION THICKNESS (CM)
C          AL  INITIAL THERMAL DIFFUSIVITY (CM2/SEC)
C          AM  THERMAL DIFFUSIVITY AT COMPLETE MELT (CM2/SEC)
C          ANECK  NECK RADIUS AT EACH NODE (CM)
C          ANEK  NECK RADIUS OF EACH NODAL AREA AT THE TIME
C                    MELTING OVERCOMES THE SINTERING PORCESS (CM)
C          ANK  DUMMY VARIABLE = ANECK(1,1)
C          AR  DUMMY VARIABLE USED IN CALCULATING REMAINING
C                    CROSS SECTICNAL POOL AREA
C          AS  TOTAL AREA ENCOMPANSING NODAL ANALYSIS
C                    ( HEIGHT OF NODES X TOTAL WIDTH)
C          AT  CROSS SECTIONAL AREA OF ONE WEDGE (CM2)
C          AV  DUMMY VARIABLE USED TO DETERMINE NEW ANGLE THETHA
C          A3  CROSS SECTIONAL AREA OF STUCK COLUMN OF MATERIAL THAT
C                    THAT RE-ENTERS THE POOL IN THE NEXT TIME INCREMENT (C
C          A4  THE CROSS SECTIONAL AREA OF THE STUCK COLUMN OF
C                    MATERIAL THAT REMAINS OUTSIDE THE POOL
C                    DURING THE NEXT TIME INCREMENT (CM2)
C          B  COEFFICIENT IN TEMPERATURE EQUATION
C          BA  ANGLE OF RESPONSE OF THE POOL (RAD)
C          BB  DUMMY VARIABLE USED IN TEMPERATURE EQUATION
C          BE DUMMY VARIABLE USED SURFACE NODAL NECK SIZE EQUATION
C          BNECK  NEW COMPUTED NECK SIZE FROM SUBROUTINE (CM)
C          CC HALF LENGTH OF POOL CORD (CM)
C          CT  COUNTER USED TO COUNT THE NUMBER OF STUCK COLUMNS
C          C1  CONSTANT USED IN TEMPERATURE EQUATIONS DETERMINED IN
C                    SUBROUTINE CONST
C          C2  CONSTANT USED IN NODAL TEMPERATURE EQUATIONS
C          C3  CONSTANT USED IN NODAL TEMPERATURE EQUATIONS
C          DA  AVERAGE DIFFUSIVITY BETWEEN NODES I+1 AND NODE I (CM2/SEC)
C          DB  AVERAGE DIFFUSIVITY BETWEEN NODES I-1 AND NODE I (CM2/SEC)
C          DC  ARC WIDTH OF STUCK NODAL COLUMNS (RAD)
C          DL  ARC LENGTH PER TIME INCREMENT (RAD/SEC)
C          DT  MAXIMUM TIME INCREMENT (SEC)
C          DX  DISTANCE BETWEEN NODES (CM)
C          EN  PORTION OF COLUMN ARC WIDTH RE-ENTERING THE
C                    STATIONARY POOL (RADIANS)
C          FT  AVERAGE TEMPERATURE OF MATERIAL IN FREE FALL ZONE (C)
C          G  ACCELLERATION DUE TO GRAVITY (CM/SEC2)
C          H  HEIGHT OF STUCK MATERIAL LEAVING  POOL (CM)
C          HT DUMMY VARIABLE USED IN COMPUTING POOL ANGLE THETHA
C          H1  HEIGHT OF STUCK MATERIAL LEAVING POOL DURING THE NEXT
```

```
C          TIME INCREMENT (CM)
C       H2  HEIGHT OF STUCK MATERIAL COLUMN OUTSIDE POOL
C       H3  DISTANCE BETWEEN LAST TWO NODES OF EACH COLUMN OF
C                STUCK MATERIAL OUTSIDE POOL (CM)
C       I  COUNTING VARIABLE USED IN DO-LOOPS
C       IFLAG  FLAG SHOWING THAT NODAL HEIGHT HSD REACHED
C                ITS MAXIMUM WHEN ≠ 1
C       II  COUNTING VARIABLE USED IN DO-LOOPS
C       III  COUNTING VARIABLE USED IN DO-LOOPS
C       IREM  FLAG SHOWING POOL MASS IS GONE WHEN = 0
C       IT  INITIAL TEMPERATURE OF POOL POWDER (C)
C       I2  DUMMY VARIABLE USED WITH THE PRINT SUBROUTINE
C       I3  DUMMY VARIABLE USED IN THE PRINT SUBROUTINE
C       J  COUNTING VARIABLE USED IN DO-LOOPS
C       JI  COUNTING VARIABLE USED IN DO-LOOPS
C       JJ  COUNTING VARIABLE USED IN DO-LOOPS
C       JJI  COUNTING VARIABLE USED IN DO-LOOPS
C       JK  DUMMY VARIABLE
C       JL  FLAG
C       JTVAL  DUMMY VARIABLE
C       K  DUMMY VARIABLE
C       KK  FLAG VARIABLE
C       KL  DUMMY VARIABLE
C       K4  DUMMY VARIABLE
C       LK  COUNTING INTEGER USED WITH PRINT SUBROUTINE
C       LT DUMMY VARIABLE
C       M  CROSS SECTIONAL OF  MASS  LEAVING POOL AND STUCK TO WALL
C       MT  MOLD TEMPERATURE (C)
C       N  NUMBER OF NODES IN EACH STATIONARY POOL COLUMN
C       NC  NUMBER OF POOL COLUMNS OF NODES
C       NEC  COUNTING VARIABLE
C       NMAX  MAXIMUM NODE HEIGHT BASED ON VOLUME OF POOL (CM)
C       NNAX  EQUALS N+1
C       NNTP  DUMMY VARIABLE WHICH EQUALS N6+N4+1
C       N2 COLUMN NUMBER OF STUCK MATERIAL
C       N3  NUMBER OF NODES IN STUCK COLUMN MINUS 2
C       N3TEMP  DUMMY VARIABLE
C       N4 DUMMY VARIABLE
C       N6  NUMBER OF NODES IN PENETRATION THICKNESS
C       OT  PORTION OF RE-ENTERING STUCK COLUMN NOT ENTERING POOL (RAD)
C       PS  POSITION OF A PARTICULAR STUCK COLUMN IN MOLD (RAD)
C       PT  PRINTING INTERVAL (SEC)
C       RA  RATIO OF RI/RO
C       RAD  INITIAL RADIUS OF MATERIAL (CM)
C       RB  DUMMY VARIABLE
C       RI  RADIUS FROM MOLD CENTER TO SURFACE OF STATIONARY POOL (CM)
C       RM  DUMMY VARIABLE
C       RO  INNER RADIUS OF MOLD (CM)
C       RPM  ROTATIONAL SPEED OF MOLD (RPM)
C       R2 DUMMY VARIABLE
C       SM  COMPLETE MELT TEMPERATURE (DEG C)
C       SR  RATIO OF FREE-FALL TIME TO TIME INTERVAL TS
C       SS  TEMPERATURE THAT MATERIAL BEGINS STICKING TO THE MOLD (C)
C       S1  DUMMY VARIABLE USED IN WEDGE AREA EQUATION
C       S2  DUMMY VARIABLE USED IN WEDGE AREA EQUATION
C       T  NODAL TEMPERATURE
C       TF  FALL TIME IN FREE FALL ZONE (SEC)
```

```
C         TH  ANGLE  (THETHA) FROM CENTER OF MOLD TO JUNCTION OF
C                   POOL SURFACE AND MOLD (RAD)
C         TM  TIME
C         TN  NEW COMPUTED NODAL TEMPERATURE (C)
C         TP  COMBINED NODAL TEMPERATURE USED IN DETERMINING
C                   AVERAGE TEMFERATURE (C)
C         TS  TIME INTERVAL USED (SEC)
C         TW  CONTACT TIME OF MATERIAL TO WALL IN POOL REGION (SEC)
C         W   ROTATIONAL SPEED OF MOLD (RAD/SEC)
C         X5  POSITION OF LEADING AREA OF STUCK MATERIAL (RAD)
C         YY  CONSTANT IN TEMPERATURE EQUATION
C
C    *****  SECTION I  *****
C
      EN=0.0
      IREM=1
      LK=0
      NEC=1
      IFLAG=0
      PT=30.0
      TM=0.0
      NC=8
      RAD=0.0125
      RI=1.360 E
      RO=6.6675
      RPM=10.0
      BA=53
      SS=110.0
      SM=138.0
      IT=20.0
      A=22.0
      B=-0.430
      YY=20.0
      G=980.0
C
C    *****  SECTION II  *****
C
      RA=RI/RO
  220 TH=(3.14159/2.0-ATAN(RA/(-RA*RA+1.0)**0.5))*2
C     DETERMINE AREA IN STATIONARY POOL
      AA=0.5*RO*RO*(TH-SIN(TH))
      AL=COND(0)/(CP(0)*RHO(0))
      AM=COND(RAD)/(CP(RAD)*RHO(RAD))
      W=0.10472*RPM
      TW=TH/W
      TS=TW/NC
      ITM=0
      ITMX=1
      TM=TM+TS
C     DETERMINE MAXIMUM PENITRATION DISTANCE
      AD=7.2*(AL*TW)**0.5
C     DETERMINE MAXIMUM TIME INCREMENT
      DT=TW/NC
C     DETERMINE NODAL DISTANCE
      DX=(DT*2*AM)**0.5
      IF(AM.LT.AL) DX=(DT*2*AL)**0.5
C     DETERMINE NUMBER OF NODES PER COLUMN
```

```
      N=(INT(AD/DX)+1)+2
      NNAX=N+1
      N2=NC+2
      CT=N2-1
C     SET INITIAL TEMPERATURE AND NECK RADIUS
      DO 125 I=1,NC
      DO 126 J=1,NNAX
      T(I,J)=IT
      ANECK(I,J)=0.0
  126 CONTINUE
  125 CONTINUE
      BA=0.0174533*BA
      WRITE(6,10)
   10 FORMAT(1H1,29HROTATIONAL MOLDING SIMULATOR )
      WRITE(6,11) RI,RO,N,A,B,EX,SS,A,SM,AM,RPM
   11 FORMAT(6X,26HPOWDER HEIGHT RADIUS(CM)= ,F10.8,/,6X,17HMOLD RADIUS(
     1CM)= ,F10.3,/,6X,21HINTIAL NO. OF NODES= ,I3,/,
     26X,19HCOEF. A OF TEMP EQ=,F10.3,/,6X,20HCOEF. B OF TEMP EQ= ,F10.3
     3,/,6X,20HNODE THICKNESS(CM)= ,F10.4,/,6X,38HSTICK TEMP(C) AND DIFF
     4USIVITY(CM2/S)= ,F10.3,3X,E10.3,/,6X,46HCOMPLETE MELT TEMP(C) AND
     5DIFFUSIVITY(CM2/S)= ,F10.3,3X,E10.3,/,6X,6HRPM= ,F10.3)
C
C     ***** SECTION III *****
C
 1000 TW=TH/W
      CC=2*RO*SIN(TH/2)
      ANK=ANECK(1,1)
      IF(CT.GT.N2) ANK=ANECK(CT,1)
      AM=COND(ANK)/(RHO(ANK)*CP(ANK))
      BE=RADX(ANK)
C     RECHECK MAXIMUM TIME INCREMENT EACH ITERATION
      DT=(BE*DX)**2/(2.0*AM)
      IF(AM.LT.AL) DT=(BE*DX)**2/(2.0*AL)
      TM=TM-TS
      IF((IREM.EQ.0).OR.(ITM.GT.0)) GOTO 109
      TS=TW/NC
  104 TTL=TS
      ITMX=1
      IF(TTL.GT.DT) TTL=DT
      IF(TTL.GT.TS1) TTL=TS1
      IF(TTL.EQ.TS) GOTO 109
      ITMX=INT(TS/TTL)+1
      TS=TTL/ITMX
  109 IF(IREM.EQ.0) TS=DT
      DL=W*TS*RO
      IF(TM.EQ.0.0) WRITE(6,20)DT,TS,DL
   20 FORMAT(1H ,/,5X,23HMAX TIME INCREMENTS(S)= ,F10.5,/,6X,21HTIME INC
     1REMENT USED= ,F10.5,/,6X,18HARC/TIME INC(CM)= ,F10.5 )
      TM=TM+TS
      IF(IREM.EQ.0) GOTO 540
      NMAX=INT(AA/(NC*DL*DX))+1
      AD=7.2*(AL*TW)**0.5
      TF=(1.3333*CC/(G*COS(BA)))**0.5
      SR=TF/TS
      IF(SR.LT.1.0) SR=1.0
C     DETERMINE AREA OF EACH WEDGE
      S1=RO*SIN(TH/2.0)
```

```
      S2=RO*COS(TH/2.0)*TAN(W*TS/2.0)
      AT=0.5*(S1+S2)*(S1-S2)*SIN(W*TS)+0.5*RO*RO*(W*TS-SIN(W*TS))
      AS=(N-0.5)*DX*DL
      IF(AS.GT.AT) AS=AT
      IF(N.LT.NMAX) GO TO 560
      N=NMAX
      IFLAG=1
  540 CONTINUE
      DO 550 I=1,NC
      T(I,N+1)=T(I,N-1)
      ANECK(I,N+1)=ANECK(I,N-1)
  550 CONTINUE
  560 CONTINUE
      NNAX=N+1
      N6=INT(AD/DX)+1
C
C     *****   SECTION IV   *****
C
C       COMPUTE NODAL TEMPERATURES AND NECK RADIUS
  580 MT=A*TM/60.0+B*(TM/60.0)**2+YY
      DO 620 I=1,NC
C     NODAL TEMPERATURE EQUATIONS FOR STATIONARY POOL
      T(I,1)=MT
      TN(1) =MT
      CALL CONST(C1,C2,C3,DB,DA,MT,MT,MT,ANECK(I,1),ANECK(I,2),
     1 BNECK(1))
      ANECK(I,1)=BNECK(1)
      DO 630 J=2,N
      CALL CONST(C1,C2,C3,DB,DA,T(I,J),T(I,J-1),T(I,J+1),ANECK(I,J),
     1 ANECK(I,J+1),BNECK(J))
      TN(J)=T(I,J)*(1-TS/C3*(DB/C1 +DA/C2))+TS/C3*(DB/C1*T(I,J-1)+
     1DA/C2*T(I,J+1))
  630 CONTINUE
      DO 640 JJ=1,N
      T(I,JJ)=TN(JJ)
      IF((JJ.EQ.NEC).AND.(TN(JJ).GT.SM)) ANEK(NEC)=BNECK(JJ)
      IF((JJ.EQ.NEC).AND.(TN(JJ).GT.SM)) NEC=NEC+1
      IF(TN(JJ).GT.SM) BNECK(JJ)=RAD
      ANECK(I,JJ)=BNECK(JJ)
  640 CONTINUE
  620 CONTINUE
      IF(CT.LT.N2) GO TO 890
C     NODAL TEMPERATURE EQUATIONS FOR STUCK MATERIAL
      DO 880 I=N2,CT
      T(I,1)=MT
      CALL CONST(C1,C2,C3,DB,DA,MT,MT,MT,ANECK(I,1),ANECK(I,2),
     1 BNECK(1))
      ANECK(I,1)=BNECK(1)
      IF(N3(I).EQ.0) GO TO 820
      IF(N3(I).EQ.1) GO TO 780
      JTVAL=N3(I)
      DO 770 J=2,JTVAL
      CALL CONST(C1,C2,C3,DB,DA,T(I,J),T(I,J-1),T(I,J+1),ANECK(I,J),
     1 ANECK(I,J+1),BNECK(J))
      TN(J)=T(I,J)*(1-TS/C3*(DB/C1+DA/C2))+TS/C3*(DB/C1*T(I,J-1)+
     1DA/C2*T(I,J+1))
  770 CONTINUE
```

```
  780 J=N3(I)+1
      CALL CONST(C1,C2,C3,DB,DA,T(I,J),T(I,J-1),T(I,J+1),ANECK(I,J),
     1 ANECK(I,J+1),BNECK(J))
      BB=TS/C3*(DB/C1*T(I,J-1)+DA/(H3(I)*C2/DX)*T(I,J+1))
      TN(J)=T(I,J)*(1-TS/C3*(DB/C1+DA/(H3(I)*C2/DX)))+BB
  820 CONTINUE
      J=N3(I)+2
      CALL CONST(C1,C2,C3,DB,DA,T(I,J),T(I,J-1),T(I,J  ),ANECK(I,J),
     1 ANECK(I,J  ),BNECK(J))
      BB=DB*TS/(H3(I)*(C3/DX)**2*(H3(I)-DX/2))
      TN(J)=T(I,J)*(1-BB)+BB*T(I,J-1)
      DO 870 JJ=1,J
      T(I,JJ)=TN(JJ)
      IF((JJ.EQ.NEC).AND.(TN(JJ).GT.SM)) ANEK(NEC)=BNECK(JJ)
      IF((JJ.EQ.NEC).AND.(TN(JJ).GT.SM)) NEC=NEC+1
      IF(TN(JJ).GT.SM) BNECK(JJ)=RAD
      ANECK(I,JJ)=BNECK(JJ)
  870 CONTINUE
  880 CONTINUE
C
  890 CONTINUE
      IF((T(NC,N).GE.SS).AND.(IREM.EQ.1).AND.(N.EQ.NMAX)) GO TO 891
      IF(T(NC,N).GE.SM) GOTO 891
      IF(TM.LT.LK*PT) GOTO 892
C
C   *****  SECTION V  *****
C
C     PRINT ROUTINE
C
  891 I3=0
      CALL PRINT(T,LK,I3)
      I3=1
      I2=0
      CALL PRINT(ANECK,I2,I3)
      IF(T(NC,N).GT.SM) GOTO29
      IF((T(NC,N).LT.SS).OR.(IREM.EQ.0)) GOTO 892
      IF(N.LT.NMAX) GOTO892
      WRITE(6,30)TM
   30 FORMAT(1H ,///,5X,34HMASS COMPLETELY GONE - TIME(SEC)= ,F10.3)
      IREM=0
      AT=0.0
      AA=0.0
      TH=0.0
      LK=LK-1
      GOTO 892
   29 CONTINUE
      WRITE(6,31)
   31 FORMAT(1X,////,5X,29H NECK RADIUS AT COMPLETE MELT    ,/,10X,
     1  4HNODE,6X,6HRADIUS             )
      DO 33 J=1,N
      WRITE(6,32) J,ANEK(J)
   32 FORMAT(10X,I5,5X,F10.6)
   33 CONTINUE
      STOP
  892 CONTINUE
      ITM=ITM+1
      IF((IREM.EQ.0).OR.(ITM.LT.ITMX)) TM=TM+TS
```

```
      IF((IREY.EQ.0).OR.(ITM.LT.ITMX)) GO TO 1000
      ITM=0
      IF(T(NC,1).GT.SS) GO TO 1200
C
C   *****  SECTION VI   *****
C
C
C     CALCULATE MIX MEAN TEMPEFATURE WHEN NO MATERIAL HAS STUCK
C
 1109 TP=0.0
      DO 1110 I=2,N
      TP=TP+T(NC,I)
 1110 CONTINUE
      TP=(TP+MT/2)/(N-0.5)
      FT=(AS*TP+(AT-AS)*IT)/AT
      DO 1140 III=2,NC
      I=NC-III+2
       DO 1142 J=1,NNAX
      T(I,J)=T(I-1,J)
      ANECK(I, J)=ANECK(I-1,J)
 1142 CONTINUE
 1140 CONTINUE
      DO 1150 I=1,NNAX
      T(1,I)=IT
      ANECK(1, I)=0.0
 1150 CONTINUE
      IT=((SR-1)*IT+FT)/SR
      TM=TM+TS
      GO TO 530
 1200 CONTINUE
C
C   *****  SECTION VII   *****
C     DETERMINE THE AMOUNT OF STICK AND NEW ANGLE
C
      DO 1220 I=2,N
      IF(T(NC,I).LE.SS) GO TO 1221
 1220 CONTINUE
 1221 CONTINUE
      RA=(SS-T(NC,I-1))/(T(NC,I)-T(NC,I-1))
      H=(RA+(I-2))*DX
      DO 1250 II=2,N
      IF(T(NC-1,II).LE.SS) GO TO 1251
 1250 CONTINUE
 1251 CONTINUE
      RB=(SS-T(NC,II-1))/(T(NC,II)-T(NC,II-1))
      H1=(RB+(II-2))*DX
      IF(INT(H/DX)-1.LT.0) GO TO 1109
      CT=CT+1
      DC(N2-1)=W*TS
      PS(N2-1)=TH/2.0
      N3(N2-1)=INT(H/DX)-1
      H3(N2-1)=H-DX*N3(N2-1)
      H2(N2-1)=H
      JTVAL=N3(N2-1)+1
      DO 1350 J=1,JTVAL
      T(N2-1,J)=T(NC,J)
      ANECK(N2-1,J)=ANECK(NC,J)
```

```
 1350 CONTINUE
      T(N2-1,N3(N2-1)+2)=SS
      ANECK(N2-1,N3(N2-1)+2)=ANECK(NC,N3(N2-1)+2)
C
C     COMPUTE MIX TEMPERATURE OF MATERIAL NOT STICKING BUT
C        ENTERING FREE-FALL ZONE
C
      TP=0.0
      DO 1380 J=I,N
      TP=TP+T(NC,J)
 1380 CONTINUE
      K=RA-0.5
      IF(K.GE.0.0)  TP=(TP-T(NC,I)*K)/(N-I-K+1)
      IF(K.LT.0.0)  TP=(TP-T(NC,I-1)*K)/(N-I-K+1)
      M=H*DL
      FT=((AS-M)*TP+(AT-AS)*IT)/(AT-M)
C     ROTATE POWDER
      DO 1440 III=2,NC
      I=NC-III+2
      DO 1445 J=1,NMAX
      T(I,J)=T(I-1,J)
      ANECK(I,J)=ANECK(I-1,J)
 1445 CONTINUE
 1440 CONTINUE
      K4=1
      IF(CT.LT.N2) GO TO 1900
C
C  *****  SECTION VIII  *****
C
C     STUCK MATL SHIFT
      DO 1470 JJI=N2,CT
      JI=CT-JJI+N2
      DC(JI)=DC(JI-1)
      PS(JI)=PS(JI-1)+W*TS
      N3(JI)=N3(JI-1)
      H3(JI)=H3(JI-1)
      H2(JI)=H2(JI-1)
      N3TEMP=N3(JI)+2
      DO 1530 J=1,N3TEMP
      T(JI,J)=T(JI-1,J)
      ANECK(JI,J)=ANECK(JI-1,J)
 1530 CONTINUE
 1470 CONTINUE
 1550 X5=6.28318-TH/2
      EN=0.0
      KL=0
      IF(PS(CT).LT.X5) GO TO 1900
C
C  *****  SECTION IX  *****
C     STUCK MATERIAL RE-ENTERING POOL ROUTINE
C
      DO 1570 JI=N2,CT
      IF(PS(JI).GE.X5) GO TO 1575
 1570 CONTINUE
 1575 CONTINUE
      EN=PS(JI)-X5
      DT=DC(JI)-EN
```

```
      IF(OT.LT.W*TS) GO TO 1610
      PS(JI)=X5
      DC(JI)=OT
      GO TO 1770
 1610 IF(OT.LT.0.0) OT=DC(JI)
      IF(OT.LT.0.0) KL=1
      OT=JI-1
      KK=0
      JL=0
      JK=N3(JI-1)+1
 1650 IF(JK.LE.N3(JI)+1 ) GO TO 1660
      JK=JK-1
      KK=1
      GO TO 1650
 1660 CONTINUE
      IF((H3(JI).GE.1.5*DX).AND.KK.EQ.1) JL=1
      IF(JL.EQ.1) JK=JK+1
      DO 1670 I=2,JK
      T(JI-1,I)=(OT*T(JI,I)+DC(JI-1)*T(JI-1,I))/(OT+DC(JI-1))
      ANECK(JI-1,I)=(OT*ANECK(JI,I)+DC(JI-1)*ANECK(JI-1,I))/(OT+
     1  DC(JI-1))
 1670 CONTINUE
      JK=JK+1
      A3=DC(JI-1)*(H3(JI-1)-DX/2)
      A4=OT*(H3(JI)-DX/2)
       IF(JL.EQ.1) A4=OT*(H3(JI)-1.5*DX)
      IF(JL.EQ.1)    T(JI,JK)=T(JI,N3(JI)+2)
      IF(JL.EQ.1) ANECK(JI,JK)=ANECK(JI,N3(JI)+2)
      IF((JL.EQ.0).AND.(KK.EQ.1)) A3=DC(JI-1)*DX
      T(JI-1,JK)=(T(JI,JK)*A4+T(JI-1,JK)*A3)/(A3+A4)
      ANECK(JI-1,JK)=(ANECK(JI,JK)*A4+ANECK(JI-1,JK)*A3)/(A3+A4)
      DC(JI-1)=DC(JI-1)+OT
      IF(KL.NE.1) GO TO 1760
      PS(JI-1)=PS(JI)
      JI=JI-1
      GO TO 1550
 1760 PS(JI-1)=X5
 1770 CONTINUE
      T(1,1)=TT
      N4=N3(JI)+1
      IF(H3(JI).GE.1.5*DX) N4=N4+1
      DO 1810 J=1,N4
      T(1,J)=T(JI,J)
      ANECK(1,J)=ANECK(JI,J)
 1810 CONTINUE
      RM=H2(JI)-(N4-0.5)*DX
      IF(RM.LE.0.0) GO TO 1840
      N4=N4+1
      T(1,N4)=(RM*T(JI,N3(JI)+2)    +(DX-RM)*IT)/DX
      ANECK(1,N4)= ANECK(JI,N3(JI)+2)
 1840 CONTINUE
      IF(IFLAG.EQ.1) GOTO 1870
      IF(N6+N4.LE.N) GO TO 1870
      NNTP=N6+N4+1
      NMAX=N+1
      DO 1860 I=2,NC
      DO 1862 J=NMAX,NNTP
```

```
      T(I,J)=T(I,N+1)
      ANECK(I,J)=0.0
 1862 CONTINUE
 1860 CONTINUE
      N=N6+N4
 1870 CONTINUE
C
      NMAX=N+1
      K4=N4+1
 1900 CONTINUE
      DO 1905 II=K4,NMAX
      T(1,II)=IT
      ANECK(1,II)=0.0
 1905 CONTINUE
      IT=((SR-1)*IT+FT)/SR
      AA=AA-M
      R2=R0
      AR=AA
      IF((CT.LT.N2).OR.(EN.LE.0.0)) GO TO 1950
      AA=AA+DL*H2(JI)
      B3=(H1+H2(JI))/2
      R2=R0-B3
      AR=AA-B3*R2*T4
 1950 CONTINUE
C
C
C ***** SECTION X *****
C
C     FIND NEW ANGLE THETHA (TH)
C
C
      HT=TH
      LT=0.0
 2010 AV=(HT+LT)/2.0
      IF(HT.EQ.LT) GO TO 2070
      RM=AV-SIN(AV)-2*AR/R2**2
      IF(RM**2.0.LT.0.0000001) GO TO 2070
      IF(RM.GT.0.0) GO TO 2060
      LT=AV
      GO TO 2010
 2060 HT=AV
      GO TO 2010
 2070 TH=AV
      TM=TM+TS
      GO TO 1000
      END
```

```
      SUBROUTINE PRINT(T,LK,K)
      DIMENSION T(200,100),N3(200)
      COMMON SS,SM,AL,AM,DX,N,TM,AA,AT,AD,TH,DL,N2,CT,NC,N3,RAD,TS
      COMMON TAIR,BMT,MT
      REAL MT
      INTEGER CT
      LK=LK+1
      BB=TH*57.29578
      IF(K.EQ.1) GOTO23
      WRITE(6,20)TM,AA,AT,AD,BB,DL,NC
   20  FORMAT(//,    11H TIME(SEC)=,F10.3,/,6X,16HTOTAL AREA(C2)= ,F10.3,
     1/,6X,12HWEDGE AREA= ,F10.4,/,6X,28HORIGINAL PENITRATION DEPTH= ,
     2F10.4,/,6X,12HANGLE(DEG)= ,F10.3,/,6X,27HARC LENGTH/TIME INCREMENT
     3= ,F10.5,/,6X,24HNO. OF WEDGES IN POOL = ,I3,/)
      WRITE(6,10) TAIR,BMT,MT
   10 FORMAT(6X,24HTEMP. OF AIR (DEG. C) =  ,F10.3,/,6X,
     1 44HTEMP. OF MOLD'S EXTERNAL SURFACE (DEG. C) =  ,F10.3,
     2 /,6X,44HTEMP. OF MOLD'S INTERIOR SURFACE (DEG. C) =  ,F10.3,///)
      WRITE(6,21)
   21  FORMAT(6X,30HTEMPERATURE HISTORY OF POWDER )
   23 IF(K.EQ.1) WRITE(6,24)
   24 FORMAT(//,12H NECK RADIUS    )
      ICOL=15
      IREP=((NC-1)/ICOL)+1
      IREM=NC-(IREP-1)*ICOL
      DO 100 KK=1,IREP
      IF(KK.EQ.IREP) ICOL=IREM
      KJ=(KK-1)*ICOL+1
      KJ1=KJ+(ICOL-1)
      IF(KK.EQ.IREP) KJ1=KJ+IREM-1
      WRITE(6,108)(J,J=KJ,KJ1)
  108  FORMAT(1X,6HAREA   ,15(I3,5X))
      DO 104 J=1,N
      IF(K.EQ.0) WRITE(6,102)J,(T(I,J),I=KJ,KJ1)
      IF(K.EQ.1) WRITE(6,103)J,(T(I,J),I=KJ,KJ1)
  102  FORMAT( 1X,I3, 3X, 15(F7.3,1X))
  103 FORMAT(1X,I3,3X,15(F7.5, 1X))
  104  CONTINUE
      WRITE(6,105)
  105  FORMAT(1X,//)
  100  CONTINUE
   97 CONTINUE
      IF(CT.LT.N2) RETURN
      ICOL=15
      IF(K.EQ.0) WRITE(6,98)
   98  FORMAT(1X,//,31H TEMPERATURE OF STUCK MATERIAL ,/)
      IF(K.EQ.1) WRITE(6,99)
   99 FORMAT(//,30H NECK RADIUS OF STUCK MATERIAL    )
      IREP=INT((CT-(N2  ))/ICOL)+1
      IREM=CT-N2+1-(IREP-1)*ICOL
      DO 200 KK=1,IREP
      KJ=(KK-1)*ICOL+N2
      IF(KK.EQ.IREP) ICOL=IREM
      KJ1=KJ+(ICOL-1)
      IF(KK.EQ.IREP) KJ1= KJ+IREM-1
```

```
      WRITE(6,108)(J,J=KJ,KJ1)
      NTN=N3(KJ)+2
      DO 204 J=1,NTN
      DO 203 II=KJ,KJ1
      NTMP=N3(II)+2
      IF(NTMP.EQ.NTN) GO TO 203
      IDIFF=NTN-NTMP
      DO 202 LL=1,IDIFF
      T(II,NTMP+LL)=0.0
  202 CONTINUE
  203 CONTINUE
      IF(K.EQ.0) WRITE(6,102)J,(T(I,J),I=KJ,KJ1)
      IF(K.EQ.1) WRITE(6,103)J,(T(I,J),I=KJ,KJ1)
  204  CONTINUE
  200  CONTINUE
  300  RETURN
      END


      SUBROUTINE CONST(C1,C2,C3,DB,DA,T1,T2,T3,ANB,ANA,BNK)
      DIMENSION N3(200)
C
C
C
      COMMON SS,SM,AL,AM,DX,N, TM,AA,AT,AD,TH,DL,N2,CT,NC,N3,RAD,TS
      A1=0.5*(ANB+ANA)
      C1=RADX(ANB)*DX
      C2=RADX(ANA)*DX
      C3=RADX(A1)*DX
      DELB=(3.0*SU(T1)*RAD/(8.6*VIS(T1)*(TM+0.5*TS)))**0.5*TS
      IF(ANB/RAD.GE.0.5) DELB=0.5*SU(T1)*TS/(VIS(T1))
      DB=COND(ANB)/(RHO(A1)*CP(A1))
      DA=COND(ANA)/(RHO(A1)*CP(A1))
      BNK=ANB+DELB
      IF(BNK.GT.RAD) BNK=RAD
      IF(DELB.GT.0.0) RETURN
      WRITE(6,10)TM,ANB,ANA,BNK,RAD,TS,SU(T1),VIS(T1) ,DELB
   10 FORMAT(1X,10(E10.5,1X))
      RETURN
      END
```

```
      FUNCTION COND(Y)
      DIMENSION N3(200)
C
C     CONDUCTIVITY FUNCTION (JOULE/(CM-SEC-DEG K))
C
C        C1 = THERMAL CONDUCTIVITY AT TEMPERATURE SS
C        C2 = THERMAL CONDUCTIVITY AT TEMPERATURE SM
C
      COMMON SS,SM,AL,AM,DX,N,TM,AA,AT,AD,TH,DL,N2,CT,NC,N3,RAD,TS
      C1=1.99E-03
      C2=4.9325E-03
      X=Y/RAD
      IF(X.GT.0.0) GOTO 10
      COND=C1
      GO TO 1
   10 IF(X.GT.1.0) GOTO 20
      COND=C1+X*(C2-C1)
      GO TO 1
   20 COND=C2
    1 CONTINUE
      RETURN
      END


      FUNCTION RHO(Y)
      DIMENSION N3(200)
C
C     DENSITY FUNCTION (KG/CM**3)
C
C     R1=DENSITY AT SS
C     R2=DENSITY AT SM
C
      COMMON SS,SM,AL,AM,DX,N,TM,AA,AT,AD,TH,DL,N2,CT,NC,N3,RAD,TS
      R1=5.0937E-04
      R2=3.8058E-04
      X=Y/RAD
      IF(X.GT.0.0) GOTO 10
      RHO=R1
      GO TO 1
   10 IF(X.GT.1.0) GOTO 20
      RHO=R1+(R2-R1)*X
      GO TO 1
   20 RHO=R2
    1 CONTINUE
      RETURN
      END
```

```
      FUNCTION CP(X)
C
C     SPECIFIC HEAT (JOULE/(KG-DEG K))
C
      CP=2302.7
      RETURN
      END

      FUNCTION RADX(Y)
      DIMENSION N3(200)
      COMMON SS,SM,AL,AM,DX,N,TM,AA,AT,AD,TH,DL,N2,CT,NC,N3,RAD,TS
C
C     THIS FUNCTION DETERMINES THE RATIO USED TO CALCULATE DX AS A FUNCT
C         OF MOLD TEMP
C
      X=Y/RAD
      IF(X.GT.0.0) GOTO 10
      RADX=1.0
      GO TO 1
   10 IF(X.GT.1.0) GOTO 20
      RADX=RHO(0.0)/RHO(Y)
      GO TO 1
   20 RADX=RHO(0.0)/RHO(RAD)
    1 CONTINUE
      RETURN
      END

      FUNCTION SU(T)
C
C         SURFACE TENSION FUNCTION (DYNES/CM)
C
      SU=31.0-0.058*(T-105)
      RETURN
      END

      FUNCTION VIS(T)
C
C         VISCOSITY FUNCTION  (POISE)
C
      VIS=5.22E06*EXP(-19.583 + 7402.5/(T+273))
      RETURN
      END
```

APPENDIX G

SAMPLE SIMULATION OUTPUT

```
ROTATIONAL MOLDING SIMULATOR
   POWDER HEIGHT RADIUS(CM)=        4.796
   MOLD RADIUS(CM)=          6.668
   INTIAL NO. OF NODES=  13
   COEF. A OF TEMP EQ=     25.500
   COEF. B OF TEMP EQ=       -.531
   NODE THICKNESS(CM)=       .0299
   STICK TEMP(C) AND DIFFUSIVITY(CM2/S)=     110.000     .170E-02
   COMPLETE MELT TEMP(C) AND DIFFUSIVITY(CM2/S)=     138.000     .243E-02
   RPM=       10.000

   MAX TIME INCREMENTS(S)=     .18334
   TIME INCREMENT USED=      .18334
   ARC/TIME INC(CM)=     1.28014

TIME(SEC)=      0.000
   TOTAL AREA(C2)=      11.927
   WEDGE AREA=      2.0527
   ORIGINAL PENITRATION DEPTH=       .3592
   ANGLE(DEG)=      88.005
   ARC LENGTH/TIME INCREMENT=     1.28014
   NO. OF WEDGES IN POOL =    8
```

TEMPERATURE HISTORY OF POWDER

AREA	1	2	3	4	5	6	7	8
1	20.000	20.000	20.000	20.000	20.000	20.000	20.000	20.000
2	20.000	20.000	20.000	20.000	20.000	20.000	20.000	20.000
3	20.000	20.000	20.000	20.000	20.000	20.000	20.000	20.000
4	20.000	20.000	20.000	20.000	20.000	20.000	20.000	20.000
5	20.000	20.000	20.000	20.000	20.000	20.000	20.000	20.000
6	20.000	20.000	20.000	20.000	20.000	20.000	20.000	20.000
7	20.000	20.000	20.000	20.000	20.000	20.000	20.000	20.000
8	20.000	20.000	20.000	20.000	20.000	20.000	20.000	20.000
9	20.000	20.000	20.000	20.000	20.000	20.000	20.000	20.000
10	20.000	20.000	20.000	20.000	20.000	20.000	20.000	20.000
11	20.000	20.000	20.000	20.000	20.000	20.000	20.000	20.000
12	20.000	20.000	20.000	20.000	20.000	20.000	20.000	20.000
13	20.000	20.000	20.000	20.000	20.000	20.000	20.000	20.000

NECK RADIUS

AREA	1	2	3	4	5	6	7	8
1	.00001	.00001	.00001	.00001	.00001	.00001	.00001	.00001
2	.00001	.00001	.00001	.00001	.00001	.00001	.00001	.00001
3	.00001	.00001	.00001	.00001	.00001	.00001	.00001	.00001
4	.00001	.00001	.00001	.00001	.00001	.00001	.00001	.00001
5	.00001	.00001	.00001	.00001	.00001	.00001	.00001	.00001
6	.00001	.00001	.00001	.00001	.00001	.00001	.00001	.00001
7	.00001	.00001	.00001	.00001	.00001	.00001	.00001	.00001
8	.00001	.00001	.00001	.00001	.00001	.00001	.00001	.00001
9	.00001	.00001	.00001	.00001	.00001	.00001	.00001	.00001
10	.00001	.00001	.00001	.00001	.00001	.00001	.00001	.00001
11	.00001	.00001	.00001	.00001	.00001	.00001	.00001	.00001
12	.00001	.00001	.00001	.00001	.00001	.00001	.00001	.00001
13	.00001	.00001	.00001	.00001	.00001	.00001	.00001	.00001

TIME(SEC)= 30.121

TOTAL AREA(C2)= 11.927

WEDGE AREA= 2.0527

ORIGINAL PENITRATION DEPTH= .4293

ANGLE(DEG)= 88.005

ARC LENGTH/TIME INCREMENT= 1.28014

NO. OF WEDGES IN POOL = 8

TEMPERATURE HISTORY OF POWDER

AREA	1	2	3	4	5	6	7	8
1	32.667	32.667	32.667	32.667	32.667	32.667	32.667	32.667
2	28.647	29.238	29.646	29.899	30.084	30.221	30.329	30.414
3	26.494	27.153	27.527	27.841	28.076	28.265	28.417	28.542
4	26.494	26.405	26.576	26.727	26.882	27.019	27.140	27.245
5	26.494	26.405	26.316	26.318	26.341	26.382	26.427	26.475
6	26.494	26.405	26.316	26.228	26.171	26.131	26.107	26.092
7	26.494	26.405	26.316	26.228	26.140	26.063	25.995	25.937
8	26.494	26.405	26.316	26.228	26.140	26.052	25.968	25.889
9	26.494	26.405	26.316	26.228	26.140	26.052	25.964	25.878
10	26.494	26.405	26.316	26.228	26.140	26.052	25.964	25.877
11	26.494	26.405	26.316	26.228	26.140	26.052	25.964	25.877
12	26.494	26.405	26.316	26.228	26.140	26.052	25.964	25.877
13	26.494	26.405	26.316	26.228	26.140	26.052	25.964	25.877

NECK RADIUS

AREA	1	2	3	4	5	6	7	8
1	.00000	.00000	.00000	.00000	.00000	.00001	.00001	.00001
2	.00000	.00000	.00000	.00000	.00000	.00000	.00001	.00001
3	.00000	.00000	.00000	.00000	.00000	.00000	.00000	.00001
4	.00000	.00000	.00000	.00000	.00000	.00000	.00000	.00001
5	.00000	.00000	.00000	.00000	.00000	.00000	.00000	.00001
6	.00000	.00000	.00000	.00000	.00000	.00000	.00000	.00001
7	.00000	.00000	.00000	.00000	.00000	.00000	.00000	.00001
8	.00000	.00000	.00000	.00000	.00000	.00000	.00000	.00001
9	.00000	.00000	.00000	.00000	.00000	.00000	.00000	.00001
10	.00000	.00000	.00000	.00000	.00000	.00000	.00000	.00001
11	.00000	.00000	.00000	.00000	.00000	.00000	.00000	.00001
12	.00000	.00000	.00000	.00000	.00000	.00000	.00000	.00001
13	.00000	.00000	.00000	.00000	.00000	.00000	.00000	.00001

TIME(SEC)= 60.241
TOTAL AREA(C2)= 11.927
WEDGE AREA= 2.0527
ORIGINAL PENITRATION DEPTH= .4293
ANGLE(DEG)= 88.005
ARC LENGTH/TIME INCREMENT= 1.28014
NO. OF WEDGES IN POOL = 8

TEMPERATURE HISTORY OF POWDER

AREA	1	2	3	4	5	6	7	8
1	45.067	45.067	45.067	45.067	45.067	45.067	45.067	45.067
2	40.381	41.072	41.550	41.847	42.066	42.228	42.356	42.457
3	37.871	38.642	39.080	39.449	39.726	39.950	40.131	40.280
4	37.871	37.767	37.968	38.146	38.329	38.490	38.634	38.759
5	37.871	37.767	37.663	37.666	37.692	37.741	37.795	37.851
6	37.871	37.767	37.663	37.559	37.492	37.445	37.416	37.398
7	37.871	37.767	37.663	37.559	37.455	37.364	37.284	37.215
8	37.871	37.767	37.663	37.559	37.455	37.351	37.252	37.158
9	37.871	37.767	37.663	37.559	37.455	37.351	37.247	37.145
10	37.871	37.767	37.663	37.559	37.455	37.351	37.247	37.144
11	37.871	37.767	37.663	37.559	37.455	37.351	37.247	37.144
12	37.871	37.767	37.663	37.559	37.455	37.351	37.247	37.144
13	37.871	37.767	37.663	37.559	37.455	37.351	37.247	37.144

NECK RADIUS

AREA	1	2	3	4	5	6	7	8
1	.00000	.00000	.00000	.00000	.00000	.00001	.00001	.00001
2	.00000	.00000	.00000	.00000	.00000	.00001	.00001	.00001
3	.00000	.00000	.00000	.00000	.00000	.00000	.00001	.00001
4	.00000	.00000	.00000	.00000	.00000	.00000	.00001	.00001
5	.00000	.00000	.00000	.00000	.00000	.00000	.00001	.00001
6	.00000	.00000	.00000	.00000	.00000	.00000	.00000	.00001
7	.00000	.00000	.00000	.00000	.00000	.00000	.00000	.00001
8	.00000	.00000	.00000	.00000	.00000	.00000	.00000	.00001
9	.00000	.00000	.00000	.00000	.00000	.00000	.00000	.00001
10	.00000	.00000	.00000	.00000	.00000	.00000	.00000	.00001
11	.00000	.00000	.00000	.00000	.00000	.00000	.00000	.00001
12	.00000	.00000	.00000	.00000	.00000	.00000	.00000	.00001
13	.00000	.00000	.00000	.00000	.00000	.00000	.00000	.00001

TIME(SEC)= 90.100

TOTAL AREA(C2)= 11.927

WEDGE AREA= 2.0527

ORIGINAL PENITRATION DEPTH= .4293

ANGLE(DEG)= 88.005

ARC LENGTH/TIME INCREMENT= 1.28014

NO. OF WEDGES IN POOL = 8

TEMPERATURE HISTORY OF POWDER

AREA	1	2	3	4	5	6	7	8
1	57.095	57.095	57.095	57.095	57.095	57.095	57.095	57.095
2	52.369	53.067	53.549	53.849	54.070	54.234	54.363	54.466
3	49.839	50.617	51.058	51.431	51.711	51.937	52.120	52.271
4	49.839	49.734	49.937	50.116	50.301	50.464	50.609	50.736
5	49.839	49.734	49.629	49.631	49.658	49.707	49.762	49.819
6	49.839	49.734	49.629	49.524	49.456	49.408	49.379	49.361
7	49.839	49.734	49.629	49.524	49.419	49.327	49.245	49.176
8	49.839	49.734	49.629	49.524	49.419	49.313	49.213	49.118
9	49.839	49.734	49.629	49.524	49.419	49.313	49.208	49.105
10	49.839	49.734	49.629	49.524	49.419	49.313	49.208	49.103
11	49.839	49.734	49.629	49.524	49.419	49.313	49.208	49.103
12	49.839	49.734	49.629	49.524	49.419	49.313	49.208	49.103
13	49.839	49.734	49.629	49.524	49.419	49.313	49.208	49.103

NECK RADIUS

AREA	1	2	3	4	5	6	7	8
1	.00000	.00000	.00000	.00000	.00001	.00001	.00001	.00001
2	.00000	.00000	.00000	.00000	.00001	.00001	.00001	.00001
3	.00000	.00000	.00000	.00000	.00000	.00001	.00001	.00001
4	.00000	.00000	.00000	.00000	.00000	.00001	.00001	.00001
5	.00000	.00000	.00000	.00000	.00000	.00001	.00001	.00001
6	.00000	.00000	.00000	.00000	.00000	.00001	.00001	.00001
7	.00000	.00000	.00000	.00000	.00000	.00001	.00001	.00001
8	.00000	.00000	.00000	.00000	.00000	.00001	.00001	.00001
9	.00000	.00000	.00000	.00000	.00000	.00001	.00001	.00001
10	.00000	.00000	.00000	.00000	.00000	.00001	.00001	.00001
11	.00000	.00000	.00000	.00000	.00000	.00001	.00001	.00001
12	.00000	.00000	.00000	.00000	.00000	.00001	.00001	.00001
13	.00000	.00000	.00000	.00000	.00000	.00001	.00001	.00001

TIME(SEC)= 120.220
TOTAL AREA(C2)= 11.927
WEDGE AREA= 2.0527
ORIGINAL PENITRATION DEPTH= .4293
ANGLE(DEG)= 88.005
ARC LENGTH/TIME INCREMENT= 1.28014
NO. OF WEDGES IN POOL = 8

TEMPERATURE HISTORY OF POWDER

AREA	1	2	3	4	5	6	7	8
1	68.962	68.962	68.962	68.962	68.962	68.962	68.962	68.962
2	64.314	65.000	65.475	65.770	65.987	66.149	66.276	66.377
3	61.825	62.590	63.025	63.392	63.667	63.890	64.070	64.218
4	61.825	61.722	61.921	62.098	62.280	62.440	62.583	62.708
5	61.825	61.722	61.618	61.621	61.647	61.695	61.749	61.806
6	61.825	61.722	61.618	61.515	61.449	61.402	61.373	61.355
7	61.825	61.722	61.618	61.515	61.412	61.321	61.241	61.173
8	61.825	61.722	61.618	61.515	61.412	61.308	61.209	61.116
9	61.825	61.722	61.618	61.515	61.412	61.308	61.205	61.103
10	61.825	61.722	61.618	61.515	61.412	61.308	61.205	61.101
11	61.825	61.722	61.618	61.515	61.412	61.308	61.205	61.101
12	61.825	61.722	61.618	61.515	61.412	61.308	61.205	61.101
13	61.825	61.722	61.618	61.515	61.412	61.308	61.205	61.101

NECK RADIUS

AREA	1	2	3	4	5	6	7	8
1	.00000	.00000	.00000	.00001	.00001	.00001	.00001	.00001
2	.00000	.00000	.00000	.00001	.00001	.00001	.00001	.00001
3	.00000	.00000	.00000	.00000	.00001	.00001	.00001	.00001
4	.00000	.00000	.00000	.00000	.00001	.00001	.00001	.00001
5	.00000	.00000	.00000	.00000	.00001	.00001	.00001	.00001
6	.00000	.00000	.00000	.00000	.00001	.00001	.00001	.00001
7	.00000	.00000	.00000	.00000	.00001	.00001	.00001	.00001
8	.00000	.00000	.00000	.00000	.00001	.00001	.00001	.00001
9	.00000	.00000	.00000	.00000	.00001	.00001	.00001	.00001
10	.00000	.00000	.00000	.00000	.00001	.00001	.00001	.00001
11	.00000	.00000	.00000	.00000	.00001	.00001	.00001	.00001
12	.00000	.00000	.00000	.00000	.00001	.00001	.00001	.00001
13	.00000	.00000	.00000	.00000	.00001	.00001	.00001	.00001

TIME(SEC)= 150.079
TOTAL AREA(C2)= 11.927
WEDGE AREA= 2.0527
ORIGINAL PENITRATION DEPTH= .4293
ANGLE(DEG)= 88.005
ARC LENGTH/TIME INCREMENT= 1.28014
NO. OF WEDGES IN POOL = 8

TEMPERATURE HISTORY OF POWDER

AREA	1	2	3	4	5	6	7	8
1	80.461	80.461	80.461	80.461	80.461	80.461	80.461	80.461
2	75.913	76.584	77.049	77.338	77.550	77.709	77.833	77.932
3	73.477	74.226	74.651	75.010	75.280	75.498	75.674	75.819
4	73.477	73.376	73.571	73.744	73.922	74.079	74.219	74.341
5	73.477	73.376	73.275	73.277	73.303	73.350	73.403	73.458
6	73.477	73.376	73.275	73.173	73.108	73.062	73.034	73.017
7	73.477	73.376	73.275	73.173	73.072	72.984	72.906	72.838
8	73.477	73.376	73.275	73.173	73.072	72.971	72.874	72.782
9	73.477	73.376	73.275	73.173	73.072	72.971	72.870	72.770
10	73.477	73.376	73.275	73.173	73.072	72.971	72.870	72.769
11	73.477	73.376	73.275	73.173	73.072	72.971	72.870	72.769
12	73.477	73.376	73.275	73.173	73.072	72.971	72.870	72.769
13	73.477	73.376	73.275	73.173	73.072	72.971	72.870	72.769

NECK RADIUS

AREA	1	2	3	4	5	6	7	8
1	.00000	.00000	.00001	.00001	.00001	.00001	.00001	.00001
2	.00000	.00000	.00001	.00001	.00001	.00001	.00001	.00001
3	.00000	.00000	.00000	.00001	.00001	.00001	.00001	.00001
4	.00000	.00000	.00000	.00001	.00001	.00001	.00001	.00001
5	.00000	.00000	.00000	.00001	.00001	.00001	.00001	.00001
6	.00000	.00000	.00000	.00001	.00001	.00001	.00001	.00001
7	.00000	.00000	.00000	.00001	.00001	.00001	.00001	.00001
8	.00000	.00000	.00000	.00001	.00001	.00001	.00001	.00001
9	.00000	.00000	.00000	.00001	.00001	.00001	.00001	.00001
10	.00000	.00000	.00000	.00001	.00001	.00001	.00001	.00001
11	.00000	.00000	.00000	.00001	.00001	.00001	.00001	.00001
12	.00000	.00000	.00000	.00001	.00001	.00001	.00001	.00001
13	.00000	.00000	.00000	.00001	.00001	.00001	.00001	.00001

TIME(SEC)= 180.200
TOTAL AREA(C2)= 11.927
WEDGE AREA= 2.0527
ORIGINAL PENITRATION DEPTH= .4293
ANGLE(DEG)= 88.005
ARC LENGTH/TIME INCREMENT= 1.28014
NO. OF WEDGES IN POOL = 8

TEMPERATURE HISTORY OF POWDER

AREA	1	2	3	4	5	6	7	8
1	91.795	91.795	91.795	91.795	91.795	91.795	91.795	91.795
2	87.351	88.007	88.461	88.743	88.951	89.106	89.227	89.324
3	84.971	85.703	86.119	86.469	86.733	86.946	87.118	87.260
4	84.971	84.872	85.063	85.232	85.406	85.559	85.696	85.816
5	84.971	84.872	84.773	84.776	84.801	84.847	84.899	84.953
6	84.971	84.872	84.773	84.674	84.611	84.566	84.538	84.522
7	84.971	84.872	84.773	84.674	84.576	84.489	84.413	84.347
8	84.971	84.872	84.773	84.674	84.576	84.477	84.382	84.292
9	84.971	84.872	84.773	84.674	84.576	84.477	84.378	84.280
10	84.971	84.872	84.773	84.674	84.576	84.477	84.378	84.279
11	84.971	84.872	84.773	84.674	84.576	84.477	84.378	84.279
12	84.971	84.872	84.773	84.674	84.576	84.477	84.378	84.279
13	84.971	84.872	84.773	84.674	84.576	84.477	84.378	84.279

NECK RADIUS

AREA	1	2	3	4	5	6	7	8
1	.00000	.00000	.00001	.00001	.00001	.00001	.00002	.00002
2	.00000	.00000	.00001	.00001	.00001	.00001	.00002	.00002
3	.00000	.00000	.00001	.00001	.00001	.00001	.00001	.00002
4	.00000	.00000	.00001	.00001	.00001	.00001	.00001	.00002
5	.00000	.00000	.00001	.00001	.00001	.00001	.00001	.00002
6	.00000	.00000	.00001	.00001	.00001	.00001	.00001	.00002
7	.00000	.00000	.00001	.00001	.00001	.00001	.00001	.00002
8	.00000	.00000	.00001	.00001	.00001	.00001	.00001	.00002
9	.00000	.00000	.00001	.00001	.00001	.00001	.00001	.00002
10	.00000	.00000	.00001	.00001	.00001	.00001	.00001	.00002
11	.00000	.00000	.00001	.00001	.00001	.00001	.00001	.00002
12	.00000	.00000	.00001	.00001	.00001	.00001	.00001	.00002
13	.00000	.00000	.00001	.00001	.00001	.00001	.00001	.00002

TIME(SEC)= 210.058
TOTAL AREA(C2)= 11.927
WEDGE AREA= 2.0527
ORIGINAL PENITRATION DEPTH= .4293
ANGLE(DEG)= 88.005
ARC LENGTH/TIME INCREMENT= 1.28014
NO. OF WEDGES IN POOL = 8

TEMPERATURE HISTORY OF POWDER

AREA	1	2	3	4	5	6	7	8
1	102.766	102.766	102.766	102.766	102.766	102.766	102.766	102.766
2	98.427	99.067	99.511	99.786	99.989	100.141	100.259	100.354
3	96.102	96.817	97.223	97.566	97.823	98.031	98.199	98.338
4	96.102	96.006	96.192	96.357	96.527	96.677	96.811	96.928
5	96.102	96.006	95.909	95.912	95.936	95.981	96.032	96.085
6	96.102	96.006	95.909	95.813	95.751	95.707	95.680	95.664
7	96.102	96.006	95.909	95.813	95.716	95.632	95.557	95.493
8	96.102	96.006	95.909	95.813	95.716	95.620	95.527	95.460
9	96.102	96.006	95.909	95.813	95.716	95.620	95.523	95.426
10	96.102	96.006	95.909	95.813	95.716	95.620	95.523	95.426
11	96.102	96.006	95.909	95.813	95.716	95.620	95.523	95.426
12	96.102	96.006	95.909	95.813	95.716	95.620	95.523	95.426
13	96.102	96.006	95.909	95.813	95.716	95.620	95.523	95.426

NECK RADIUS

AREA	1	2	3	4	5	6	7	8
1	.00000	.00001	.00001	.00001	.00001	.00002	.00002	.00002
2	.00000	.00001	.00001	.00001	.00001	.00002	.00002	.00002
3	.00000	.00000	.00001	.00001	.00001	.00001	.00002	.00002
4	.00000	.00000	.00001	.00001	.00001	.00001	.00002	.00002
5	.00000	.00000	.00001	.00001	.00001	.00001	.00002	.00002
6	.00000	.00000	.00001	.00001	.00001	.00001	.00002	.00002
7	.00000	.00000	.00001	.00001	.00001	.00001	.00002	.00002
8	.00000	.00000	.00001	.00001	.00001	.00001	.00002	.00002
9	.00000	.00000	.00001	.00001	.00001	.00001	.00002	.00002
10	.00000	.00000	.00001	.00001	.00001	.00001	.00002	.00002
11	.00000	.00000	.00001	.00001	.00001	.00001	.00002	.00002
12	.00000	.00000	.00001	.00001	.00001	.00001	.00002	.00002
13	.00000	.00000	.00001	.00001	.00001	.00001	.00002	.00002

TIME(SEC)= 240.145
TOTAL AREA(C2)= 11.225
WEDGE AREA= 1.9385
ORIGINAL PENITRATION DEPTH= .4246
ANGLE(DEG)= 86.090
ARC LENGTH/TIME INCREMENT= 1.25229
NO. OF WEDGES IN POOL = 8

TEMPERATURE HISTORY OF POWDER

AREA	1	2	3	4	5	6	7	8
1	113.555	113.555	113.555	113.555	113.555	113.555	113.555	113.555
2	108.853	109.602	110.102	110.413	110.644	110.820	110.961	111.078
3	106.417	107.213	107.697	108.083	108.382	108.629	108.835	109.013
4	106.417	106.387	106.626	106.829	107.037	107.229	107.406	107.571
5	106.417	106.387	106.344	106.374	106.433	106.517	106.611	106.714
6	106.417	106.387	106.344	106.278	106.247	106.240	106.256	106.290
7	106.417	106.387	106.344	106.278	106.214	106.166	106.134	106.120
8	106.417	106.387	106.344	106.278	106.214	106.155	106.105	106.068
9	106.417	106.387	106.344	106.278	106.214	106.155	106.101	106.057
10	106.417	106.387	106.344	106.278	106.214	106.155	106.101	106.055
11	106.417	106.387	106.344	106.278	106.214	106.155	106.101	106.055
12	106.417	106.387	106.344	106.278	106.214	106.155	106.101	106.055
13	106.417	106.387	106.344	106.278	106.214	106.155	106.101	106.055

TEMPERATURE OF STUCK MATERIAL

AREA	10	11	12	13	14	15	16	17	18	19	20	21
1	113.555	113.555	113.555	113.555	113.555	113.555	113.555	113.555	113.555	113.555	113.555	113.555
2	110.824	111.503	112.037	112.434	112.797	113.061	113.239	113.349	113.412	113.449	113.474	113.495

NECK RADIUS

AREA	1	2	3	4	5	6	7	8
1	.00000	.00001	.00001	.00001	.00002	.00002	.00002	.00003
2	.00000	.00001	.00001	.00001	.00002	.00002	.00002	.00003
3	.00000	.00001	.00001	.00001	.00001	.00002	.00002	.00002
4	.00000	.00001	.00001	.00001	.00001	.00002	.00002	.00002
5	.00000	.00001	.00001	.00001	.00001	.00002	.00002	.00002
6	.00000	.00001	.00001	.00001	.00001	.00002	.00002	.00002
7	.00000	.00001	.00001	.00001	.00001	.00002	.00002	.00002
8	.00000	.00001	.00001	.00001	.00001	.00002	.00002	.00002
9	.00000	.00001	.00001	.00001	.00001	.00002	.00002	.00002
10	.00000	.00001	.00001	.00001	.00001	.00002	.00002	.00002
11	.00000	.00001	.00001	.00001	.00001	.00002	.00002	.00002
12	.00000	.00001	.00001	.00001	.00001	.00002	.00002	.00002
13	.00000	.00001	.00001	.00001	.00001	.00002	.00002	.00002

NECK RADIUS OF STUCK MATERIAL

AREA	10	11	12	13	14	15	16	17	18	19	20	21
1	.00003	.00003	.00004	.00004	.00004	.00005	.00005	.00005	.00006	.00006	.00006	.00007
[illegible]	[illegible]	[illegible]	[illegible]	[illegible]	[illegible]	.00005	.00005	.00005	.00006	.00006	.00006	.00007

TIME(SEC)= 270.061
TOTAL AREA(C2)= 3.261
WEDGE AREA= .3601
ORIGINAL PENITRATION DEPTH= .3136
ANGLE(DEG)= 46.973
ARC LENGTH/TIME INCREMENT= .68328
NO. OF WEDGES IN POOL = 8

TEMPERATURE HISTORY OF POWDER

AREA	1	2	3	4	5	6	7	8
1	124.018	124.018	124.018	124.018	124.018	124.018	124.018	124.018
2	122.028	122.041	122.063	122.063	122.078	122.092	122.111	122.107
3	120.216	120.244	120.290	120.289	120.317	120.340	120.374	120.354
4	118.702	118.741	118.799	118.788	118.797	118.799	118.813	118.758
5	117.497	117.544	117.579	117.496	117.436	117.361	117.315	117.216
6	116.587	116.426	116.274	116.052	115.886	115.730	115.633	115.525
7	114.870	114.420	114.183	114.018	113.888	113.778	113.720	113.679
8	111.016	111.359	111.526	111.685	111.708	111.760	111.813	111.874
9	109.433	109.648	109.828	110.040	110.153	110.278	110.386	110.495
10	109.287	109.302	109.334	109.406	109.462	109.538	109.614	109.696
11	109.287	109.283	109.275	109.276	109.279	109.295	109.320	109.355
12	109.287	109.283	109.274	109.264	109.253	109.245	109.243	109.249
13	109.287	109.283	109.274	109.264	109.251	109.239	109.231	109.226
14	109.287	109.283	109.274	109.264	109.251	109.239	109.229	109.223
15	109.287	109.283	109.274	109.264	109.251	109.239	109.229	109.222
16	109.287	109.283	109.274	109.264	109.251	109.239	109.229	109.222
17	109.287	109.283	109.274	109.264	109.251	109.239	109.229	109.222

TEMPERATURE OF STUCK MATERIAL

AREA	10	11	12	13	14	15	16	17	18	19	20	21	22	23	24
1	124.018	124.018	124.018	124.018	124.018	124.018	124.018	124.018	124.018	124.018	124.018	124.018	124.018	124.018	124.018
2	122.109	122.089	122.052	122.059	122.037	122.028	122.020	122.020	121.998	121.987	121.976	121.968	121.969	121.950	121.941
3	120.352	120.303	120.213	120.219	120.174	120.154	120.135	120.134	120.093	120.074	120.054	120.040	120.045	120.013	119.998
4	118.725	118.595	118.434	118.432	118.368	118.338	118.308	118.304	118.261	118.238	118.217	118.204	118.217	118.183	118.170
5	117.133	116.886	116.665	116.659	116.593	116.564	116.533	116.533	116.519	116.504	116.492	116.491	116.516	116.495	116.487
6	115.416	115.073	114.864	114.853	114.815	114.808	114.798	114.819	114.873	114.882	114.894	114.916	114.968	114.973	114.990
7	113.607	113.268	113.105	113.154	113.176	113.219	113.259	113.329	113.468	113.513	113.559	113.615	113.697	113.739	113.791
8	111.921	111.699	111.660	111.777	111.882	111.998	112.117	112.258	111.400	111.552	111.706	111.859	112.009	112.136	112.305
9	110.197	110.453	110.715	110.945	111.153	111.373	111.612	111.852	0.000	0.000	0.000	0.000	0.000	0.000	0.000

AREA	25	26	27	28	29	30	31	32	33	34	35	36	37	38	39
1	124.018	124.018	124.018	124.018	124.018	124.018	124.018	124.018	124.018	124.018	[illegible]	124.018	124.018	[illegible]	124.018
2	121.935	121.925	121.927	121.914	121.908	121.900	[illegible]	[illegible]	121.893	[illegible]	[illegible]	121.880	121.871	[illegible]	121.850
3	119.987	119.974	119.980	119.960	119.953	119.941	119.930	119.923	119.938	119.932	119.930	119.924	119.912	119.868	119.879
4	118.162	118.153	118.169	118.152	118.151	118.143	118.137	118.138	118.166	118.167	118.175	118.180	118.181	118.156	118.180
5	116.472	116.478	116.511	116.509	116.525	116.532	116.540	116.556	116.604	116.620	116.645	116.666	116.686	116.685	116.726
6	115.002	115.034	115.093	115.115	115.158	115.188	115.221	115.261	115.332	115.369	115.419	115.467	115.518	115.566	115.627
7	113.842	113.908	113.998	114.050	114.105	114.166	114.229	114.299	114.393	114.456	114.534	114.615	114.708	114.828	114.909
8	112.482	112.647	112.814	112.920	113.054	113.182	113.315	113.452	113.584	113.695	113.835	113.997	114.193	114.486	114.594

AREA	40	41	42	43	44	45	46	47	48	49	50	51
1	124.018	124.018	124.018	124.018	124.018	124.018	124.018	124.018	124.018	124.018	124.018	124.018
2	121.860	121.873	121.884	121.898	121.908	121.925	121.933	121.946	121.959	121.973	121.989	122.017
3	119.901	119.925	119.938	119.944	119.967	120.002	120.020	120.046	120.074	120.104	120.138	120.194
4	118.218	118.258	118.269	118.275	118.313	118.366	118.396	118.438	118.483	118.531	118.584	118.668
5	116.787	116.852	116.862	116.893	116.950	117.023	117.067	117.126	117.190	117.259	117.336	117.451
6	115.713	115.807	115.808	115.867	115.946	116.039	116.098	116.174	116.259	116.352	116.453	116.582
	[illegible]	[illegible]	114.474	114.627	114.774	114.913	115.011	115.131	115.276	115.437	115.610	115.806
	[illegible]	[illegible]	[illegible]	[illegible]	[illegible]	0.000	0.000	0.000	0.000	0.000	0.000	0.000

NECK RADIUS

AREA	1	2	3	4	5	6	7	8
1	.00049	.00049	.00049	.00049	.00049	.00050	.00050	.00050
2	.00048	.00048	.00049	.00049	.00049	.00049	.00047	.00047
3	.00035	.00036	.00036	.00036	.00036	.00036	.00037	.00037
4	.00033	.00032	.00028	.00028	.00024	.00024	.00025	.00025
5	.00022	.00023	.00023	.00023	.00023	.00023	.00024	.00024
6	.00011	.00011	.00012	.00012	.00012	.00012	.00012	.00012
7	.00011	.00011	.00011	.00011	.00011	.00012	.00012	.00012
8	.00011	.00011	.00011	.00011	.00001	.00001	.00001	.00001
9	.00000	.00000	.00000	.00001	.00001	.00001	.00001	.00001
10	.00000	.00000	.00000	.00001	.00001	.00001	.00001	.00001
11	.00000	.00000	.00000	.00001	.00001	.00001	.00001	.00001
12	.00000	.00000	.00000	.00001	.00001	.00001	.00001	.00001
13	.00000	.00000	.00000	.00001	.00001	.00001	.00001	.00001
14	.00000	.00000	.00000	.00001	.00001	.00001	.00001	.00001
15	.00000	.00000	.00000	.00001	.00001	.00001	.00001	.00001
16	.00000	.00000	.00000	.00001	.00001	.00001	.00001	.00001
17	.00000	.00000	.00000	.00001	.00001	.00001	.00001	.00001

NECK RADIUS OF STUCK MATERIAL

AREA	10	11	12	13	14	15	16	17	18	19	20	21	22	23	24
1	.00050	.00040	.00040	.00040	.00040	.00040	.00040	.00041	.00041	.00041	.00041	.00042	.00042	.00042	.00042
2	.00045	.00039	.00039	.00039	.00039	.00039	.00040	.00040	.00040	.00040	.00041	.00041	.00041	.00041	.00041
3	.00037	.00037	.00037	.00038	.00038	.00038	.00038	.00039	.00039	.00039	.00039	.00040	.00040	.00040	.00040
4	.00025	.00025	.00025	.00025	.00025	.00026	.00026	.00026	.00026	.00027	.00027	.00027	.00027	.00027	.00028
5	.00024	.00024	.00024	.00025	.00025	.00025	.00025	.00026	.00026	.00026	.00026	.00026	.00025	.00025	.00023
6	.00013	.00013	.00013	.00013	.00013	.00013	.00014	.00014	.00014	.00014	.00014	.00015	.00015	.00015	.00015
7	.00012	.00012	.00013	.00013	.00013	.00013	.00013	.00014	.00014	.00014	.00014	.00014	.00015	.00015	.00015
8	.00002	.00002	.00002	.00002	.00002	.00002	.00003	.00003	.00003	.00003	.00003	.00004	.00004	.00004	.00004
9	.00002	.00002	.00002	.00002	.00002	.00002	.00003	.00003	0.00000	0.00000	0.00000	0.00000	0.00000	0.00000	0.00000

AREA	25	26	27	28	29	30	31	32	33	34	35	36	37	38	39
1	.00042	.00043	.00043	.00043	.00043	.00044	.00044	.00044	.00044	.00044	.00044	.00045	.00045	.00045	.00045
2	.00042	.00042	.00042	.00042	.00043	.00043	.00043	.00044	.00044	.00044	.00044	.00044	.00044	.00045	.00045
3	.00040	.00041	.00041	.00041	.00041	.00042	.00042	.00042	.00042	.00042	.00043	.00043	.00043	.00043	.00043
4	.00028	.00028	.00028	.00028	.00029	.00029	.00029	.00030	.00031	.00031	.00031	.00033	.00036	.00042	.00042
5	.00016	.00016	.00017	.00017	.00017	.00017	.00017	.00018	.00018	.00018	.00018	.00019	.00019	.00019	.00019
6	.00015	.00016	.00016	.00016	.00016	.00017	.00017	.00017	.00017	.00017	.00018	.00018	.00018	.00019	.00019
7	.00015	.00016	.00016	.00016	.00005	.00006	.00006	.00006	.00006	.00006	.00007	.00007	.00007	.00007	.00008
8	.00004	.00005	.00005	.00005	.00005	.00005	.00006	.00006	.00006	.00006	.00006	.00007	.00007	.00007	.00007

AREA	40	41	42	43	44	45	46	47	48	49	50	51
1	.00046	.00046	.00046	.00047	.00047	.00047	.00047	.00047	.00048	.00048	.00048	.00049
2	.00045	.00045	.00046	.00046	.00046	.00047	.00047	.00047	.00047	.00047	.00048	.00048
3	.00043	.00042	.00040	.00033	.00033	.00034	.00034	.00034	.00034	.00035	.00035	.00035
4	.00042	.00041	.00039	.00032	.00032	.00033	.00033	.00033	.00033	.00034	.00034	.00033
5	.00019	.00020	.00020	.00020	.00020	.00021	.00021	.00021	.00021	.00022	.00022	.00022
6	.00019	.00019	.00019	.00020	.00020	.00020	.00020	.00021	.00021	.00021	.00021	.00011
7	.00008	.00008	.00008	.00008	.00009	.00009	.00009	.00009	.00010	.00010	.00010	.00011
8	.00008	.00008	0.00000	0.00000	0.00000	0.00000	0.00000	0.00000	0.00000	0.00000	0.00000	0.00000

TIME(SEC)= 276.381
TOTAL AREA(C2)= .909
WEDGE AREA= .0294
ORIGINAL PENITRATION DEPTH= .2050
ANGLE(DEG)= 20.060
ARC LENGTH/TIME INCREMENT= .29180
NO. OF WEDGES IN POOL = 8

TEMPERATURE HISTORY OF POWDER

AREA	1	2	3	4	5	6	7	8
1	126.195	126.195	126.195	126.195	126.195	126.195	126.195	126.195
2	123.981	123.981	123.981	123.993	123.993	123.994	123.994	123.994
3	121.986	121.986	121.986	122.009	122.009	122.012	122.012	122.012
4	120.209	120.209	120.209	120.245	120.245	120.247	120.247	120.246
5	118.709	118.709	118.709	118.760	118.760	118.754	118.749	118.743
6	117.483	117.483	117.482	117.545	117.537	117.486	117.464	117.440
7	116.580	116.564	116.536	116.571	116.521	116.311	116.248	116.187
8	115.811	115.637	115.483	115.365	115.234	114.785	114.703	114.630
9	113.274	113.222	113.181	113.019	113.006	112.704	112.709	112.708
10	110.264	110.480	110.666	110.765	110.884	110.845	110.939	111.012
11	109.999	110.039	110.092	110.136	110.182	110.158	110.218	110.266

TEMPERATURE OF STUCK MATERIAL

AREA	10	11	12	13	14	15	16	17	18	19	20	21	22	23	24
1	126.195	126.195	126.195	126.195	126.195	126.195	126.195	126.195	126.195	126.195	126.195	126.195	126.195	126.195	126.195
2	124.001	124.001	124.008	124.008	124.017	124.017	124.027	124.027	124.032	124.032	124.042	124.041	124.051	124.050	124.058
3	122.025	122.025	122.039	122.039	122.056	122.055	122.076	122.074	122.084	122.081	122.101	122.097	122.116	122.111	122.126
4	120.266	120.264	120.286	120.283	120.307	120.302	120.330	120.323	120.336	120.327	120.352	120.341	120.367	120.354	120.371
5	118.767	118.758	118.782	118.769	118.793	118.777	118.801	118.782	118.789	118.768	118.783	118.760	118.768	118.744	118.755
6	117.453	117.423	117.435	117.401	117.412	117.376	117.386	117.349	117.343	117.305	117.311	117.273	117.270	117.234	117.236
7	116.169	116.109	116.093	116.036	116.025	115.970	115.959	115.910	115.891	115.845	115.838	115.795	115.780	115.743	115.736
8	114.590	114.532	114.502	114.453	114.435	114.392	114.373	114.339	114.324	114.293	114.286	114.258	114.242	114.224	114.223
9	112.710	112.721	112.727	112.739	112.755	112.761	112.755	112.766	112.775	112.783	112.794	112.800	112.803	112.821	112.846
10	111.101	111.193	111.259	111.331	111.388	111.437	111.431	111.483	111.515	111.560	111.597	111.641	111.683	111.740	111.815
11	110.028	110.056	110.089	110.122	110.161	110.210	110.363	110.421	110.551	110.638	110.738	110.875	111.059	111.160	111.370

AREA	25	26	27	28	29	30	31	32	33	34	35	36	37	38	39
1	126.195	126.195	126.195	126.195	126.195	126.195	126.195	126.195	126.195	126.195	126.195	126.195	126.195	126.195	126.195
2	124.056	124.063	124.067	124.064	124.071	124.067	124.071	124.067	124.068	124.073	124.068	124.071	124.074	124.068	124.072
3	122.120	122.131	122.138	122.129	122.142	122.132	122.138	122.128	122.129	122.137	122.125	122.129	122.135	122.123	122.128
4	120.356	120.367	120.373	120.357	120.371	120.354	120.358	120.340	120.338	120.348	120.328	120.332	120.340	120.321	120.331
5	118.730	118.736	118.738	118.711	118.725	118.698	118.699	118.673	118.666	118.672	118.647	118.650	118.657	118.635	118.645
6	117.200	117.206	117.202	117.170	117.182	117.150	117.147	117.120	117.108	117.113	117.087	117.091	117.100	117.078	117.091
7	115.702	115.726	115.718	115.689	115.683	115.655	115.655	115.635	115.625	115.633	115.615	115.626	115.641	115.628	115.649
8	114.208	114.286	114.290	114.278	114.285	114.274	114.285	114.281	114.283	114.301	114.301	114.324	114.352	114.357	114.392
9	112.868	113.027	113.051	113.064	113.090	113.103	113.133	113.153	113.175	113.211	113.233	113.274	113.321	113.345	113.387
10	111.882	111.165	111.272	111.349	111.428	111.515	111.602	111.666	111.759	111.861	111.931	112.008	112.121	112.170	112.313
11	111.485	0.000	0.000	0.000	0.000	0.000	0.000	0.000	0.000	0.000	0.000	0.000	0.000	0.000	0.000

AREA	40	41	42	43	44	45	46	47	48	49	50	51	52	53	54
1	126.195	126.195	126.195	126.195	126.195	126.195	126.195	126.195	126.195	126.195	126.195	126.195	126.195	126.195	126.195
2	124.065	124.062	124.060	124.053	124.037	124.038	124.030	124.027	124.021	124.013	123.995	123.997	124.002	123.995	123.997
3	122.115	122.108	122.101	122.087	122.051	122.053	122.039	122.030	122.009	121.996	121.952	121.939	121.948	121.937	121.941
4	120.312	120.303	120.302	120.283	120.237	120.239	120.221	120.208	120.174	120.158	120.092	120.067	120.083	120.071	120.079
5	118.623	118.607	118.600	118.579	118.512	118.516	118.498	118.484	118.448	118.434	118.361	118.344	118.369	118.360	118.375
6	117.071	117.053	117.042	117.025	116.944	116.953	116.941	116.931	116.899	116.892	116.823	116.820	116.857	116.857	116.883
7	115.638	115.625	115.617	115.611	115.528	115.547	115.547	115.546	115.531	115.537	115.486	115.504	115.557	115.571	115.611
[illegible]	[illegible]	[illegible]	114.402	114.412	114.349	114.382	114.396	114.413	114.427	114.450	114.434	114.478	114.551	114.580	114.636
[illegible]	[illegible]	[illegible]	[illegible]	[illegible]	[illegible]	[illegible]	[illegible]	113.582	113.641	113.681	113.713	113.789	113.884	113.928	114.000
[illegible]	[illegible]	[illegible]	[illegible]	[illegible]	[illegible]	[illegible]	[illegible]	[illegible]	[illegible]	[illegible]	[illegible]	[illegible]	113.592	113.651	113.742

AREA	55	56	57	58	59	60	61	62	63	64	65	66	67	68	69
1	126.195	126.195	126.195	126.195	126.195	126.195	126.195	126.195	126.195	126.195	126.195	126.195	126.195	126.195	126.195
2	123.999	123.994	123.998	123.997	124.003	123.999	123.999	124.007	124.003	124.003	124.005	124.011	124.009	124.011	124.010
3	121.947	121.938	121.948	121.947	121.960	121.952	121.954	121.970	121.964	121.966	121.971	121.984	121.980	121.987	121.987
4	120.090	120.080	120.097	120.100	120.119	120.111	120.116	120.139	120.133	120.139	120.144	120.153	120.150	120.151	120.155
5	118.394	118.388	118.415	118.422	118.451	118.446	118.459	118.493	118.491	118.503	118.516	118.536	118.538	118.550	118.560
6	116.912	116.915	116.949	116.966	117.004	117.007	117.027	117.052	117.058	117.079	117.103	117.138	117.148	117.175	117.196
7	115.653	115.668	115.706	115.735	115.787	115.802	115.836	115.876	115.892	115.925	115.963	116.015	116.036	116.083	116.116
8	114.692	114.722	114.753	114.797	114.866	114.893	114.947	115.002	115.029	115.075	115.128	115.200	115.231	115.287	115.335
9	114.067	114.109	113.497	113.593	113.715	113.774	113.892	113.990	114.040	114.118	114.213	114.343	114.398	114.526	114.614
10	113.820	113.874	0.000	0.000	0.000	0.000	0.000	0.000	0.000	0.000	0.000	0.000	0.000	0.000	0.000

AREA	70	71	72	73	74	75	76	77
1	126.195	126.195	126.195	126.195	126.195	126.195	126.195	126.195
2	124.009	124.008	124.000	123.960	123.947	123.958	123.961	123.971
3	121.992	121.991	121.985	121.936	121.913	121.936	121.943	121.963
4	120.167	120.168	120.167	120.116	120.090	120.126	120.139	120.171
5	118.582	118.589	118.595	118.556	118.536	118.586	118.607	118.654
6	117.229	117.243	117.261	117.249	117.246	117.311	117.343	117.407
7	116.163	116.186	116.218	116.251	116.274	116.355	116.399	116.482
8	115.395	115.428	115.476	115.573	115.632	115.727	115.783	115.886
9	114.707	114.757	114.848	115.141	115.289	115.409	115.486	115.620

NECK RADIUS

AREA	1	2	3	4	5	6	7	8
1	.00050	.00050	.00050	.00051	.00051	.00051	.00051	.00051
2	.00050	.00050	.00050	.00050	.00050	.00050	.00050	.00050
3	.00048	.00048	.00048	.00048	.00048	.00048	.00048	.00048
4	.00035	.00035	.00035	.00035	.00035	.00035	.00035	.00035
5	.00034	.00034	.00034	.00034	.00034	.00035	.00035	.00035
6	.00022	.00022	.00022	.00022	.00022	.00023	.00023	.00023
7	.00022	.00022	.00022	.00022	.00022	.00022	.00022	.00022
8	.00011	.00011	.00011	.00011	.00011	.00011	.00011	.00011
9	.00011	.00011	.00011	.00011	.00011	.00011	.00011	.00011
10	.00000	.00000	.00000	.00000	.00000	.00000	.00001	.00001
11	.00000	.00000	.00000	.00000	.00000	.00000	.00001	.00001

NECK RADIUS OF STUCK MATERIAL

AREA	10	11	12	13	14	15	16	17	18	19	20	21	22	23	24
1	.00051	.00051	.00052	.00052	.00052	.00052	.00052	.00052	.00052	.00052	.00052	.00052	.00053	.00053	.00053
2	.00050	.00050	.00051	.00051	.00051	.00051	.00051	.00051	.00051	.00051	.00052	.00052	.00052	.00052	.00052
3	.00049	.00049	.00049	.00049	.00049	.00049	.00049	.00049	.00050	.00050	.00050	.00050	.00050	.00050	.00050
4	.00036	.00036	.00036	.00036	.00036	.00036	.00037	.00037	.00037	.00037	.00037	.00037	.00037	.00037	.00037
5	.00035	.00035	.00035	.00035	.00035	.00035	.00034	.00034	.00033	.00033	.00030	.00030	.00025	.00025	.00025
6	.00023	.00023	.00023	.00023	.00023	.00023	.00024	.00024	.00024	.00024	.00024	.00024	.00024	.00024	.00024
7	.00022	.00022	.00023	.00023	.00023	.00023	.00023	.00023	.00023	.00023	.00023	.00023	.00024	.00024	.00024
8	.00011	.00011	.00011	.00011	.00012	.00012	.00012	.00012	.00012	.00012	.00012	.00012	.00013	.00013	.00013
9	.00011	.00011	.00011	.00011	.00012	.00012	.00012	.00012	.00012	.00012	.00012	.00012	.00012	.00012	.00013
10	.00001	.00001	.00001	.00001	.00001	.00001	.00001	.00001	.00001	.00002	.00002	.00002	.00002	.00002	.00002
11	.00001	.00001	.00001	.00001	.00001	.00001	.00001	.00001	.00001	.00002	.00002	.00002	.00002	.00002	.00002

AREA	25	26	27	28	29	30	31	32	33	34	35	36	37	38	39
1	.00053	.00053	.00053	.00053	.00054	.00054	.00054	.00054	.00054	.00055	.00055	.00055	.00055	.00055	.00055
2	.00052	.00052	.00052	.00052	.00053	.00053	.00053	.00053	.00053	.00054	.00054	.00054	.00054	.00054	.00054
3	.00050	.00051	.00051	.00051	.00051	.00051	.00051	.00051	.00052	.00052	.00052	.00052	.00052	.00052	.00052
4	.00037	.00038	.00038	.00038	.00038	.00038	.00038	.00038	.00039	.00039	.00039	.00040	.00040	.00040	.00042
5	.00025	.00026	.00026	.00026	.00026	.00026	.00026	.00026	.00026	.00027	.00027	.00027	.00027	.00027	.00027
6	.00024	.00025	.00025	.00025	.00025	.00025	.00025	.00025	.00025	.00026	.00026	.00026	.00026	.00026	.00026
7	.00024	.00024	.00022	.00022	.00014	.00014	.00014	.00014	.00014	.00014	.00014	.00015	.00015	.00015	.00015
8	.00013	.00013	.00013	.00013	.00013	.00013	.00014	.00014	.00014	.00014	.00014	.00014	.00014	.00014	.00015
9	.00013	.00013	.00013	.00013	.00013	.00013	.00014	.00013	.00014	.00014	.00014	.00014	.00014	.00014	.00004
10	.00002	.00002	.00002	.00003	.00003	.00003	.00003	.00003	.00003	.00003	.00003	.00004	.00004	.00004	.00004
11	.00002	0.00000	0.00000	0.00000	0.00000	0.00000	0.00000	0.00000	0.00000	0.00000	0.00000	0.00000	0.00000	0.00000	0.00000

AREA	40	41	42	43	44	45	46	47	48	49	50	51	52	53	54
1	.00055	.00055	.00055	.00055	.00056	.00056	.00056	.00056	.00056	.00056	.00057	.00057	.00057	.00057	.00058
2	.00054	.00054	.00055	.00055	.00055	.00055	.00055	.00055	.00056	.00056	.00056	.00056	.00056	.00056	.00057
3	.00052	.00052	.00053	.00053	.00053	.00052	.00052	.00052	.00050	.00050	.00048	.00043	.00043	.00043	.00044
4	.00042	.00043	.00047	.00047	.00051	.00051	.00051	.00051	.00049	.00049	.00046	.00041	.00042	.00042	.00042
5	.00027	.00027	.00028	.00028	.00028	.00028	.00028	.00028	.00028	.00028	.00029	.00029	.00029	.00029	.00030
6	.00026	.00027	.00027	.00027	.00027	.00027	.00027	.00028	.00028	.00028	.00028	.00028	.00029	.00029	.00029
7	.00015	.00015	.00016	.00016	.00016	.00016	.00016	.00016	.00016	.00016	.00017	.00017	.00017	.00017	.00017
8	.00015	.00015	.00015	.00015	.00015	.00016	.00016	.00016	.00016	.00016	.00016	.00016	.00017	.00017	.00017
9	.00004	.00004	.00004	.00005	.00005	.00005	.00005	.00005	.00005	.00005	.00006	.00006	.00006	.00006	.00006
10	.00004	.00004	.00004	.00004	.00005	.00005	.00005	.00005	.00005	.00005	.00005	.00006	.00006	.00006	.00006

AREA	55	56	57	58	59	60	61	62	63	64	65	66	67	68	69
1	.00058	.00058	.00058	.00058	.00058	.00058	.00059	.00059	.00059	.00059	.00059	.00059	.00059	.00060	.00060
2	.00057	.00057	.00057	.00057	.00058	.00058	.00058	.00058	.00058	.00058	.00058	.00059	.00059	.00059	.00059
3	.00044	.00044	.00044	.00044	.00044	.00044	.00045	.00045	.00045	.00045	.00045	.00046	.00046	.00046	.00046
4	.00042	.00042	.00042	.00043	.00043	.00043	.00043	.00043	.00043	.00042	.00041	.00037	.00037	.00033	.00033
5	.00030	.00030	.00030	.00030	.00030	.00030	.00031	.00031	.00031	.00031	.00031	.00032	.00032	.00032	.00032
6	.00029	.00029	.00029	.00029	.00029	.00029	.00028	.00019	.00019	.00020	.00020	.00020	.00020	.00020	.00021
7	.00018	.00017	.00018	.00018	.00018	.00018	.00018	.00019	.00019	.00019	.00019	.00019	.00019	.00020	.00020
8	.00017	.00017	.00017	.00018	.00018	.00018	.00018	.00018	.00018	.00019	.00019	.00019	.00019	.00009	.00009
9	.00006	.00007	.00007	.00007	.00007	.00007	.00007	.00008	.00008	.00008	.00008	.00008	.00008	.00009	.00009
10	.00006	.00006	0.00000	0.00000	0.00000	0.00000	0.00000	0.00000	0.00000	0.00000	0.00000	0.00000	0.00000	0.00000	0.00000

AREA	70	71	72	73	74	75	76	77
1	.00060	.00060	.00061	.00050	.00050	.00050	.00050	.00050
2	.00057	.00057	.00055	.00049	.00049	.00049	.00049	.00050
3	.00046	.00046	.00047	.00047	.00047	.00047	.00047	.00048
4	.00034	.00034	.00034	.00034	.00034	.00035	.00035	.00035
5	.00033	.00033	.00033	.00033	.00033	.00034	.00034	.00034
6	.00021	.00021	.00021	.00021	.00021	.00022	.00022	.00022
7	.00020	.00020	.00020	.00021	.00021	.00021	.00021	.00022
8	.00009	.00009	.00010	.00010	.00010	.00010	.00010	.00011
9	.00009	.00009	.00009	.00010	.00010	.00010	.00010	.00010

TIME(SEC)= 300.008
TOTAL AREA(C2)= 0.000
WEDGE AREA= 0.0000
ORIGINAL PENITRATION DEPTH= .2050
ANGLE(DEG)= 0.000
ARC LENGTH/TIME INCREMENT= 1.57144
NO. OF WEDGES IN POOL = 8

TEMPERATURE HISTORY OF POWDER

AREA	1	2	3	4	5	6	7	8
1	134.228	134.228	134.228	134.228	134.228	134.228	134.228	134.228
2	132.091	132.091	132.091	132.092	132.091	132.079	132.079	132.079
3	130.056	130.057	130.057	130.058	130.057	130.033	130.033	130.032
4	128.205	128.206	128.206	128.208	128.207	128.172	128.171	128.170
5	126.586	126.587	126.588	126.590	126.588	126.542	126.541	126.539
6	125.179	125.180	125.181	125.183	125.181	125.125	125.125	125.122
7	124.021	124.022	124.023	124.025	124.023	123.958	123.958	123.955
8	123.099	123.100	123.101	123.103	123.101	123.029	123.028	123.025
9	122.438	122.439	122.440	122.442	122.440	122.363	122.362	122.359
10	122.033	122.034	122.035	122.038	122.035	121.955	121.954	121.951
11	121.898	121.899	121.900	121.902	121.900	121.819	121.818	121.815

TEMPERATURE OF STUCK MATERIAL

AREA	10	11	12	13	14	15	16	17	18	19	20	21	22	23	24
1	134.228	134.228	134.228	134.228	134.228	134.228	134.228	134.228	134.228	134.228	134.228	134.228	134.228	134.228	134.228
2	131.957	131.955	131.959	131.959	131.964	131.969	132.008	132.008	132.024	132.028	132.037	132.047	132.065	132.068	132.086
3	129.786	129.780	129.788	129.788	129.798	129.810	129.888	129.888	129.921	129.928	129.946	129.966	130.002	130.009	130.044
4	127.790	127.782	127.793	127.794	127.809	127.826	127.947	127.948	127.998	128.009	128.036	128.066	128.122	128.132	128.186
5	126.018	126.007	126.021	126.022	126.042	126.066	126.228	126.229	126.295	126.311	126.339	126.380	126.440	126.454	126.528
6	124.445	124.430	124.449	124.450	124.474	124.506	124.719	124.720	124.806	124.826	124.864	124.917	124.998	125.016	125.111
7	123.110	123.091	123.113	123.115	123.144	123.183	123.451	123.453	123.560	123.585	123.633	123.699	123.802	123.824	123.940
8	121.994	121.971	121.997	121.999	122.033	122.082	122.410	122.412	122.542	122.573	122.632	122.712	122.839	122.866	123.005
9	121.126	121.097	121.127	121.129	121.169	121.228	121.622	121.624	121.780	121.817	121.886	121.982	122.134	122.165	122.329
10	120.496	120.461	120.495	120.497	120.543	120.614	121.080	121.082	121.265	121.309	121.390	121.502	121.681	121.718	121.908
11	119.755	119.696	119.745	119.748	119.814	119.930	120.640	120.643	120.900	120.961	121.070	121.223	121.459	121.506	121.744

AREA	25	26	27	28	29	30	31	32	33	34	35	36	37	38	39
1	134.228	134.228	134.228	134.228	134.228	134.228	134.228	134.228	134.228	134.228	134.228	134.228	134.228	134.228	134.228
2	132.090	132.095	132.103	132.106	132.111	132.115	132.120	132.121	132.128	132.135	132.137	132.141	132.148	132.148	132.160
3	130.054	130.064	130.080	130.085	130.096	130.104	130.114	130.116	130.129	130.144	130.148	130.154	130.169	130.169	130.194
4	128.201	128.217	128.240	128.248	128.265	128.277	128.292	128.296	128.314	128.338	128.344	128.355	128.379	128.379	128.420
5	126.548	126.570	126.602	126.613	126.634	126.651	126.672	126.676	126.701	126.732	126.740	126.756	126.787	126.787	126.842
6	125.136	125.165	125.206	125.219	125.246	125.267	125.293	125.299	125.331	125.369	125.379	125.398	125.438	125.438	125.506
7	123.972	124.007	124.053	124.070	124.085	124.111	124.143	124.149	124.188	124.234	124.247	124.269	124.318	124.317	124.400
8	123.043	123.086	123.141	123.162	123.181	123.213	123.250	123.258	123.303	123.357	123.372	123.398	123.455	123.454	123.552
9	122.374	122.425	122.491	122.515	122.539	122.577	122.619	122.627	122.681	122.742	122.759	122.788	122.854	122.853	122.955
10	121.960	121.620	121.723	121.761	121.798	121.857	121.916	121.928	122.007	122.093	122.119	122.156	122.249	122.245	122.396
11	121.810	0.000	0.000	0.000	0.000	0.000	0.000	0.000	0.000	0.000	0.000	0.000	0.000	0.000	0.000

AREA	40	41	42	43	44	45	46	47	48	49	50	51	52	53	54
1	134.228	134.228	134.228	134.228	134.228	134.228	134.228	134.228	134.228	134.228	134.228	134.228	134.228	134.228	134.228
2	132.162	132.166	132.173	132.174	132.189	132.193	132.194	132.201	132.221	132.224	132.243	132.257	132.269	132.272	132.280
3	130.197	130.205	130.218	130.221	130.250	130.257	130.259	130.272	130.304	130.311	130.340	130.354	130.378	130.385	130.400
4	128.424	128.441	128.471	128.476	128.531	128.542	128.544	128.563	128.610	128.621	128.662	128.676	128.712	128.722	128.746
5	126.847	126.869	126.906	126.913	126.985	127.001	127.004	127.030	127.099	127.114	127.177	127.207	127.254	127.268	127.299
6	125.513	125.540	125.584	125.594	125.685	125.705	125.708	125.743	125.835	125.854	125.939	125.985	126.044	126.062	126.100
7	124.408	124.441	124.492	124.504	124.617	124.641	124.645	124.688	124.805	124.828	124.938	125.001	125.072	125.093	125.138
8	123.561	123.600	123.659	123.673	123.810	123.838	123.843	123.895	124.038	124.065	124.202	124.281	124.364	124.389	124.442
9	122.966	123.011	123.079	123.095	123.259	123.291	123.296	123.357	123.529	123.560	123.726	123.823	123.918	123.947	124.006
[illegible]	[illegible]	[illegible]	[illegible]	[illegible]	122.838	122.878	122.884	122.970	123.211	123.251	123.484	123.614	123.729	123.764	123.834

AREA	55	56	57	58	59	60	61	62	63	64	65	66	67	68	69
1	134.228	134.228	134.228	134.228	134.228	134.228	134.228	134.228	134.228	134.228	134.228	134.228	134.228	134.228	134.228
2	132.285	132.288	132.295	132.303	132.313	132.316	132.327	132.336	132.339	132.344	132.352	132.364	132.368	132.382	132.389
3	130.410	130.417	130.431	130.446	130.467	130.474	130.495	130.514	130.519	130.530	130.546	130.571	130.578	130.607	130.622
4	128.761	128.770	128.792	128.815	128.846	128.856	128.888	128.914	128.921	128.937	128.958	128.984	128.995	129.028	129.052
5	127.319	127.332	127.362	127.393	127.434	127.448	127.491	127.525	127.536	127.557	127.586	127.625	127.639	127.688	127.720
6	126.125	126.141	126.180	126.219	126.269	126.286	126.338	126.364	126.377	126.404	126.442	126.493	126.511	126.575	126.617
7	125.168	125.188	125.236	125.283	125.343	125.364	125.428	125.461	125.477	125.510	125.555	125.619	125.641	125.721	125.772
8	124.475	124.499	124.558	124.613	124.683	124.707	124.782	124.824	124.842	124.880	124.934	125.010	125.036	125.121	125.180
9	124.043	124.070	123.727	123.809	123.911	123.947	124.061	124.125	124.151	124.205	124.286	124.397	124.434	124.568	124.652
10	123.877	123.910	0.000	0.000	0.000	0.000	0.000	0.000	0.000	0.000	0.000	0.000	0.000	0.000	0.000

AREA	70	71	72	73	74	75	76	77
1	134.228	134.228	134.228	134.228	134.228	134.228	134.228	134.228
2	132.392	132.396	132.398	132.422	132.445	132.456	132.464	132.476
3	130.634	130.641	130.653	130.723	130.770	130.792	130.807	130.832
4	129.072	129.083	129.105	129.222	129.293	129.327	129.350	129.388
5	127.750	127.763	127.795	127.962	128.060	128.104	128.135	128.185
6	126.654	126.671	126.714	126.933	127.058	127.118	127.151	127.214
7	125.817	125.838	125.891	126.164	126.318	126.384	126.430	126.505
8	125.234	125.258	125.322	125.653	125.838	125.913	125.967	126.054
9	124.727	124.759	124.852	125.333	125.584	125.677	125.745	125.853

NECK RADIUS

AREA	1	2	3	4	5	6	7	8
1	.00092	.00092	.00092	.00093	.00093	.00093	.00093	.00093
2	.00091	.00091	.00091	.00091	.00091	.00091	.00091	.00091
3	.00087	.00087	.00087	.00087	.00087	.00087	.00087	.00087
4	.00072	.00072	.00072	.00073	.00073	.00073	.00073	.00073
5	.00070	.00070	.00070	.00070	.00070	.00070	.00070	.00070
6	.00057	.00057	.00057	.00057	.00057	.00057	.00057	.00057
7	.00055	.00055	.00055	.00056	.00056	.00056	.00056	.00056
8	.00043	.00043	.00043	.00044	.00044	.00044	.00044	.00044
9	.00042	.00042	.00042	.00043	.00043	.00043	.00043	.00043
10	.00031	.00032	.00032	.00032	.00032	.00032	.00032	.00032
11	.00031	.00031	.00031	.00031	.00032	.00032	.00032	.00032

NECK RADIUS OF STUCK MATERIAL

AREA	10	11	12	13	14	15	16	17	18	19	20	21	22	23	24
1	.00093	.00093	.00093	.00093	.00094	.00094	.00094	.00094	.00094	.00094	.00094	.00094	.00094	.00094	.00095
2	.00091	.00091	.00091	.00091	.00092	.00092	.00092	.00092	.00092	.00092	.00092	.00092	.00093	.00093	.00093
3	.00087	.00087	.00088	.00088	.00088	.00088	.00088	.00088	.00088	.00088	.00089	.00089	.00089	.00089	.00089
4	.00073	.00073	.00073	.00073	.00073	.00073	.00074	.00074	.00074	.00074	.00074	.00074	.00074	.00074	.00075
5	.00070	.00070	.00070	.00070	.00071	.00071	.00069	.00069	.00069	.00069	.00066	.00066	.00061	.00061	.00061
6	.00057	.00057	.00057	.00057	.00057	.00057	.00058	.00058	.00058	.00058	.00058	.00058	.00059	.00059	.00059
7	.00055	.00055	.00056	.00056	.00056	.00056	.00056	.00056	.00056	.00056	.00057	.00057	.00057	.00057	.00057
8	.00043	.00043	.00044	.00044	.00044	.00044	.00044	.00044	.00044	.00044	.00045	.00045	.00045	.00045	.00045
9	.00043	.00043	.00043	.00043	.00043	.00043	.00043	.00043	.00044	.00044	.00044	.00044	.00044	.00044	.00045
10	.00031	.00031	.00032	.00032	.00032	.00032	.00032	.00032	.00032	.00033	.00033	.00033	.00033	.00033	.00033
11	.00031	.00031	.00031	.00031	.00031	.00031	.00032	.00032	.00032	.00032	.00032	.00033	.00033	.00033	.00033

AREA	25	26	27	28	29	30	31	32	33	34	35	36	37	38	39
1	.00095	.00095	.00095	.00095	.00095	.00095	.00096	.00096	.00096	.00096	.00096	.00096	.00096	.00096	.00096
2	.00093	.00093	.00093	.00093	.00094	.00094	.00094	.00094	.00094	.00095	.00095	.00095	.00095	.00095	.00095
3	.00089	.00090	.00090	.00090	.00090	.00090	.00090	.00090	.00090	.00091	.00091	.00091	.00091	.00091	.00091
4	.00075	.00075	.00075	.00075	.00075	.00075	.00076	.00076	.00076	.00077	.00077	.00077	.00078	.00078	.00079
5	.00061	.00061	.00061	.00061	.00062	.00062	.00062	.00062	.00062	.00062	.00062	.00063	.00063	.00063	.00063
6	.00059	.00059	.00059	.00059	.00060	.00060	.00060	.00060	.00060	.00060	.00060	.00061	.00061	.00061	.00061
7	.00057	.00057	.00055	.00055	.00047	.00047	.00048	.00048	.00048	.00048	.00048	.00048	.00049	.00049	.00049
8	.00045	.00045	.00046	.00046	.00046	.00046	.00046	.00046	.00046	.00047	.00047	.00047	.00047	.00047	.00048
9	.00045	.00045	.00045	.00045	.00045	.00045	.00046	.00046	.00046	.00046	.00046	.00046	.00046	.00046	.00036
10	.00034	.00034	.00034	.00034	.00034	.00034	.00034	.00034	.00035	.00035	.00035	.00035	.00035	.00035	.00036
11	.00033	0.00000	0.00000	0.00000	0.00000	0.00000	0.00000	0.00000	0.00000	0.00000	0.00000	0.00000	0.00000	0.00000	0.00000

AREA	40	41	42	43	44	45	46	47	48	49	50	51	52	53	54
1	.00096	.00097	.00097	.00097	.00097	.00097	.00097	.00098	.00098	.00098	.00098	.00099	.00099	.00099	.00099
2	.00095	.00095	.00096	.00096	.00096	.00096	.00096	.00096	.00096	.00096	.00097	.00097	.00097	.00097	.00098
3	.00091	.00091	.00092	.00092	.00091	.00091	.00091	.00091	.00089	.00089	.00087	.00082	.00082	.00082	.00083
4	.00079	.00081	.00085	.00085	.00089	.00088	.00088	.00088	.00086	.00086	.00084	.00079	.00079	.00079	.00080
5	.00063	.00063	.00064	.00064	.00064	.00064	.00064	.00064	.00064	.00064	.00065	.00065	.00065	.00065	.00066
6	.00061	.00061	.00062	.00062	.00062	.00062	.00062	.00062	.00063	.00063	.00063	.00063	.00063	.00063	.00064
7	.00049	.00049	.00049	.00049	.00049	.00050	.00050	.00050	.00050	.00050	.00050	.00051	.00051	.00051	.00051
8	.00048	.00048	.00048	.00048	.00048	.00049	.00049	.00049	.00049	.00049	.00049	.00050	.00050	.00050	.00050
9	.00036	.00037	.00037	.00037	.00037	.00037	.00037	.00038	.00038	.00038	.00038	.00038	.00039	.00039	.00039
10	.00036	.00036	.00036	.00036	.00037	.00037	.00037	.00037	.00037	.00038	.00038	.00038	.00038	.00038	.00039

AREA	55	56	57	58	59	60	61	62	63	64	65	66	67	68	69
1	.00099	.00099	.00099	.00100	.00100	.00100	.00101	.00101	.00101	.00101	.00101	.00101	.00101	.00102	.00102
2	.00098	.00098	.00098	.00098	.00098	.00098	.00099	.00099	.00099	.00099	.00099	.00100	.00100	.00100	.00100
3	.00083	.00083	.00083	.00083	.00083	.00083	.00084	.00084	.00084	.00084	.00084	.00085	.00085	.00085	.00085
4	.00080	.00080	.00080	.00080	.00080	.00080	.00080	.00080	.00080	.00080	.00079	.00075	.00075	.00071	.00071
5	.00066	.00066	.00066	.00066	.00067	.00067	.00067	.00067	.00067	.00067	.00068	.00068	.00068	.00068	.00069
6	.00064	.00064	.00064	.00064	.00064	.00064	.00063	.00054	.00054	.00055	.00055	.00055	.00055	.00056	.00056
7	.00051	.00052	.00052	.00052	.00052	.00052	.00053	.00053	.00053	.00053	.00053	.00054	.00054	.00054	.00054
8	.00051	.00051	.00051	.00051	.00051	.00051	.00052	.00052	.00052	.00052	.00052	.00053	.00053	.00043	.00043
9	.00039	.00039	.00039	.00040	.00040	.00040	.00040	.00040	.00041	.00041	.00041	.00041	.00042	.00042	.00042
10	.00039	.00039	0.00000	0.00000	0.00000	0.00000	0.00000	0.00000	0.00000	0.00000	0.00000	0.00000	0.00000	0.00000	0.00000

AREA	70	71	72	73	74	75	76	77
1	.00102	.00102	.00103	.00092	.00092	.00092	.00092	.00092
2	.00098	.00098	.00096	.00090	.00090	.00090	.00090	.00090
3	.00086	.00086	.00086	.00086	.00086	.00087	.00087	.00087
4	.00071	.00071	.00072	.00072	.00072	.00072	.00072	.00073
5	.00069	.00069	.00069	.00070	.00070	.00070	.00070	.00070
6	.00056	.00056	.00056	.00057	.00057	.00057	.00057	.00057
7	.00055	.00055	.00055	.00055	.00056	.00056	.00056	.00056
8	.00043	.00043	.00043	.00044	.00044	.00044	.00045	.00045
9	[illegible]	[illegible]	[illegible]	[illegible]	[illegible]	.00044	.00044	.00044

TIME(SEC)= 330.036
TOTAL AREA(CZ)= 0.000
WEDGE AREA= 0.0000
ORIGINAL PENITRATION DEPTH= .2050
ANGLE(DEG)= 0.000
ARC LENGTH/TIME INCREMENT= .42824
NO. OF WEDGES IN POOL = 8

TEMPERATURE HISTORY OF POWDER

AREA	1	2	3	4	5	6	7	8
1	144.199	144.199	144.199	144.199	144.199	144.199	144.199	144.199
2	143.243	143.243	143.243	143.243	143.243	143.286	143.286	143.286
3	142.371	142.371	142.371	142.372	142.372	142.315	142.315	142.315
4	141.374	141.374	141.375	141.375	141.375	141.514	141.514	141.514
5	140.641	140.641	140.641	140.642	140.642	140.491	140.491	140.491
6	139.714	139.714	139.714	139.716	139.715	139.824	139.824	139.824
7	139.093	139.093	139.093	139.095	139.095	138.994	138.993	138.993
8	136.965	136.965	136.965	136.968	136.968	136.890	136.890	136.889
9	135.594	135.594	135.594	135.598	135.597	135.536	135.536	135.535
10	134.833	134.834	134.834	134.838	134.838	134.793	134.793	134.792
11	134.591	134.591	134.591	134.596	134.595	134.553	134.553	134.552

TEMPERATURE OF STUCK MATERIAL

AREA	10	11	12	13	14	15	16	17	18	19	20	21	22	23	24
1	144.199	144.199	144.199	144.199	144.199	144.199	144.199	144.199	144.199	144.199	144.199	144.199	144.199	144.199	144.199
2	143.165	143.162	143.164	143.164	143.169	143.131	143.184	143.184	143.215	143.218	143.219	143.237	143.253	143.254	143.274
3	142.076	142.070	142.075	142.075	142.085	142.163	142.230	142.230	142.253	142.260	142.289	142.301	142.336	142.352	142.390
4	141.187	141.179	141.185	141.185	141.199	141.141	141.306	141.306	141.389	141.398	141.410	141.456	141.504	141.512	141.389
5	140.216	140.204	140.213	140.213	140.232	140.322	140.508	140.509	140.579	140.591	140.635	140.672	140.740	140.764	140.660
6	139.453	139.438	139.449	139.450	139.472	139.490	139.764	139.765	139.879	139.894	139.931	139.991	140.073	140.094	139.598
7	136.910	136.885	136.904	136.905	136.940	137.027	137.504	137.504	137.685	137.711	137.780	137.873	138.011	138.049	138.980
8	134.899	134.865	134.891	134.892	134.937	135.040	135.645	135.646	135.881	135.918	136.009	136.133	136.320	136.368	136.730
9	133.457	133.414	133.446	133.448	133.500	133.609	134.280	134.281	134.551	134.597	134.704	134.853	135.081	135.136	135.398
10	132.484	132.432	132.470	132.472	132.531	132.648	133.380	133.382	133.679	133.735	133.856	134.029	134.294	134.355	134.646
11	131.403	131.317	131.376	131.378	131.463	131.639	132.684	132.686	133.082	133.165	133.325	133.559	133.913	133.990	134.360

AREA	25	26	27	28	29	30	31	32	33	34	35	36	37	38	39
1	144.199	144.199	144.199	144.199	144.199	144.199	144.199	144.199	144.199	144.199	144.199	144.199	144.199	144.199	144.199
2	143.281	143.246	143.274	143.233	143.235	143.239	143.269	143.270	143.238	143.269	143.270	143.273	143.248	143.247	143.255
3	142.306	142.377	142.293	142.355	142.359	142.373	142.296	142.299	142.362	142.312	142.314	142.320	142.375	142.373	142.384
4	141.500	141.386	141.489	141.393	141.397	141.411	141.495	141.498	141.431	141.511	141.515	141.523	141.477	141.473	141.504
5	140.472	140.656	140.541	140.654	140.661	140.686	140.598	140.603	140.700	140.655	140.660	140.671	140.753	140.749	140.788
6	139.800	139.737	139.866	139.812	139.818	139.844	139.929	139.935	139.912	139.995	140.002	140.015	140.007	140.002	140.068
7	138.965	139.122	139.124	139.201	139.208	139.241	139.239	139.246	139.318	139.363	139.351	139.366	139.431	139.425	139.506
8	136.850	137.028	137.124	137.202	137.210	137.258	137.321	137.331	137.416	137.502	137.515	137.537	137.620	137.612	137.759
9	135.484	135.690	135.784	135.864	135.876	135.936	136.000	136.013	136.114	136.214	136.231	136.259	136.362	136.352	136.515
10	134.728	134.269	134.400	134.479	134.513	134.607	134.679	134.698	134.824	134.952	134.984	135.026	135.164	135.148	135.383
11	134.461	0.000	0.000	0.000	0.000	0.000	0.000	0.000	0.000	0.000	0.000	0.000	0.000	0.000	0.000

AREA	40	41	42	43	44	45	46	47	48	49	50	51	52	53	54
1	144.199	144.199	144.199	144.199	144.199	144.199	144.199	144.199	144.199	144.199	144.199	144.199	144.199	144.199	144.199
2	143.256	143.281	143.270	143.271	143.305	143.308	143.308	143.304	143.324	143.298	143.325	143.330	143.328	143.331	143.339
3	142.385	142.359	142.406	142.408	142.423	142.429	142.429	142.463	142.426	142.471	142.458	142.472	142.509	142.502	142.502
4	141.507	141.569	141.552	141.556	141.652	141.659	141.659	141.585	141.675	141.603	141.698	141.718	141.695	141.718	141.725
5	140.791	140.774	140.844	140.849	140.909	140.919	140.773	140.903	140.838	140.929	140.944	140.932	141.030	140.988	141.021
6	140.072	140.138	140.154	140.159	140.009	140.023	140.170	140.028	140.240	140.170	140.339	140.342	140.288	140.357	140.353
7	139.510	139.542	139.606	139.613	139.462	139.478	139.293	139.498	139.557	139.649	139.540	139.622	139.801	139.744	139.777
8	137.766	137.841	137.928	137.939	138.677	138.698	138.827	138.848	139.113	139.127	139.135	139.224	139.234	139.210	139.335
9	136.525	136.617	136.730	136.745	137.137	137.167	137.219	137.376	137.764	137.843	138.560	138.785	138.731	138.916	138.956
[illegible]	[illegible]	[illegible]	[illegible]	[illegible]	136.187	136.234	136.244	136.409	136.920	137.020	137.618	138.025	138.643	138.665	138.886

AREA	55	56	57	58	59	60	61	62	63	64	65	66	67	68	69
1	144.199	144.199	144.199	144.199	144.199	144.199	144.199	144.199	144.199	144.199	144.199	144.199	144.199	144.199	144.199
2	143.327	143.340	143.368	143.379	143.383	143.385	143.394	143.396	143.390	143.398	143.394	143.405	143.408	143.420	143.426
3	142.526	142.511	142.583	142.586	142.612	142.616	142.618	142.621	142.624	142.615	142.640	142.640	142.640	142.677	142.693
4	141.698	141.744	141.852	141.882	141.898	141.885	141.901	141.910	141.894	141.919	141.915	141.951	141.962	142.005	142.027
5	141.062	141.011	141.223	141.236	141.244	141.251	141.249	141.254	141.263	141.258	141.307	141.327	141.334	141.417	141.453
6	140.304	140.417	140.659	140.702	140.655	140.615	140.650	140.680	140.667	140.712	140.731	140.802	140.825	140.920	140.962
7	139.876	139.784	140.212	140.085	140.078	140.097	140.145	140.178	140.200	140.226	140.299	140.368	140.391	140.527	140.583
8	139.255	139.459	139.529	139.568	139.602	139.613	139.730	139.797	139.815	139.879	139.947	140.055	140.091	140.246	140.311
9	139.119	139.051	138.317	138.566	138.881	138.981	139.220	139.332	139.381	139.470	139.579	139.728	139.776	139.981	140.064
10	138.851	139.055	0.000	0.000	0.000	0.000	0.000	0.000	0.000	0.000	0.000	0.000	0.000	0.000	0.000

AREA	70	71	72	73	74	75	76	77
1	144.199	144.199	144.199	144.199	144.199	144.199	144.199	144.199
2	143.438	143.441	143.449	143.520	143.555	143.563	143.573	143.584
3	142.703	142.709	142.740	142.878	142.943	142.969	142.982	143.007
4	142.064	142.072	142.100	142.311	142.413	142.438	142.467	142.499
5	141.482	141.492	141.553	141.828	141.953	142.000	142.028	142.074
6	141.022	141.035	141.090	141.434	141.594	141.636	141.679	141.730
7	140.638	140.654	140.738	141.137	141.315	141.376	141.417	141.480
8	140.386	140.404	140.489	140.941	141.144	141.202	141.254	141.320
9	140.153	140.175	140.284	140.818	141.049	141.119	141.174	141.251

NECK RADIUS

AREA	1	2	3	4	5	6	7	8
1	.01250	.01250	.01250	.01250	.01250	.01250	.01250	.01250
2	.01250	.01250	.01250	.01250	.01250	.01250	.01250	.01250
3	.01250	.01250	.01250	.01250	.01250	.01250	.01250	.01250
4	.01250	.01250	.01250	.01250	.01250	.01250	.01250	.01250
5	.01250	.01250	.01250	.01250	.01250	.01250	.01250	.01250
6	.01250	.01250	.01250	.01250	.01250	.01250	.01250	.01250
7	.01250	.01250	.01250	.01250	.01250	.01250	.01250	.01250
8	.00093	.00093	.00093	.00094	.00094	.00094	.00094	.00094
9	.00092	.00092	.00092	.00092	.00092	.00092	.00092	.00092
10	.00080	.00080	.00080	.00080	.00080	.00080	.00080	.00080
11	.00079	.00079	.00080	.00080	.00080	.00080	.00080	.00080

NECK RADIUS OF STUCK MATERIAL

AREA	10	11	12	13	14	15	16	17	18	19	20	21	22	23	24
1	.01250	.01250	.01250	.01250	.01250	.01250	.01250	.01250	.01250	.01250	.01250	.01250	.01250	.01250	.01250
2	.01250	.01250	.01250	.01250	.01250	.01250	.01250	.01250	.01250	.01250	.01250	.01250	.01250	.01250	.01250
3	.01250	.01250	.01250	.01250	.01250	.01250	.01250	.01250	.01250	.01250	.01250	.01250	.01250	.01250	.01250
4	.01250	.01250	.01250	.01250	.01250	.01250	.01250	.01250	.01250	.01250	.01250	.01250	.01250	.01250	.01250
5	.01250	.01250	.01250	.01250	.01250	.01250	.01250	.01250	.01250	.01250	.01250	.01250	.01250	.01250	.01250
6	.01250	.01250	.01250	.01250	.01250	.01250	.01250	.01250	.01250	.01250	.01250	.01250	.01250	.01250	.01250
7	.00106	.00106	.00106	.00106	.00106	.00106	.00107	.00107	.00107	.00107	.00108	.00108	.01250	.01250	.01250
8	.00092	.00092	.00092	.00092	.00093	.00093	.00093	.00093	.00094	.00094	.00094	.00094	.00095	.00095	.00095
9	.00090	.00090	.00090	.00090	.00091	.00091	.00091	.00091	.00092	.00092	.00092	.00092	.00093	.00093	.00093
10	.00078	.00078	.00078	.00078	.00079	.00079	.00080	.00080	.00080	.00080	.00081	.00081	.00081	.00081	.00082
11	.00077	.00077	.00077	.00077	.00077	.00077	.00079	.00079	.00079	.00079	.00080	.00080	.00080	.00081	.00081

AREA	25	26	27	28	29	30	31	32	33	34	35	36	37	38	39
1	.01250	.01250	.01250	.01250	.01250	.01250	.01250	.01250	.01250	.01250	.01250	.01250	.01250	.01250	.01250
2	.01250	.01250	.01250	.01250	.01250	.01250	.01250	.01250	.01250	.01250	.01250	.01250	.01250	.01250	.01250
3	.01250	.01250	.01250	.01250	.01250	.01250	.01250	.01250	.01250	.01250	.01250	.01250	.01250	.01250	.01250
4	.01250	.01250	.01250	.01250	.01250	.01250	.01250	.01250	.01250	.01250	.01250	.01250	.01250	.01250	.01250
5	.01250	.01250	.01250	.01250	.01250	.01250	.01250	.01250	.01250	.01250	.01250	.01250	.01250	.01250	.01250
6	.01250	.01250	.01250	.01250	.01250	.01250	.01250	.01250	.01250	.01250	.01250	.01250	.01250	.01250	.01250
7	.01250	.01250	.01250	.01250	.01250	.01250	.01250	.01250	.01250	.01250	.01250	.01250	.01250	.01250	.01250
8	.00095	.00096	.00096	.00096	.00096	.00096	.00097	.00097	.00097	.00097	.00097	.00097	.00098	.00098	.00098
9	.00094	.00094	.00094	.00094	.00095	.00095	.00095	.00095	.00095	.00095	.00095	.00096	.00096	.00096	.00086
10	.00082	.00082	.00082	.00082	.00082	.00083	.00083	.00083	.00083	.00084	.00084	.00084	.00084	.00084	.00085
11	.00081	0.00000	0.00000	0.00000	0.00000	0.00000	0.00000	0.00000	0.00000	0.00000	0.00000	0.00000	0.00000	0.00000	0.00000

AREA	40	41	42	43	44	45	46	47	48	49	50	51	52	53	54
1	.01250	.01250	.01250	.01250	.01250	.01250	.01250	.01250	.01250	.01250	.01250	.01250	.01250	.01250	.01250
2	.01250	.01250	.01250	.01250	.01250	.01250	.01250	.01250	.01250	.01250	.01250	.01250	.01250	.01250	.01250
3	.01250	.01250	.01250	.01250	.01250	.01250	.01250	.01250	.01250	.01250	.01250	.01250	.01250	.01250	.01250
4	.01250	.01250	.01250	.01250	.01250	.01250	.01250	.01250	.01250	.01250	.01250	.01250	.01250	.01250	.01250
5	.01250	.01250	.01250	.01250	.01250	.01250	.01250	.01250	.01250	.01250	.01250	.01250	.01250	.01250	.01250
6	.01250	.01250	.01250	.01250	.01250	.01250	.01250	.01250	.01250	.01250	.01250	.01250	.01250	.01250	.01250
7	.01250	.01250	.01250	.01250	.01250	.01250	.01250	.01250	.01250	.01250	.01250	.01250	.01250	.01250	.01250
8	.00098	.00098	.00099	.00099	.01250	.01250	.01250	.01250	.01250	.01250	.01250	.01250	.01250	.01250	.01250
9	.00086	.00086	.00087	.00087	.00087	.00087	.00088	.00088	.00088	.00088	.01250	.01250	.01250	.01250	.01250
10	.00085	.00085	.00085	.00086	.00086	.00086	.00086	.00087	.00087	.00087	.00088	.01250	.01250	.01250	.01250

AREA	55	56	57	58	59	60	61	62	63	64	65	66	67	68	69
1	.01250	.01250	.01250	.01250	.01250	.01250	.01250	.01250	.01250	.01250	.01250	.01250	.01250	.01250	.01250
2	.01250	.01250	.01250	.01250	.01250	.01250	.01250	.01250	.01250	.01250	.01250	.01250	.01250	.01250	.01250
3	.01250	.01250	.01250	.01250	.01250	.01250	.01250	.01250	.01250	.01250	.01250	.01250	.01250	.01250	.01250
4	.01250	.01250	.01250	.01250	.01250	.01250	.01250	.01250	.01250	.01250	.01250	.01250	.01250	.01250	.01250
5	.01250	.01250	.01250	.01250	.01250	.01250	.01250	.01250	.01250	.01250	.01250	.01250	.01250	.01250	.01250
6	.01250	.01250	.01250	.01250	.01250	.01250	.01250	.01250	.01250	.01250	.01250	.01250	.01250	.01250	.01250
7	.01250	.01250	.01250	.01250	.01250	.01250	.01250	.01250	.01250	.01250	.01250	.01250	.01250	.01250	.01250
8	.01250	.01250	.01250	.01250	.01250	.01250	.01250	.01250	.01250	.01250	.01250	.01250	.01250	.01250	.01250
9	.01250	.01250	.01250	.01250	.01250	.01250	.01250	.01250	.01250	.01250	.01250	.01250	.01250	.01250	.01250
10	.01250	.01250	0.00000	0.00000	0.00000	0.00000	0.00000	0.00000	0.00000	0.00000	0.00000	0.00000	0.00000	0.00000	0.00000

AREA	70	71	72	73	74	75	76	77
1	.01250	.01250	.01250	.01250	.01250	.01250	.01250	.01250
2	.01250	.01250	.01250	.01250	.01250	.01250	.01250	.01250
3	.01250	.01250	.01250	.01250	.01250	.01250	.01250	.01250
4	.01250	.01250	.01250	.01250	.01250	.01250	.01250	.01250
5	.01250	.01250	.01250	.01250	.01250	.01250	.01250	.01250
6	.01250	.01250	.01250	.01250	.01250	.01250	.01250	.01250
7	.01250	.01250	.01250	.01250	.01250	.01250	.01250	.01250
			[illegible]	.01250	.01250	.01250	.01250	.01250

TIME(SEC)= 333.366
TOTAL AREA(C2)= 0.000
WEDGE AREA= 0.0000
ORIGINAL PENITRATION DEPTH= .2050
ANGLE(DEG)= 0.000
ARC LENGTH/TIME INCREMENT= .42824
NO. OF WEDGES IN POOL = 8

TEMPERATURE HISTORY OF POWDER

AREA	1	2	3	4	5	6	7	8
1	145.288	145.288	145.288	145.288	145.288	145.288	145.288	145.288
2	144.339	144.323	144.323	144.324	144.323	144.336	144.336	144.344
3	143.410	143.428	143.428	143.429	143.429	143.401	143.401	143.386
4	142.557	142.512	142.512	142.513	142.512	142.549	142.548	142.569
5	141.734	141.773	141.773	141.774	141.774	141.715	141.715	141.693
6	141.028	140.969	140.969	140.970	140.970	141.013	141.013	141.032
7	140.345	140.390	140.390	140.392	140.392	140.320	140.320	140.299
8	139.607	139.573	139.573	139.575	139.574	139.583	139.583	139.589
9	139.160	139.195	139.195	139.197	139.197	139.131	139.131	139.115
10	138.643	138.652	138.652	138.654	138.654	138.612	138.612	138.604
11	138.337	138.365	138.365	138.368	138.368	138.305	138.305	138.291

TEMPERATURE OF STUCK MATERIAL

AREA	10	11	12	13	14	15	16	17	18	19	20	21	22	23	24
1	145.288	145.288	145.288	145.288	145.288	145.288	145.288	145.288	145.288	145.288	145.288	145.288	145.288	145.288	145.288
2	144.256	144.253	144.255	144.255	144.248	144.266	144.271	144.271	144.302	144.278	144.306	144.309	144.311	144.326	144.330
3	143.237	143.230	143.235	143.235	143.261	143.261	143.329	143.329	143.294	143.340	143.310	143.332	143.387	143.371	143.398
4	142.324	142.314	142.321	142.321	142.311	142.355	142.327	142.328	142.433	142.377	142.453	142.471	142.491	142.531	142.529
5	141.441	141.428	141.437	141.437	141.475	141.490	141.529	141.530	141.511	141.588	141.559	141.611	141.646	141.631	141.689
6	140.683	140.667	140.679	140.679	140.685	140.742	140.611	140.611	140.793	140.750	140.849	140.900	140.900	140.952	140.967
7	139.985	139.966	139.979	139.980	140.013	140.059	139.947	139.948	140.036	140.108	140.126	140.213	140.061	140.070	140.244
8	137.851	137.821	137.843	137.844	137.889	137.973	139.252	139.252	139.466	139.486	139.573	139.670	139.495	139.549	139.698
9	136.154	136.113	136.143	136.144	136.205	136.314	137.360	137.361	137.682	137.753	137.868	138.036	138.868	138.911	139.204
10	134.934	134.882	134.919	134.920	134.990	135.122	136.071	136.073	136.463	136.551	136.699	136.916	137.441	137.515	137.993
11	133.545	133.450	133.513	133.516	133.616	133.823	135.105	135.108	135.622	135.740	135.946	136.253	136.770	136.874	137.489

AREA	25	26	27	28	29	30	31	32	33	34	35	36	37	38	39
1	145.288	145.288	145.288	145.288	145.288	145.288	145.288	145.288	145.288	145.288	145.288	145.288	145.288	145.288	145.288
2	144.332	144.336	144.346	144.344	144.346	144.354	144.359	144.365	144.364	144.367	144.369	144.371	144.382	144.381	144.387
3	143.407	143.426	143.425	143.443	143.446	143.445	143.452	143.444	143.467	143.486	143.490	143.495	143.499	143.502	143.517
4	142.525	142.558	142.590	142.587	142.591	142.617	142.632	142.649	142.650	142.663	142.668	142.675	142.697	142.694	142.710
5	141.732	141.791	141.795	141.833	141.839	141.842	141.857	141.847	141.892	141.931	141.938	141.927	141.929	141.948	141.972
6	140.955	141.061	141.117	141.123	141.130	141.172	141.196	141.218	141.237	141.225	141.233	141.246	141.267	141.259	141.303
7	140.325	140.465	140.488	140.541	140.550	140.570	140.593	140.591	140.654	140.630	140.642	140.605	140.629	140.655	140.730
8	139.722	139.927	139.998	140.027	140.038	140.091	140.122	140.142	140.029	140.021	140.036	140.064	140.129	140.109	140.250
9	138.856	139.532	139.594	139.649	139.662	139.709	139.743	139.754	139.500	139.558	139.577	139.593	139.707	139.697	139.903
10	138.550	137.459	137.647	137.763	137.807	137.940	138.022	138.053	138.600	138.915	138.947	139.041	139.260	139.211	139.550
11	137.662	0.000	0.000	0.000	0.000	0.000	0.000	0.000	0.000	0.000	0.000	0.000	0.000	0.000	0.000

AREA	40	41	42	43	44	45	46	47	48	49	50	51	52	53	54
1	145.288	145.288	145.288	145.288	145.288	145.288	145.288	145.288	145.288	145.288	145.288	145.288	145.288	145.288	145.288
2	144.388	144.395	144.392	144.397	144.422	144.431	144.434	144.438	144.473	144.479	144.516	144.532	144.543	144.548	144.557
3	143.519	143.519	143.552	143.551	143.608	143.602	143.599	143.634	143.699	143.709	143.772	143.810	143.839	143.845	143.860
4	142.713	142.735	142.735	142.749	142.836	142.861	142.870	142.886	142.990	143.011	143.119	143.168	143.201	143.214	143.239
5	141.976	141.987	142.052	142.053	142.186	142.181	142.177	142.243	142.377	142.399	142.525	142.597	142.653	142.666	142.695
6	141.308	141.357	141.384	141.405	141.578	141.615	141.626	141.665	141.841	141.874	142.048	142.127	142.182	142.202	142.242
7	140.737	140.784	140.881	140.889	141.118	141.126	141.125	141.213	141.417	141.451	141.638	141.740	141.816	141.836	141.877
8	140.259	140.346	140.426	140.450	140.726	140.766	140.776	140.847	141.086	141.129	141.356	141.464	141.538	141.564	141.614
	[illegible]	[illegible]	140.139	140.157	140.482	140.508	140.513	140.612	140.875	140.920	141.160	141.283	141.372	141.398	141.449
	[illegible]	[illegible]	[illegible]	[illegible]	[illegible]	[illegible]	140.325	140.434	140.739	140.790	141.067	141.204	141.297	141.327	141.386

AREA	55	56	57	58	59	60	61	62	63	64	65	66	67	68	69
1	145.288	145.288	145.288	145.288	145.288	145.288	145.288	145.288	145.288	145.288	145.288	145.288	145.288	145.288	145.288
2	144.556	144.567	144.566	144.576	144.587	144.590	144.603	144.610	144.612	144.618	144.625	144.637	144.640	144.657	144.664
3	143.874	143.874	143.882	143.898	143.921	143.928	143.953	143.967	143.971	143.982	143.999	144.020	144.027	144.061	144.075
4	143.238	143.270	143.268	143.295	143.327	143.337	143.875	143.395	143.401	143.419	143.441	143.474	143.485	143.534	143.555
5	142.720	142.722	142.735	142.768	142.812	142.826	142.874	142.900	142.909	142.931	142.962	143.004	143.017	143.082	143.110
6	142.243	142.289	142.286	142.329	142.382	142.397	142.457	142.489	142.499	142.527	142.563	142.615	142.632	142.710	142.744
7	141.908	141.917	141.932	141.979	142.041	142.061	142.130	142.166	142.179	142.210	142.253	142.313	142.331	142.422	142.461
8	141.622	141.673	141.672	141.727	141.796	141.817	141.895	141.937	141.950	141.985	142.033	142.100	142.121	142.222	142.266
9	141.480	141.500	141.357	141.426	141.511	141.538	141.635	141.687	141.704	141.746	141.805	141.889	141.914	142.037	142.091
10	141.403	141.451	0.000	0.000	0.000	0.000	0.000	0.000	0.000	0.000	0.000	0.000	0.000	0.000	0.000

AREA	70	71	72	73	74	75	76	77
1	145.288	145.288	145.288	145.288	145.288	145.288	145.288	145.288
2	144.672	144.674	144.684	144.735	144.758	144.765	144.771	144.778
3	144.090	144.095	144.114	144.215	144.261	144.275	144.285	144.301
4	143.578	143.584	143.613	143.762	143.829	143.849	143.865	143.888
5	143.139	143.147	143.185	143.379	143.466	143.493	143.514	143.543
6	142.780	142.790	142.835	143.070	143.177	143.208	143.235	143.269
7	142.502	142.514	142.567	142.839	142.962	142.998	143.027	143.068
8	142.312	142.325	142.383	142.687	142.825	142.865	142.897	142.942
9	142.145	142.161	142.231	142.592	142.752	142.798	142.835	142.886

NECK RADIUS

AREA	1	2	3	4	5	6	7	8
1	.01250	.01250	.01250	.01250	.01250	.01250	.01250	.01250
2	.01250	.01250	.01250	.01250	.01250	.01250	.01250	.01250
3	.01250	.01250	.01250	.01250	.01250	.01250	.01250	.01250
4	.01250	.01250	.01250	.01250	.01250	.01250	.01250	.01250
5	.01250	.01250	.01250	.01250	.01250	.01250	.01250	.01250
6	.01250	.01250	.01250	.01250	.01250	.01250	.01250	.01250
7	.01250	.01250	.01250	.01250	.01250	.01250	.01250	.01250
8	.01250	.01250	.01250	.01250	.01250	.01250	.01250	.01250
9	.01250	.01250	.01250	.01250	.01250	.01250	.01250	.01250
10	.01250	.01250	.01250	.01250	.01250	.01250	.01250	.01250
11	.01250	.01250	.01250	.01250	.01250	.01250	.01250	.01250

NECK RADIUS OF STUCK MATERIAL

AREA	10	11	12	13	14	15	16	17	18	19	20	21	22	23	24
1	.01250	.01250	.01250	.01250	.01250	.01250	.01250	.01250	.01250	.01250	.01250	.01250	.01250	.01250	.01250
2	.01250	.01250	.01250	.01250	.01250	.01250	.01250	.01250	.01250	.01250	.01250	.01250	.01250	.01250	.01250
3	.01250	.01250	.01250	.01250	.01250	.01250	.01250	.01250	.01250	.01250	.01250	.01250	.01250	.01250	.01250
4	.01250	.01250	.01250	.01250	.01250	.01250	.01250	.01250	.01250	.01250	.01250	.01250	.01250	.01250	.01250
5	.01250	.01250	.01250	.01250	.01250	.01250	.01250	.01250	.01250	.01250	.01250	.01250	.01250	.01250	.01250
6	.01250	.01250	.01250	.01250	.01250	.01250	.01250	.01250	.01250	.01250	.01250	.01250	.01250	.01250	.01250
7	.01250	.01250	.01250	.01250	.01250	.01250	.01250	.01250	.01250	.01250	.01250	.01250	.01250	.01250	.01250
8	.00098	.00098	.00099	.00099	.00099	.00099	.01250	.01250	.01250	.01250	.01250	.01250	.01250	.01250	.01250
9	.00096	.00096	.00096	.00096	.00097	.00097	.00098	.00098	.00098	.00098	.00099	.01250	.01250	.01250	.01250
10	.00084	.00084	.00084	.00084	.00085	.00085	.00086	.00086	.00086	.00086	.00087	.00087	.00087	.00088	.00088
11	.00083	.00083	.00083	.00083	.00083	.00083	.00085	.00085	.00085	.00085	.00086	.00086	.00087	.00087	.00087

AREA	25	26	27	28	29	30	31	32	33	34	35	36	37	38	39
1	.01250	.01250	.01250	.01250	.01250	.01250	.01250	.01250	.01250	.01250	.01250	.01250	.01250	.01250	.01250
2	.01250	.01250	.01250	.01250	.01250	.01250	.01250	.01250	.01250	.01250	.01250	.01250	.01250	.01250	.01250
3	.01250	.01250	.01250	.01250	.01250	.01250	.01250	.01250	.01250	.01250	.01250	.01250	.01250	.01250	.01250
4	.01250	.01250	.01250	.01250	.01250	.01250	.01250	.01250	.01250	.01250	.01250	.01250	.01250	.01250	.01250
5	.01250	.01250	.01250	.01250	.01250	.01250	.01250	.01250	.01250	.01250	.01250	.01250	.01250	.01250	.01250
6	.01250	.01250	.01250	.01250	.01250	.01250	.01250	.01250	.01250	.01250	.01250	.01250	.01250	.01250	.01250
7	.01250	.01250	.01250	.01250	.01250	.01250	.01250	.01250	.01250	.01250	.01250	.01250	.01250	.01250	.01250
8	.01250	.01250	.01250	.01250	.01250	.01250	.01250	.01250	.01250	.01250	.01250	.01250	.01250	.01250	.01250
9	.01250	.01250	.01250	.01250	.01250	.01250	.01250	.01250	.01250	.01250	.01250	.01250	.01250	.01250	.01250
10	.01250	.00088	.00088	.00089	.00089	.00089	.01250	.01250	.01250	.01250	.01250	.01250	.01250	.01250	.01250
11	.00088	0.00000	0.00000	0.00000	0.00000	0.00000	0.00000	0.00000	0.00000	0.00000	0.00000	0.00000	0.00000	0.00000	0.00000

AREA	40	41	42	43	44	45	46	47	48	49	50	51	52	53	54
1	.01250	.01250	.01250	.01250	.01250	.01250	.01250	.01250	.01250	.01250	.01250	.01250	.01250	.01250	.01250
2	.01250	.01250	.01250	.01250	.01250	.01250	.01250	.01250	.01250	.01250	.01250	.01250	.01250	.01250	.01250
3	.01250	.01250	.01250	.01250	.01250	.01250	.01250	.01250	.01250	.01250	.01250	.01250	.01250	.01250	.01250
4	.01250	.01250	.01250	.01250	.01250	.01250	.01250	.01250	.01250	.01250	.01250	.01250	.01250	.01250	.01250
5	.01250	.01250	.01250	.01250	.01250	.01250	.01250	.01250	.01250	.01250	.01250	.01250	.01250	.01250	.01250
6	.01250	.01250	.01250	.01250	.01250	.01250	.01250	.01250	.01250	.01250	.01250	.01250	.01250	.01250	.01250
7	.01250	.01250	.01250	.01250	.01250	.01250	.01250	.01250	.01250	.01250	.01250	.01250	.01250	.01250	.01250
8	.01250	.01250	.01250	.01250	.01250	.01250	.01250	.01250	.01250	.01250	.01250	.01250	.01250	.01250	.01250
9	.01250	.01250	.01250	.01250	.01250	.01250	.01250	.01250	.01250	.01250	.01250	.01250	.01250	.01250	.01250
10	.01250	.01250	.01250	.01250	.01250	.01250	.01250	.01250	.01250	.01250	.01250	.01250	.01250	.01250	.01250

AREA	55	56	57	58	59	60	61	62	63	64	65	66	67	68	69
1	.01250	.01250	.01250	.01250	.01250	.01250	.01250	.01250	.01250	.01250	.01250	.01250	.01250	.01250	.01250
2	.01250	.01250	.01250	.01250	.01250	.01250	.01250	.01250	.01250	.01250	.01250	.01250	.01250	.01250	.01250
3	.01250	.01250	.01250	.01250	.01250	.01250	.01250	.01250	.01250	.01250	.01250	.01250	.01250	.01250	.01250
4	.01250	.01250	.01250	.01250	.01250	.01250	.01250	.01250	.01250	.01250	.01250	.01250	.01250	.01250	.01250
5	.01250	.01250	.01250	.01250	.01250	.01250	.01250	.01250	.01250	.01250	.01250	.01250	.01250	.01250	.01250
6	.01250	.01250	.01250	.01250	.01250	.01250	.01250	.01250	.01250	.01250	.01250	.01250	.01250	.01250	.01250
7	.01250	.01250	.01250	.01250	.01250	.01250	.01250	.01250	.01250	.01250	.01250	.01250	.01250	.01250	.01250
8	.01250	.01250	.01250	.01250	.01250	.01250	.01250	.01250	.01250	.01250	.01250	.01250	.01250	.01250	.01250
9	.01250	.01250	.01250	.01250	.01250	.01250	.01250	.01250	.01250	.01250	.01250	.01250	.01250	.01250	.01250
10	.01250	.01250	0.00000	0.00000	0.00000	0.00000	0.00000	0.00000	0.00000	0.00000	0.00000	0.00000	0.00000	0.00000	0.00000

AREA	70	71	72	73	74	75	76	77
1	.01250	.01250	.01250	.01250	.01250	.01250	.01250	.01250
2	.01250	.01250	.01250	.01250	.01250	.01250	.01250	.01250
3	.01250	.01250	.01250	.01250	.01250	.01250	.01250	.01250
4	.01250	.01250	.01250	.01250	.01250	.01250	.01250	.01250
5	.01250	.01250	.01250	.01250	.01250	.01250	.01250	.01250
6	.01250	.01250	.01250	.01250	.01250	.01250	.01250	.01250
7	.01250	.01250	.01250	.01250	.01250	.01250	.01250	.01250
[illegible]	[illegible]	[illegible]	[illegible]	[illegible]	.01250	.01250	.01250	.01250

NECK RADIUS AT COMPLETE MELT

NODE	RADIUS
1	.001145
2	.001219
3	.001216
4	.001104
5	.001108
6	.001002
7	.001007
8	.000902
9	.000900
10	.000888
11	.000856

ROTATIONAL MOLDING SIMULATION

WITH OVEN CONVECTION HEATING

```
      PROGRAM RH485(INPUT,OUTPUT,TAPE5=INPUT,TAPE6=OUTPUT,TAPE8)
      DIMENSION TN(100),T(200,100),DC(200),PS(200),N3(200),H3(200)
     C ,H2(200),ANECK(200,100),BNECK(100),ANEK(100)
      COMMON SS,SM,AL,AM,DX,N,TM,AA,AT,AD,TH,DL,N2,CT,NC,N3,RAD,TS
      COMMON TAIR,BMT,MT
      INTEGER CT,KL
      REAL H,I3,H2,K,M,IT,HT,LT,MT,H1,MTN
      DATA ANECK,BNECK/20000*0.0,100*0.0/
C
C   GLOSSARY
C
C          AA  TOTAL CROSS SECTIONAL POOL AREA (CM2)
C          ACNST  DUMMY VARIABLE
C          ACONST  DUMMY VARIABLE
C          AD  PENITRATION THICKNESS (CM)
C          AH  CONVECTION COEFFICIENT OF OVEN AIR (J/CM2-SEC-K)
C          AL  INITIAL POWDER THERMAL DIFFUSIVITY (CM2/SEC)
C          ALCP  SPECIFIC HEAT OF ALUMINUM MOLD (J/KG-C)
C          ALDIFF  THERMAL DIFFUSIVITY OF ALUMINUM MOLD (CM2/SEC)
C          ALK  THERMAL CONDUCTIVITY OF MOLD (J/CM-SEC-K)
C          ALRHO DENSITY OF ALUMINUM MOLD (KG/CM3)
C          AM  THERMAL DIFFUSIVITY AT COMPLETE MELT (CM2/SEC)
C          ANECK  NECK RADIUS AT EACH NODE (CM)
C          ANEK  NECK RADIUS OF EACH NODAL AREA AT THE TIME
C                    MELTING OVERCOMES THE SINTERING PORCESS (CM)
C          ANK  DUMMY VARIABLE = ANECK(1,1)
C          AR  DUMMY VARIABLE USED IN CALCULATING REMAINING
C                    CROSS SECTIONAL POOL AREA
C          AS  TOTAL AREA ENCOMPANSING NODAL ANALYSIS
C                    ( HEIGHT OF NODES X TOTAL WIDTH)
C          AT  CROSS SECTIONAL AREA OF ONE WEDGE (CM2)
C          ATEST  DUMMY VARIABLE
C          AV  DUMMY VARIABLE USED TO DETERMINE NEW ANGLE THETHA
C          A3  CROSS SECTIONAL AREA OF STUCK COLUMN OF MATERIAL THAT
C                    THAT RE-ENTERS THE POOL IN THE NEXT TIME INCREMENT (
C          A4  THE CROSS SECTIONAL AREA OF THE STUCK COLUMN OF
C                    MATERIAL THAT REMAINS OUTSIDE THE POOL
C                    DURING THE NEXT TIME INCREMENT (CM2)
C          BA  ANGLE OF RESPONSE OF THE POOL (RAD)
C          BB  DUMMY VARIABLE USED IN TEMPERATURE EQUATION
C          BE DUMMY VARIABLE USED SURFACE NODAL NECK SIZE EQUATION
C          BMT  EXTERIOR TEMP OF MOLD (DEG C)
C          BMTN  EXTERIOR TEMP OF MOLD DURING
C                    THE NEXT TIME INCREMENT (DEG C)
C          BNECK - NEW COMPUTED NECK SIZE FROM SUBROUTINE (CM)
C          CC HALF LENGTH OF POOL CORD (CM)
C          CT  COUNTER USED TO COUNT THE NUMBER OF STUCK COLUMNS
C          C1  CONSTANT USED IN TEMPERATURE EQUATIONS DETERMINED IN
C                    SUBROUTINE CONST
C          C2  CONSTANT USED IN NODAL TEMPERATURE EQUATIONS
C          C3  CONSTANT USED IN NODAL TEMPERATURE EQUATIONS
C          DA  AVERAGE DIFFUSIVITY BETWEEN NODES I+1 AND NODE I (CM2/SEC)
C          DB  AVERAGE DIFFUSIVITY BETWEEN NODES I-1 AND NODE I (CM2/SEC)
C          DC  ARC WIDTH OF STUCK NODAL COLUMNS (RAD)
C          DL  ARC LENGTH PER TIME INCREMENT (RAD/SEC)
```

```
C         DT  MAXIMUM TIME INCREMENT (SEC)
C         DX  DISTANCE BETWEEN NODES (CM)
C         DXMOLD  THICKNESS OF MOLD(CM)
C         EN  PORTION OF COLUMN ARC WIDTH RE-ENTERING THE
C                   STATIONARY POOL (RADIANS)
C         FT  AVERAGE TEMPERATURE OF MATERIAL IN FREE FALL ZONE (C)
C         G  ACCELLERATION DUE TO GRAVITY (CM/SEC2)
C         H  HEIGHT OF STUCK MATERIAL LEAVING  POOL (CM)
C         HT DUMMY VARIABLE USEE IN COMPUTING POOL ANGLE THETHA
C         H1  HEIGHT OF STUCK MATERIAL LEAVING POOL DURING THE NEXT
C                   TIME INCREMENT (CM)
C         H2  HEIGHT OF STUCK MATERIAL COLUMN OUTSIDE POOL
C         H3  DISTANCE BETWEEN LAST TWO NODES OF EACH COLUMN OF
C                   STUCK MATERIAL OUTSIDE POOL (CM)
C         I  COUNTING VARIABLE USED IN DO-LOOPS
C         IFLAG  FLAG SHOWING THAT NODAL HEIGHT HSD REACHED
C                   ITS MAXIMUM WHEN ≠ 1
C         II  COUNTING VARIABLE USED IN DO-LOOPS
C         III  COUNTING VARIABLE USED IN DO-LOOPS
C         IREM  FLAG SHOWING POOL MASS IS GONE WHEN = 0
C         IT  INITIAL TEMPERATURE OF POOL POWDER (C)
C         ITM  COUNTER
C         ITMX  NUMBER OF ITERATIONS BEFORE MOLD ROTATION
C         I2  DUMMY VARIABLE USED WITH THE PRINT SUBROUTINE
C         I3  DUMMY VARIABLE USED IN THE PRINT SUBROUTINE
C         J  COUNTING VARIABLE USED IN DO-LOOPS
C         JI  COUNTING VARIABLE USED IN DO-LOOPS
C         JJ  COUNTING VARIABLE USED IN DO-LOOPS
C         JJI  COUNTING VARIABLE USED IN DO-LOOPS
C         JK  DUMMY VARIABLE
C         JL  FLAG
C         JTVAL  DUMMY VARIABLE
C         K  DUMMY VARIABLE
C         KK  FLAG VARIABLE
C         KL  DUMMY VARIABLE
C         K4  DUMMY VARIABLE
C         LK  COUNTING INTEGER USED WITH PRINT SUBROUTINE
C         LT DUMMY VARIABLE
C         M  CROSS SECTIONAL OF  MASS  LEAVING POOL AND STUCK TO WALL
C         MT  INTERIOR MOLD SURFACE TEMP (DEG C)
C         MTN  INTERIOR MOLD SURFACE TEMP ONE TIME INCREMENT
C                   LATTER (DEG C)
C         N  NUMBER OF NODES IN EACH STATIONARY POOL COLUMN
C         NC  NUMBER OF POOL COLUMNS OF NODES
C         NEC  COUNTING VARIABLE
C         NMAX  MAXIMUM NODE HEIGHT BASED ON VOLUME OF POOL (CM)
C         NNAX  EQUALS N+1
C         NNTP  DUMMY VARIABLE WHICH EQUALS N6+N4+1
C         N2 COLUMN NUMBER OF STUCK MATERIAL
C         N3  NUMBER OF NODES IN STUCK COLUMN MINUS 2
C         N3TEMP  DUMMY VARIABLE
C         N4 DUMMY VARIABLE
C         N6  NUMBER OF NODES IN PENITRATION THICKNESS
C         OT  PORTION OF RE-ENTERING STUCK COLUMN NOT ENTERING POOL (RAD)
C         PS  POSITION OF A PARTICULAR STUCK COLUMN IN MOLD (RAD)
C         PT  PRINTING INTERVAL (SEC)
C         RA  RATIO OF RI/RO
```

```
C         RAD  INITIAL RADIUS OF MATERIAL (CM)
C         RB   DUMMY VARIABLE
C         RI   RADIUS FROM MOLD CENTER TO SURFACE OF STATIONARY POOL (CM)
C         RM   DUMMY VARIABLE
C         RO   INNER RADIUS OF MOLD (CM)
C         RPM  ROTATIONAL SPEED OF MOLD (RPM)
C         R2 DUMMY VARIABLE
C         SM   COMPLETE MELT TEMPERATURE (DEG C)
C         SR   RATIO OF FREE-FALL TIME TO TIME INTERVAL TS
C         SS   TEMPERATURE THAT MATERIAL BEGINS STICKING TO THE MOLD (C)
C         S1   DUMMY VARIABLE USED IN WEDGE AREA EQUATION
C         S2   DUMMY VARIABLE USED IN WEDGE AREA EQUATION
C         T   NODAL TEMPERATURE
C         TAIR  TEMPERATURE OF OVEN AIR (DEG C)
C         TF   FALL TIME IN FREE FALL ZONE (SEC)
C         TH   ANGLE  (THETHA) FROM CENTER OF MOLD TO JUNCTION OF
C                    POOL SURFACE AND MOLD (RAD)
C         TM TIME
C         TN   NEW COMPUTED NODAL TEMPERATURE (C)
C         TP   COMBINED NODAL TEMPERATURE USED IN DETERMINING
C                    AVERAGE TEMPERATURE (C)
C         TS   TIME INTERVAL USED (SEC)
C         TS1  DUMMY VARIABLE
C         TTL  DUMMY VARIABLE
C         TW   CONTACT TIME OF MATERIAL TO WALL IN POOL REGION (SEC)
C         W  ROTATIONAL SPEED OF MOLD (RAD/SEC)
C         X5   POSITION OF LEADING AREA OF STUCK MATERIAL (RAD)
C
C ***** SECTION I *****
C
      EN=0.0
      IREM=1
      LK=0
      NEC=1
      IFLAG=0
      PT=30.0
      TM=0.0
      NC=8
      RAD=0.0125
      RI=1.3606
      RO=6.6675
      RPM=10.0
      BA=53
      SS=110.0
      SM=138.0
      IT=20.0
      DXMOLD=0.655
      ALRHO=2.707E-03
      ALCP=8.7085E+02
      ALK=2.025
      AH=5.678E-00
      TAIR=371.0
      MT=IT
      BMT=IT
      ALDIFF= ALK/( ALRHO* ALCP)
      G=980.0
C
```

```
C  *****   SECTION II   *****
C
      RA=RI/RO
  220 TH=(3.14159/2.0-ATAN(RA/(-RA*RA+1.0)**0.5))*2
C     DETERMINE AREA IN STATIONARY POOL
      AA=0.5*RO*RO*(TH-SIN(TH))
      AL=COND(0)/(CP(0)*RHO(0))
      AM=COND(RAD)/(CP(RAD)*RHO(RAD))
      W=0.10472*RPM
      TW=TH/W
      TS=TW/NC
      ITM=0
      ITMX=1
      ACNST=2/(DXMOLD*ALRHO*ALCP)*(AH+ALK/DXMOLD)
      TS1=1/ACNST
      TM=TM+TS
C     DETERMINE MAXIMUM PENITRATION DISTANCE
      AD=7.2*(AL*TW)**0.5
C     DETERMINE MAXIMUM TIME INCREMENT
      DT=TW/NC
C     DETERMINE NODAL DISTANCE
      DX=(DT*2*AM)**0.5
      IF(AM.LT.AL) DX=(DT*2*AL)**0.5
C     DETERMINE NUMBER OF NODES PER COLUMN
      N=(INT(AD/DX)+1)+2
      NNAX=N+1
      N2=NC+2
      CT=N2-1
C     SET INITIAL TEMPERATURE AND NECK RADIUS
      DO 125 I=1,NC
      DO 126 J=1,NNAX
      T(I,J)=IT
      ANECK(I,J)=0.0
  126 CONTINUE
  125 CONTINUE
      BA=0.0174533*BA
      WRITE(6,10)
   10 FORMAT(1H1,29HROTATIONAL MOLDING SIMULATOR )
      WRITE(6,12) TAIR,AH,DXMOLD,ALDIFF
   12 FORMAT(1X,//,6X,24HTEMP. OF AIR (DEG. C) =    ,F10.3,/,6X,
     133HCONVECTION COEF. (J/CM2-SEC-K) =    ,E10.3,/,6X,
     222HMOLD THICKNESS (CM) = ,F10.5,/,6X,
     3 27HMOLD DIFFUSIVITY (CM2/S) = ,F10.5)
      WRITE(6,11)RI,RO,N,DX,SS,AL,SM,AM,RPM
   11 FORMAT(6X,25HPOWDER HEIGHT RADIUS(CM)= ,F10.3,/,6X,17HMOLD RADIUS(
     1CM)= ,F10.3,/,6X,21HINTIAL NO. OF NODES= ,I3,/,
     3    6X,20HNODE THICKNESS(CM)= ,F10.4,/,6X,38HSTICK TEMP(C) AND DIFF
     4USIVITY(CM2/S)= ,F10.3,3X,E10.3,/,6X,46HCOMPLETE MELT TEMP(C) AND
     5DIFFUSIVITY(CM2/S)= ,F10.3,3X,E10.3,/,6X,6HRPM= ,F10.3)
C
C  *****   SECTION III   *****
C
 1000 TW=TH/W
      CC=2*RO*SIN(TH/2)
      ANK=ANECK(1,1)
      IF(CT.GT.N2) ANK=ANECK(CT,1)
      AM=COND(ANK)/(RHO(ANK)*CP(ANK))
```

```
      BE=RADX(ANK)
C     RECHECK MAXIMUM TIME INCREMENT EACH ITERATION
      DT=(BE*DX)**2/(2.0*AM)
      IF(AM.LT.AL) DT=(BE*DX)**2/(2.0*AL)
      TM=TM-TS
      IF((IREM.EQ.0).OR.(ITM.GT.0)) GOTO 109
      TS=TW/NC
  108 TTL=TS
      ITMX=1
      IF(TTL.GT.DT) TTL=DT
      IF(TTL.GT.TS1) TTL=TS1
      IF(TTL.EQ.TS) GOTO 109
      ITMX=INT(TS/TTL)+1
      TS=TTL/ITMX
  109 IF(IREM.EQ.0) TS=DT
      DL=W*TS*RO
      IF(TM.EQ.0.0) WRITE(6,20)DT,TS,DL
   20 FORMAT(1H ,/,6X,23HMAX TIME INCREMENTS(S)= ,F10.5,/,6X,21HTIME INC
     1REMENT USED= ,F10.5,/,6X,18HARC/TIME INC(CM) = ,F10.5 )
      TM=TM+TS
      IF(IREM.EQ.0) GOTO 540
      NMAX=INT(AA/(NC*DL*DX))+1
      AD=7.2*(AL*TW)**0.5
      TF=(1.3333*CC/(G*COS(BA)))**0.5
      SR=TF/TS
      IF(SR.LT.1.0) SR=1.0
C     DETERMINE AREA OF EACH WEDGE
      S1=RO*SIN(TH/2.0)
      S2=RO*COS(TH/2.0)*TAN(W*TS/2.0)
      AT=0.5*(S1+S2)*(S1-S2)*SIN(W*TS)+0.5*RO*RO*(W*TS-SIN(W*TS))
      AS=(N-0.5)*DX*DL
      IF(AS.GT.AT) AS=AT
      IF(N.LT.NMAX) GO TO 560
      N=NMAX
      IFLAG=1
  540 CONTINUE
      DO 550 I=1,NC
      T(I,N+1)=T(I,N-1)
      ANECK(I,N+1)=ANECK(I,N-1)
  550 CONTINUE
  560 CONTINUE
      NNAX=N+1
      N6=INT(AD/DX)+1
C
C ***** SECTION IV *****
C
C       COMPUTE NODAL TEMPERATURES AND NECK RADIUS
C
C
C   COMPUTE EXTERIOR AND INTERIOR MOLD SURFACE TEMPERATURES
C
  580 CONTINUE
      ACONST=2*TS/(DXMOLD*ALRHO*ALCP)
  590 BMTN=BMT*(1.0-ACONST*(AH+ALK/DXMOLD))+
     1 ACONST*(AH*TAIR+ALK*MT/DXMOLD)
      MTN=MT*(1.0-ACONST*ALK/DXMOLD)+ACONST*ALK*BMT/DXMOLD
      DO 620 I=1,NC
```

```
C       NODAL TEMPERATURE EQUATICNS FOR STATIONARY POOL
        T(I,1)=MT
        TN(1) =MT
        CALL CONST(C1,C2,C3,DB,DA,MT,MT,MT,ANECK(I,1),ANECK(I,2),
      1 BNECK(1))
        ANECK(I,1)=BNECK(1)
        DO 630 J=2,N
        CALL CONST(C1,C2,C3,DB,DA,T(I,J),T(I,J-1),T(I,J+1),ANECK(I,J),
      1 ANECK(I,J+1),BNECK(J))
        TN(J)=T(I,J)*(1-TS/C3*(DB/C1 +DA/C2))+TS/C3*(DB/C1*T(I,J-1)+
      1DA/C2*T(I,J+1))
  630   CONTINUE
        DO 640 JJ=1,N
        T(I,JJ)=TN(JJ)
        IF((JJ.EQ.NEC).AND.(TN(JJ).GT.SM)) ANEK(NEC)=BNECK(JJ)
        IF((JJ.EQ.NEC).AND.(TN(JJ).GT.SM)) NEC=NEC+1
        IF(TN(JJ).GT.SM) BNECK(JJ)=RAD
        ANECK(I,JJ)=BNECK(JJ)
  640   CONTINUE
  620   CONTINUE
        IF(CT.LT.N2) GO TO 890
C       NODAL TEMPERATURE EQUATICNS FOR STUCK MATERIAL
        DO 880 I=N2,CT
        T(I,1)=MT
        CALL CONST(C1,C2,C3,DB,DA,MT,MT,MT,ANECK(I,1),ANECK(I,2),
      1 BNECK(1))
        ANECK(I,1)=BNECK(1)
        IF(N3(I).EQ.0) GO TO 820
        IF(N3(I).EQ.1) GO TO 780
        JTVAL=N3(I)
        DO 770 J=2,JTVAL
        CALL CONST(C1,C2,C3,DB,DA,T(I,J),T(I,J-1),T(I,J+1),ANECK(I,J),
      1 ANECK(I,J+1),BNECK(J))
        TN(J)=T(I,J)*(1-TS/C3*(DE/C1+DA/C2))+TS/C3*(DB/C1*T(I,J-1)+
      1DA/C2*T(I,J+1))
  770   CONTINUE
  780   J=N3(I)+1
        CALL CONST(C1,C2,C3,DB,DA,T(I,J),T(I,J-1),T(I,J+1),ANECK(I,J),
      1 ANECK(I,J+1),BNECK(J))
        BB=TS/C3*(DB/C1*T(I,J-1)+DA/(H3(I)*C2/DX)*T(I,J+1))
        TN(J)=T(I,J)*(1-TS/C3*(DB/C1+DA/(H3(I)*C2/DX)))+BB
  820   CONTINUE
        J=N3(I)+2
        CALL CONST(C1,C2,C3,DB,DA,T(I,J),T(I,J-1),T(I,J  ),ANECK(I,J),
      1 ANECK(I,J  ),BNECK(J))
        BB=DB*TS/(H3(I)*(C3/DX)**2*(H3(I)-DX/2))
        TN(J)=T(I,J)*(1-BB)+BB*T(I,J-1)
        DO 870 JJ=1,J
        T(I,JJ)=TN(JJ)
        IF((JJ.EQ.NEC).AND.(TN(JJ).GT.SM)) ANEK(NEC)=BNECK(JJ)
        IF((JJ.EQ.NEC).AND.(TN(JJ).GT.SM)) NEC=NEC+1
        IF(TN(JJ).GT.SM) BNECK(JJ)=RAD
        ANECK(I,JJ)=BNECK(JJ)
  870   CONTINUE
  880   CONTINUE
C
  890   CONTINUE
```

```
      BMT=BMTN
      MT=MTN
      IF(((T(NC,N).GE.SS).AND.( IREM.EQ.1).AND.(N.EQ.NMAX)) GO TO 891
      IF(T(NC,N).GE.SM) GOTO 891
      IF(TM.LT.LK*PT) GOTO 892
C
C     ***** SECTION V *****
C
C     PRINT ROUTINE
C
  891 I3=0
      CALL PRINT(T,LK,I3)
      I3=1
      I2=0
      CALL PRINT(ANECK,I2,I3)
      IF(T(NC,N).GT.SM) GOTO29
      IF((T(NC,N).LT.SS).OR.(IREM.EQ.0)) GOTO 892
      IF(N.LT.NMAX) GOTO892
      WRITE(6,30)TM
   30 FORMAT(1H ,///,5X,34HMASS COMPLETELY GONE - TIME(SEC)= ,F10.3)
      IREM=0
      AT=0.0
      AA=0.0
      TH=0.0
      LK=LK-1
      GOTO 892
   29 CONTINUE
      WRITE(6,31)
   31 FORMAT(1X,////,5X,29H NECK RADIUS AT COMPLETE MELT    ,/,10X,
     1  4HNODE,6X,6HRADIUS        )
      DO 33 J=1,N
      WRITE(6,32) J,ANEK(J)
   32 FORMAT(10X,I5,5X,F10.6)
   33 CONTINUE
      STOP
  892 CONTINUE
      ITM=ITM+1
      IF((IREM.EQ.0).OR.(ITM.LT.ITMX)) TM=TM+TS
      IF((IREM.EQ.0).OR.(ITM.LT.ITMX)) GO TO 1000
      ITM=0
      IF(T(NC,1).GT.SS) GO TO 1200
C
C     ***** SECTION VI *****
C
C
C     CALCULATE MIX MEAN TEMPERATURE WHEN NO MATERIAL HAS STUCK
C
 1109 TP=0.0
      DO 1110 I=2,N
      TP=TP+T(NC,I)
 1110 CONTINUE
      TP=(TP+MT/2)/(N-0.5)
      FT=(AS*TP+(AT-AS)*IT)/AT
      DO 1140 III=2,NC
      I=NC-III+2
       DO 1142 J=1,NMAX
      T(I,J)=T(I-1,J)
```

```
      ANECK(I,J)=ANECK(I-1,J)
 1142 CONTINUE
 1140 CONTINUE
      DO 1150 I=1,NNAX
      T(1,I)=IT
      ANECK(1,I)=0.0
 1150 CONTINUE
      IT=((SR-1)*IT+FT)/SR
      TM=TM+TS
      GO TO 580
 1200 CONTINUE
C
C     *****  SECTION VII  *****
C     DETERMINE THE AMOUNT OF STICK AND NEW ANGLE
C
      DO 1220 I=2,N
      IF(T(NC,I).LE.SS) GO TO 1221
 1220 CONTINUE
 1221 CONTINUE
      RA=(SS-T(NC,I-1))/(T(NC,I)-T(NC,I-1))
      H=(RA+(I-2))*DX
      DO 1250 II=2,N
      IF(T(NC-1,II).LE.SS) GO TO 1251
 1250 CONTINUE
 1251 CONTINUE
      RB=(SS-T(NC,II-1))/(T(NC,II)-T(NC,II-1))
      H1=(RB+(II-2))*DX
      IF(INT(H/DX)-1.LT.0) GO TO 1109
      CT=CT+1
      DC(N2-1)=W*TS
      PS(N2-1)=TH/2.0
      N3(N2-1)=INT(H/DX)-1
      H3(N2-1)=H-DX*N3(N2-1)
      H2(N2-1)=H
      JTVAL=N3(N2-1)+1
      DO 1350 J=1,JTVAL
      T(N2-1,J)=T(NC,J)
      ANECK(N2-1,J)=ANECK(NC,J)
 1350 CONTINUE
      T(N2-1,N3(N2-1)+2)=SS
      ANECK(N2-1,N3(N2-1)+2)=ANECK(NC,N3(N2-1)+2)
C
C     COMPUTE MIX TEMPERATURE OF MATERIAL NOT STICKING BUT
C        ENTERING FREE-FALL ZONE
C
      TP=0.0
      DO 1380 J=I,N
      TP=TP+T(NC,J)
 1380 CONTINUE
      K=RA-0.5
      IF(K.GE.0.0)  TP=(TP-T(NC,I)*K)/(N-I-K+1)
      IF(K.LT.0.0)  TP=(TP-T(NC,I-1)*K)/(N-I-K+1)
      M=H*DL
      FT=((AS-M)*TP+(AT-AS)*IT)/(AT-M)
C   ROTATE POWDER
      DO 1440 III=2,NC
      I=NC-III+2
```

```
      DO 1445 J=1,NMAX
      T(I,J)=T(I-1,J)
      ANECK(I,J)=ANECK(I-1,J)
 1445 CONTINUE
 1440 CONTINUE
      K4=1
      IF(CT.LT.N2) GO TO 1900
C
C     ***** SECTION VIII *****
C
C     STUCK MATL SHIFT
      DO 1470 JJI=N2,CT
      JI=CT-JJI+N2
      DC(JI)=DC(JI-1)
      PS(JI)=PS(JI-1)+W*TS
      N3(JI)=N3(JI-1)
      H3(JI)=H3(JI-1)
      H2(JI)=H2(JI-1)
      N3TEMP=N3(JI)+2
      DO 1530 J=1,N3TEMP
      T(JI,J)=T(JI-1,J)
      ANECK(JI,J)=ANECK(JI-1,J)
 1530 CONTINUE
 1470 CONTINUE
 1550 X5=6.28318-TH/2
      EN=0.0
      KL=0
      IF(PS(CT).LT.X5) GO TO 1900
C
C     ***** SECTION IX *****
C     STUCK MATERIAL RE-ENTERING POOL ROUTINE
C
      DO 1570 JI=N2,CT
      IF(PS(JI).GE.X5) GO TO 1575
 1570 CONTINUE
 1575 CONTINUE
      EN=PS(JI)-X5
      OT=DC(JI)-EN
      IF(OT.LT.W*TS) GO TO 1610
      PS(JI)=X5
      DC(JI)=OT
      GO TO 1770
 1610 IF(OT.LT.0.0) OT=DC(JI)
      IF(OT.LT.0.0) KL=1
      CT=JI-1
      KK=0
      JL=0
      JK=N3(JI-1)+1
 1650 IF(JK.LE.N3(JI)+1 ) GO TO 1660
      JK=JK-1
      KK=1
      GO TO 1650
 1660 CONTINUE
      IF((H3(JI).GE.1.5*DX).AND.KK.EQ.1) JL=1
      IF(JL.EQ.1) JK=JK+1
      DO 1670 I=2,JK
      T(JI-1,I)=(OT*T(JI,I)+DC(JI-1)*T(JI-1,I))/(OT+DC(JI-1))
```

```
      ANECK(JI-1,I)=(OT*ANECK(JI,I)+DC(JI-1)*ANECK(JI-1,I))/(OT+
     1  DC(JI-1))
 1670 CONTINUE
      JK=JK+1
      A3=DC(JI-1)*(H3(JI-1)-DX/2)
      A4=OT*(H3(JI)-DX/2)
       IF(JL.EQ.1) A4=OT*(H3(JI)-1.5*DX)
      IF(JL.EQ.1)    T(JI,JK)=T(JI,N3(JI)+2)
      IF(JL.EQ.1) ANECK(JI,JK)=ANECK(JI,N3(JI)+2)
      IF((JL.EQ.0).AND.(KK.EQ.1)) A3=DC(JI-1)*DX
      T(JI-1,JK)=(T(JI,JK)*A4+T(JI-1,JK)*A3)/(A3+A4)
      ANECK(JI-1,JK)=(ANECK(JI,JK)*A4+ANECK(JI-1,JK)*A3)/(A3+A4)
      DC(JI-1)=DC(JI-1)+OT
      IF(KL.NE.1) GO TO 1760
      PS(JI-1)=PS(JI)
      JI=JI-1
      GO TO 1550
 1760  PS(JI-1)=X5
 1770  CONTINJE
      T(1,1)=MT
      N4=N3(JI)+1
      IF(H3(JI).GE.1.5*DX) N4=N4+1
      DO 1810 J=1,N4
      T(1,J)=T(JI,J)
      ANECK(1,J)=ANECK(JI,J)
 1810  CONTINUE
      RM=H2(JI)-(N4-0.5)*DX
      IF(RM.LE.0.0) GO TO 1840
      N4=N4+1
      T(1,N4)=(RM*T(JI,N3(JI)+2)    +(DX-RM)*IT)/DX
      ANECK(1,N4)= ANECK(JI,N3(JI)+2)
 1840  CONTINJE
      IF(IFLAG.EQ.1) GOTO 1870
      IF(N6+N4.LE.N) GO TO 1870
      NNTP=N6+N4+1
      NNAX=N+1
      DO 1860 I=2,NC
      DO 1862 J=NNAX,NNTP
      T(I,J)=T(I,N+1)
      ANECK(I,J)=0.0
 1862  CONTINJE
 1860  CONTINJE
      N=N6+N4
 1870  CONTINJE
C
      NNAX=N+1
      K4=N4+1
 1900 CONTINUE
      DO 1905 II=K4,NNAX
      T(1,II)=IT
      ANECK(1,II)=0.0
 1905  CONTINJE
      IT=((SR-1)*IT+FT)/SR
      AA=AA-M
      R2=R0
      AR=AA
      IF((CT.LT.N2).OR.(EN.LE.E.0)) GO TO 1950
```

```
      AA=AA+DL*H2(JI)
      BB=(H1+H2(JI))/2
      R2=R0-BB
      AR=AA-BB*R2*TH
 1950 CONTINUE
C
C
C   ***** SECTION X  *****
C
C     FIND NEW ANGLE THETHA (TH)
C
C
      HT=TH
      LT=0.0
 2010 AV=(HT+LT)/2.0
      IF(HT.EQ.LT) GO TO 2070
      RM=AV-SIN(AV)-2*AR/R2**2
      IF(RM**2.0.LT.0.0000001) GO TO 2070
      IF(RM.GT.0.0) GO TO 2060
      LT=AV
      GO TO 2010
 2060 HT=AV
      GO TO 2010
 2070 TH=AV
      TM=TM+TS
      GO TO 1000
      END
```

```
      SUBROUTINE PRINT(T,LK,K)
      DIMENSION T(200,100),N3(200)
      COMMON SS,SM,AL,AM,DX,N, TM,AA,AT,AD,TH,DL,N2,CT,NC,N3,RAD,TS
      COMMON TAIR,BMT,MT
      REAL MT
      INTEGER CT
      LK=LK+1
      BB=TH*57.29578
      IF(K.EQ.1) GOTO23
      WRITE(6,20)TM,AA,AT,AD,BB,DL,NC
   20 FORMAT(//,   11H TIME(SEC)=,F10.3,/,6X,16HTOTAL AREA(C2)= ,F10.3,
     1/,6X,12HWEDGE AREA= ,F10.4,/,6X,28HORIGINAL PENITRATION DEPTH= ,
     2F10.4,/,6X,12HANGLE(DEG)= ,F10.3,/,6X,27HARC LENGTH/TIME INCREMENT
     3= ,F10.5,/,6X,24HNO. OF WEDGES IN POOL = ,I3,/)
      WRITE(6,10) TAIR,BMT,MT
   10 FORMAT(6X,24HTEMP. OF AIR (DEG. C) =  ,F10.3,/,6X,
     1 44HTEMP. OF MOLD'S EXTERNAL SURFACE (DEG. C) =  ,F10.3,
     2 /,6X,44HTEMP. OF MOLD'S INTERIOR SURFACE (DEG. C) =  ,F10.3,///)
      WRITE(6,21)
   21  FORMAT(6X,30HTEMPERATURE HISTORY OF POWDER )
   23 IF(K.EQ.1) WRITE(6,24)
   24 FORMAT(//,12H NECK RADIUS   )
      ICOL=15
      IREP=((NC-1)/ICOL)+1
      IREM=NC-(IREP-1)*ICOL
      DO 100 KK=1,IREP
      IF(KK.EQ.IREP) ICOL=IREM
      KJ=(KK-1)*ICOL+1
      KJ1=KJ+(ICOL-1)
      IF(KK.EQ.IREP) KJ1=KJ+IREM-1
      WRITE(6,108)(J,J=KJ,KJ1)
  108  FORMAT(1X,5HAREA  ,15(I3,5X))
      DO 104 J=1,N
      IF(K.EQ.0) WRITE(6,102)J,(T(I,J),I=KJ,KJ1)
      IF(K.EQ.1) WRITE(6,103)J,(T(I,J),I=KJ,KJ1)
  102  FORMAT(1X,I3,3X,15(F7.3,1X))
  103 FORMAT(1X,I3,3X,15(F7.5,1X))
  104  CONTINUE
      WRITE(6,105)
  105  FORMAT(1X,//)
  100  CONTINUE
   97 CONTINUE
      IF(CT.LT.N2) RETURN
      ICOL=15
      IF(K.EQ.0) WRITE(6,98)
   98  FORMAT(1X,//,31H TEMPERATURE OF STUCK MATERIAL ,/)
      IF(K.EQ.1) WRITE(6,99)
   99 FORMAT(//,30H NECK RADIUS OF STUCK MATERIAL    )
      IREP=INT((CT-(N2 -1))/ICOL)+1
      IREM=CT-N2+1-(IREP-1)*ICOL
      DO 200 KK=1,IREP
      KJ=(KK-1)*ICOL+N2
      IF(KK.EQ.IREP) ICOL=IREM
      KJ1=KJ+(ICOL-1)
      IF(KK.EQ.IREP) KJ1= KJ+IREM-1
```

```
      WRITE(6,108)(J,J=KJ,KJ1)
      NTN=N3(KJ)+2
      DO 204 J=1,NTN
      DO 203 II=KJ,KJ1
      NTMP=N3(II)+2
      IF(NTMP.EQ.NTN) GO TO 203
      IDIFF=NTN-NTMP
      DO 202 LL=1,IDIFF
      T(II,NTMP+LL)=0.0
  202 CONTINUE
  203 CONTINUE
      IF(K.EQ.0) WRITE(6,102)J,(T(I,J),I=KJ,KJ1)
      IF(K.EQ.1) WRITE(6,103)J,(T(I,J),I=KJ,KJ1)
  204  CONTINUE
  200  CONTINUE
  300  RETURN
      END


      SUBROUTINE CONST(C1,C2,C3,DB,DA,T1,T2,T3,ANB,ANA,BNK)
      DIMENSION N3(200)
C
C
C
      COMMON SS,SM,AL,AM,DX,N,TM,AA,AT,AD,TH,DL,N2,CT,NC,N3,RAD,TS
      A1=0.5*(ANB+ANA)
      C1=RADX(ANB)*DX
      C2=RADX(ANA)*DX
      C3=RADX(A1)*DX
      DELB=(3.0*SU(T1)*RAD/(8.0*VIS(T1)*(TM+0.5*TS)))**0.5*TS
      IF(ANB/RAD.GE.0.5) DELB=0.5*SU(T1)*TS/(VIS(T1))
      DB=COND(ANB)/(RHO(A1)*CP(A1))
      DA=COND(ANA)/(RHO(A1)*CP(A1))
      BNK=ANB+DELB
      IF(BNK.GT.RAD) BNK=RAD
      IF(DELB.GT.0.0) RETURN
      WRITE(6,10)TM,ANB,ANA,BNK,RAD,TS,SU(T1),VIS(T1) ,DELB
   10 FORMAT(1X,10(E10.5,1X))
      RETURN
      END
```

```
      FUNCTION RHO(Y)
      DIMENSION N3(200)
C
C     DENSITY FUNCTION (<G/CM**3)
C
C     R1=DENSITY AT SS
C     R2=DENSITY AT SM
C
      COMMON SS,SM,AL,AM,DX,N, IM,AA,AT,AD,TH,DL,N2,CT,NC,N3,RAD,TS
      R1=5.0937E-04
      R2=8.8058E-04
      X=Y/RAD
      IF(X.GT.0.0) GOTO 10
      RHO=R1
      GO TO 1
   10 IF(X.GT.1.0) GOTO 20
      RHO=R1+(R2-R1)*X
      GO TO 1
   20 RHO=R2
    1 CONTINUE
      RETURN
      END
```

```
      FUNCTION COND(Y)
      DIMENSION N3(200)
C
C     CONDUCTIVITY FUNCTION (JOULE/(CM-SEC-DEG K))
C
C        C1 = THERMAL CONDUCTIVITY AT TEMPERATURE SS
C        C2 = THERMAL CONDUCTIVITY AT TEMPERATURE SM
C
      COMMON SS,SM,AL,AM,DX,N, IM,AA,AT,AD,TH,DL,N2,CT,NC,N3,RAD,TS
      C1=1.99E-03
      C2=4.9325E-03
      X=Y/RAD
      IF(X.GT.0.0) GOTO 10
      COND=C1
      GO TO 1
   10 IF(X.GT.1.0) GOTO 20
      COND=C1+X*(C2-C1)
      GO TO 1
   20 COND=C2
    1 CONTINUE
      RETURN
      END
```

=-LONG/-OT,ARG=-COMMON/-FIXED,CS= USER/-FIXED,DB=-TB/-SB/-SL/ ER/-ID/-PMD/
N5.

```
      FUNCTION RADX(Y)
      DIMENSION N3(200)
      COMMON SS,SM,AL,AM,DX,N,TM,AA,AT,AD,TH,DL,N2,GT,NG,N3,RAD,TS
C
C     THIS FUNCTION DETERMINES THE RATIO USED TO CALCULATE DX AS A FUNC
C         OF MOLD TEMP
C
      X=Y/RAD
      IF(X.GT.0.0) GOTO 10
      RADX=1.0
      GO TO 1
   10 IF(X.GT.1.0) GOTO 20
      RADX=RHO(0.0)/RHO(Y)
      GO TO 1
   20 RADX=RHO(0.0)/RHO(RAD)
    1 CONTINUE
      RETURN
      END

      FUNCTION CP(X)
C
C     SPECIFIC HEAT (JOULE/(KG-DEG K))
C
      CP=2302.7
      RETURN
      END

      FUNCTION SU(T)
C
C         SURFACE TENSION FUNCTION (DYNES/CM)
C
      SU=31.0-0.058*(T-105)
      RETURN
      END

      FUNCTION VIS(T)
C
C         VISCOSITY FUNCTION  (POISE)
C
      VIS=5.22E06*EXP(-19.583 + 7402.5/(T+273))
      RETURN
      END
```

SELECTED BIBLIOGRAPHY

(1) Frenkel, J., "Viscous Flow of Crystalline Bodies Under The Action of Surface Tension", Journal of Physics, Vol IX, NO 5, 1945, pp 385-391.

(2) Kuczynski, G. C., "Study of the Sintering of Glass", Journal of Applied Physics, Vol 20, Dec 1949, pp 1160-1163.

(3) Kuczynski, Neuville and Toner, "Study of Sintering of Poly(methyl Methacrylate)", Journal of Applied Polymer Science, Vol 14, 1970, pp 2069-2077.

(4) Lontz, J. F., "Sintering of Polymer Materials", Fundamental Phenomena in the Material Sciences, Vol 1, (L.J. Bonis and H.H. Hausner, eds), Plenvn Press, New York, 1964, pp 25-47.

(5) Dillion, R. E., Matheson, L. A. and Bradford, E. B., "Sintering of Synthetic Latex Particles", J. Colloid Sci 6, 1951, pp 108-117.

(6) Tadmor and Gogos, Principles of Polymer Processing, John Wiley & Sons, New York, NY, 1979, pg 147.

(7) Bigg, D.M. and Epstein, M. M., "Molding Polymeric Powders by Compaction and Sintering", Science Technology Polymer Process, Processing Int. Conf 1979, pp 897-919.

(8) Narkis, M., "Sintering Behavior of Poly (Methyl Methacrylate) Particles", Polymer Engineering and Science, Oct 1979, Vol 19, No 13, pp 889-892.

(9) Steiner, G. F., Manson, J. A. and Nippert, C. R., "Characterization of Polymer Glasses By Sintering Techniques", Paper presented to American Chemical Society, Chicago, 13-18 Sept 1970, pp 105-111.

(10) Schonhorn, H., Frisch, H. I., Kwei, T. K., "Kinetics of Wetting of Surfaces by Polymer Melts", Journal of Applied Physics, Vol 17, No 13, Nov 66, pp 4967-4973.

(11) Halldin, G. W. and Kamel, I.L., "Powder Processing of UHMV-PE, II. Sintering", Society of Plastic Engineers, 35th Annual Technical Conference, Apr 1977, pp 298-300.

(12) Ross, Thomas, J., "Review of Polymer Powder Sintering", SPE 37th Annual Technical Conference, Vol 15, May 1979, pp 909-912.

(13) Kuczynski, G. C. and Zaplatynskyj, I., "Sintering of Glass", Journal of the American Ceramic Society, Vol 39, No 10, pp 249-350.

(14) Rao, M. and Throne, J. L., "Theory of Rotational Molding - Part III: Sintering - Melting and Degradation", in Proceedings 30th Annual SPE Technical Conference: Shaping the Future with Plastics, 15-18 May 1972, Chicago, pp 759-761.

(15) Rosenzweig, N. and Narkis, M., "Coalescence Phenomenology of Spherical Polymer Particles By Sintering", Polymer, Sep 1980, Vol 21, pp 988-989.

(16) Jayaraman, G. S., Wallace, J. F., Geil, P. H. and Baer, E., "Cold Compaction Molding and Sintering of Polystyrene", Polymer Engineering and Science, Aug 1976, Vol 16, No 8, pp 529-536.

(17) Mackenzie, J. K. and Shuttleworth, R., "A Phenomenological Theory of Sintering", Proc Phys Society, LXII, 12, pp 833-852.

(18) Throne, James L., Plastic Process Engineering, Marcel Dekker, inc., New York, NY, 1979, pg 60.

(19) Mohan, A., Soni, N. C. and Moorthy, V. K., "Refinements in Determination of Sintering Mechanisms", Transactions of the Indian Ceramic Society, Vol 38, July-Aug 1979, pp 117-124.

(20) Menges, G., Schulze-Kadelbach, R., Reichstein, H., Thebing, U. and Schmity, J., "Examination of the Principles for Sintering Plastic Materials", Rheology Acta, Mar 1980, pp 633-641.

(21) Rosenzweig, N. and Narkis, M., "Dimensional Variations of Two Spherical Polymeric Particles During Sintering", Polymer Engineering and Science, July 1981, Vol 21, No 10, pp 582-585.

(22) Ramamoorthy, P. and Treybal, R., "Drop Coalescence in Liquid-Liquid Fluidized Beds", A.I.CH.E. Journal, Vol 24, No 6, Nov 1978, pp 985-992.

(23) Lang, S. B. and Wilke, C. R., "A Hydrodynamic Mechanism for the Coalescence of Liquid Drops. I. Theory of Coalescence at a Planar Interface", Industrial Engineering, Chemical Fundamentals, Vol 10, No 3, 1971, pp 328-340.

(24) Lang, S. B. and Wilke, C. R., "A Hydrodynamic Mechanism for the Coalescence of Liquid Drops. II. Experimental Studies", Industrial Engineering Chemical Fundamental, Vol 10, No 3, pp 341-352.

(25) Shaler, A. J., "Seminar on the Kinetics of Sintering (with Discussions)", Metals Transactions, Vol 185 Nov 1949, pp 796-804.

(26) Vanderhoff, J. W., Tarkowski, H. L., Jenkins, M. C. and Bradford, E. B., "Theoretical Consideration of the Interfacial Forces Involved in the Coalescence of Latex Particles", Journal of Macromolecular Chemistry, Apr 1966, pp 361-397.

(27) Brown, George, "Formation of Films from Polymer Dispersions", Journal of Polymer Science, Vol XXII, 1956, pp 423-434.

(28) Leidi, M., Hartland, S., "The Effect of Vertical Forces on the Coalescence of Two Dimensional Drops", Proc. R. Soc. Lond. 349, 1976, pp 343-354.

(29) Myer, Glen E., Analytical Methods in Heat Transfer, McGraw - Hill Book Co., 1971, pg 198.

(30) Vanderbeck, William E., The Prediction of Sintering Time in the Roto-molding of Polymeric Materials, Thesis, NJIT, Newark, NJ, 1979, pg 71.

(31) Rao, M. and Throne, J. L., "Theory of Rotational Molding - Part I: Heat Transfer", Soc. Plast. Eng., Tech Pap., 72, 18(Pt. 2), pp 752-756

(32) Rao, M. and Throne, J. L., "Theory of Rotational Molding - Part II: Fluid Flow", Soc. Plast. Eng., Tech Pap., 72, 18(Pt. 2), pp 757-761.

(33) Progelhof, R. C., Throne, J. L., and Ruetsch, R. R., "Methods for Predicting the Thermal Conductivity of Composite Systems: A Review", Polymer Engineering And Science, Sept 76, Vol 16, No 9, pp 615-625.

(34) Yagi, Sakae, Kunii, and Daizo, "Studies of Effective Thermal Conductivies in Packed Beds", A.I.Ch.E. Journal, Sept 57.

(35) Werley, K. and Gilligan, J., "The Temperature Distribution of a Sphere Placed in a Directed Uniform Heat Flux", Journal of Heat Transfer, May 81, Vol 103, pg. 399.

(36) Sass, Allan, "Simulation of the Heat Transfer Phenomena in a Rotary Kiln", I & ED Process Design & Development, Vol 6, No 4, Oct 67, pp 532-535.

(37) Murphy, K., "The Melting Process in Polyethylene Powder Beds", ME 490 Paper, NJIT, Newark, NJ, Dec 81.

(38) Merrill, Ronald, "Thermal Conduction Through an Evacuated Idealized Powder Over the Temperature Range of 100 to 500 K", NASA Technical Note #D-5063, March 1969.

(39) Mac Adams, John L., "How to Predict Physical Properties of Rotomolded Parts", SPE Tech Paper, Oct 1975, pp 64-71.

(40) Luikov, Shashkov, Vasiliev, and Fraiman, "Thermal Conductivity of Porous Systems", Heat Mass Transfer, Vol 11, Apr 66, pp 117-140.

(41) Lehmberg, J., Hehl, M., and Schugerl, K., "Transverse Mixing And Heat Transfer in Horizontal Rotary Drum Reactors",

(42) Kramers, H., and Croockewit, P., "The Passage of Granular Solids Through Inclined Rotary Kilns", Chem. Eng. Sci., Vol 1, No 6, 1952.

(43) Wes, G., Drinkenburg, A., and Stemerding, S., "Heat Transfer in a Horizontal Rotary Drum Reactor", Powder Tech., 1976

(44) Kunii, Daizo and Smith, "Heat Transfer Characteristics of Porous Rocks", A.I.Ch.E. Journal, March 1960.

(45) Cho, S.H., and Sunderland, J.E., "Heat Conduction Problems With Melting and Freezing", J. of Heat Transfer, Aug 1969, pg 421.

(46) Fraiman, Y., Luikow, A., and Shashkov, A., "Thermal Conductivity of Porous Systems", J. of Heat Mass Transfer, Vol 11, 1968, pp. 117-140.

(47) Beek, W.J. and Stammers, E., "The Melting of a Polymer on a Hot Surface", Polymer Eng & Science, Jan 69, Vol 9, No 1, pg 49.

(48) Baer, E., Geil, P., Jayaraman, G., and Wallace, J., "Cold Compaction Molding and Sintering of Polystyrene", Polymer Eng & Sci, Aug 1976, Vol 16, No 8, pg 529.

(49) Hartland, S., and Leidi, M., "The Effect of Vertical Force on the Coalescence of Two Dimensional Drops", Proc. R. Soc. Lond. A., Vol 349, 1976, pp 343-354.

(50) Carrow, G.E., "Crosslinkable Rotational Molding High Density Polyethylene", S.P.E. 30th Annual Tech. Conf., May 1972, pp 762-765.

(51) Rao and Toor, "Heat Transfer Between Particles in Packed Beds", Ind. Eng. Chem. Fund., 1984, 23, pp. 294-298.

(52) Ristic, "Kuczynski's Theory of Sintering and Recent Investigations of the Process", International Journal of Science of Sintering, Vol 16, 1984, No 2.

(53) Lewandowski, A., "A Study of Surface Kinetic Angles of Plastic Powders In a Rotating Drum", NCE Thesis, Newark, NJ.

(54) Mercadante, F., "Flow Characteristics of A Granular Matter In a Rotating Cylinder", NCE Thesis, Newark, NJ, 1973.

(55) Krieth, Frank, Principles of Heat Transfer, 2nd Ed., Scranton, Pa., The Ronald Press Company, 1963.

(56) Myers, Glen E., Analytical Methods in Conduction Heat Transfer, New York, McGraw-Hill, 1971.

(57) Technical Information Sheet(TIS) of Marlex LX470 Phillips Chemical Company, Bartlesville, OK, May 1981.

(58) Technical Service Memorandum No. 243 (TSM-243), Marlex Polyolefin Resins, Phillips Chemical Company, Bartlesville, OK, June 1983.

(59) Schenck, Hildebrand, Jr., Fortran Methods in Heat Flow, New York, The Ronald Press Company, 1963.